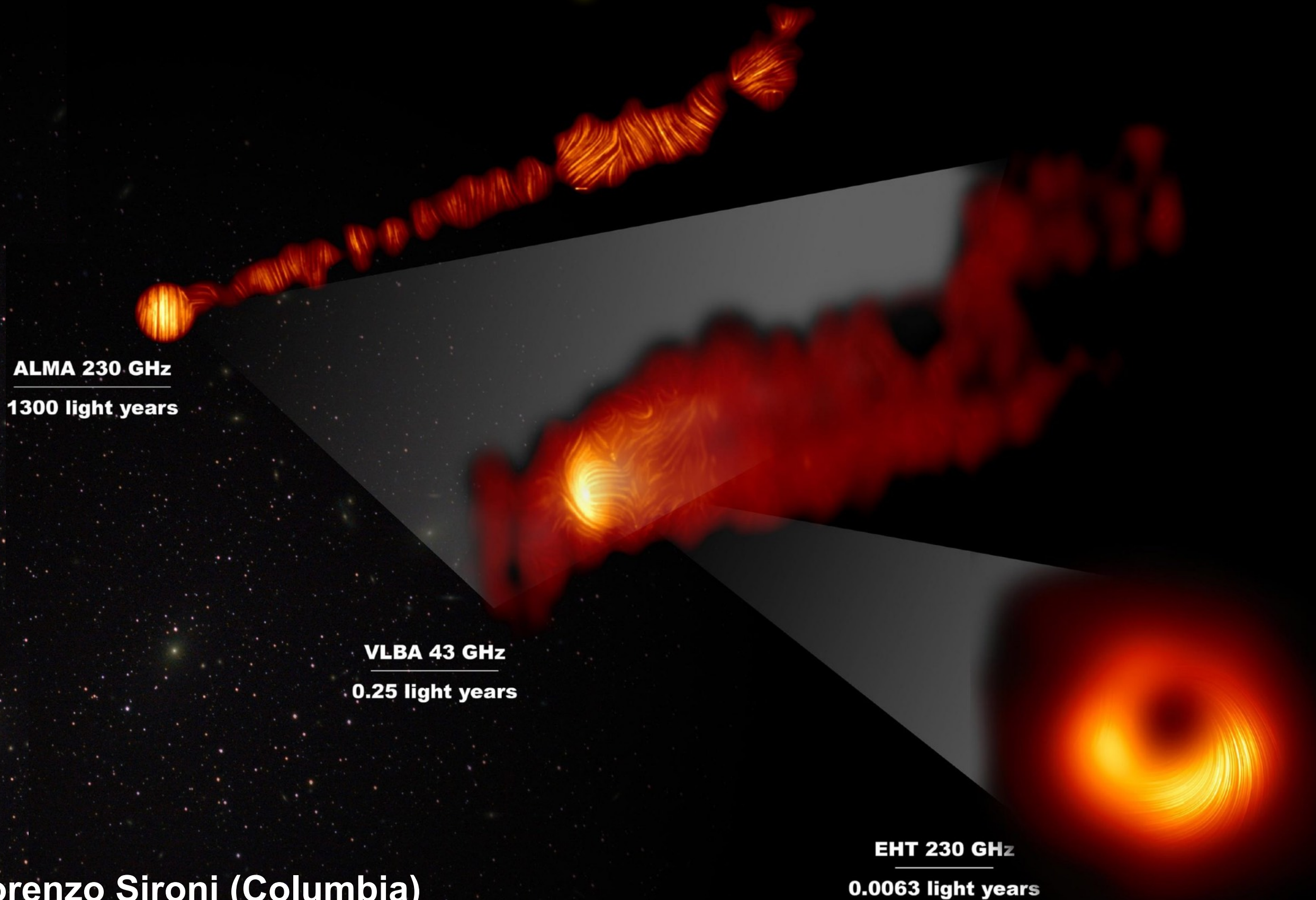


# Reconnection-powered emission



**ALMA 230 GHz**  
**1300 light years**

**VLBA 43 GHz**  
**0.25 light years**

**EHT 230 GHz**  
**0.0063 light years**

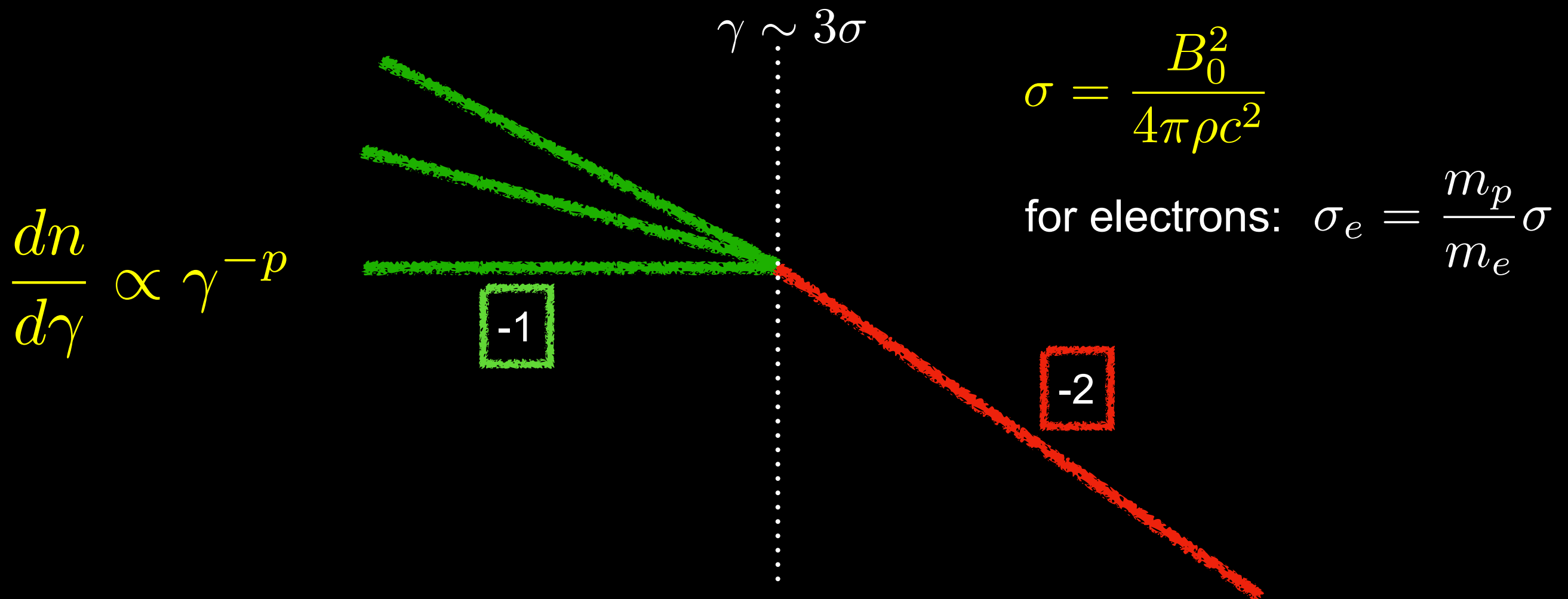
**Lorenzo Sironi (Columbia)**

***Foundations of CR Astrophysics, Varenna 2022***

# Overarching summary

Relativistic reconnection can:

- efficiently dissipate magnetic energy (at rate  $\sim 0.1 c$ ).
- produce non-thermal particles with hard power-law slopes.



# Outline

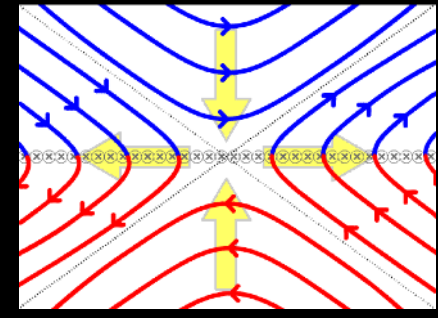
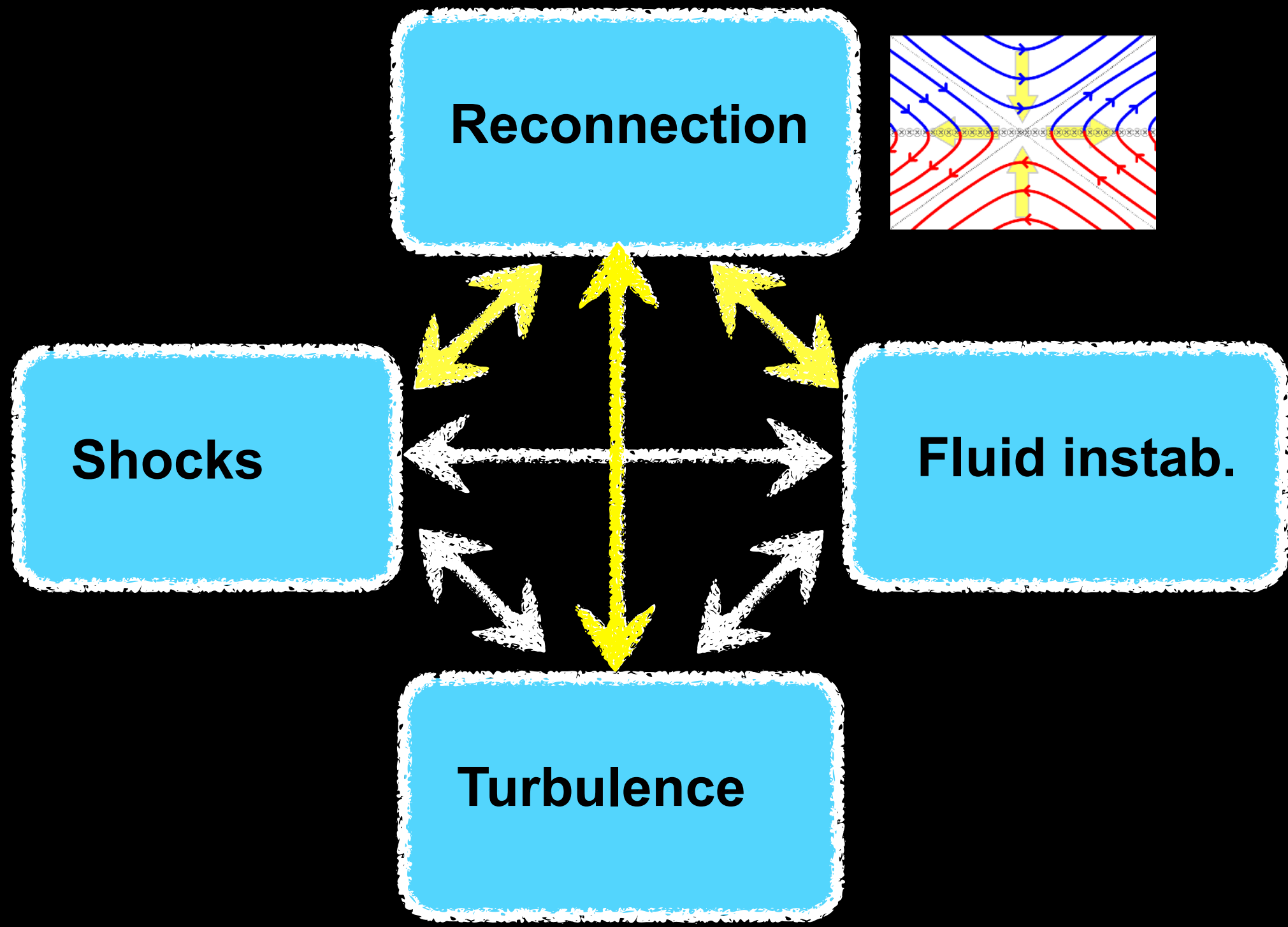
for a recent review, <https://www.nature.com/articles/s42254-021-00419-x>

## What is magnetic reconnection?

- The Sweet-Parker model of magnetic reconnection.
- The regime of relativistic reconnection.
- The physics of particle acceleration in relativistic reconnection.

## What can magnetic reconnection do?

- Where/How do reconnection layers form?
- Reconnection-powered particle acceleration and emission.



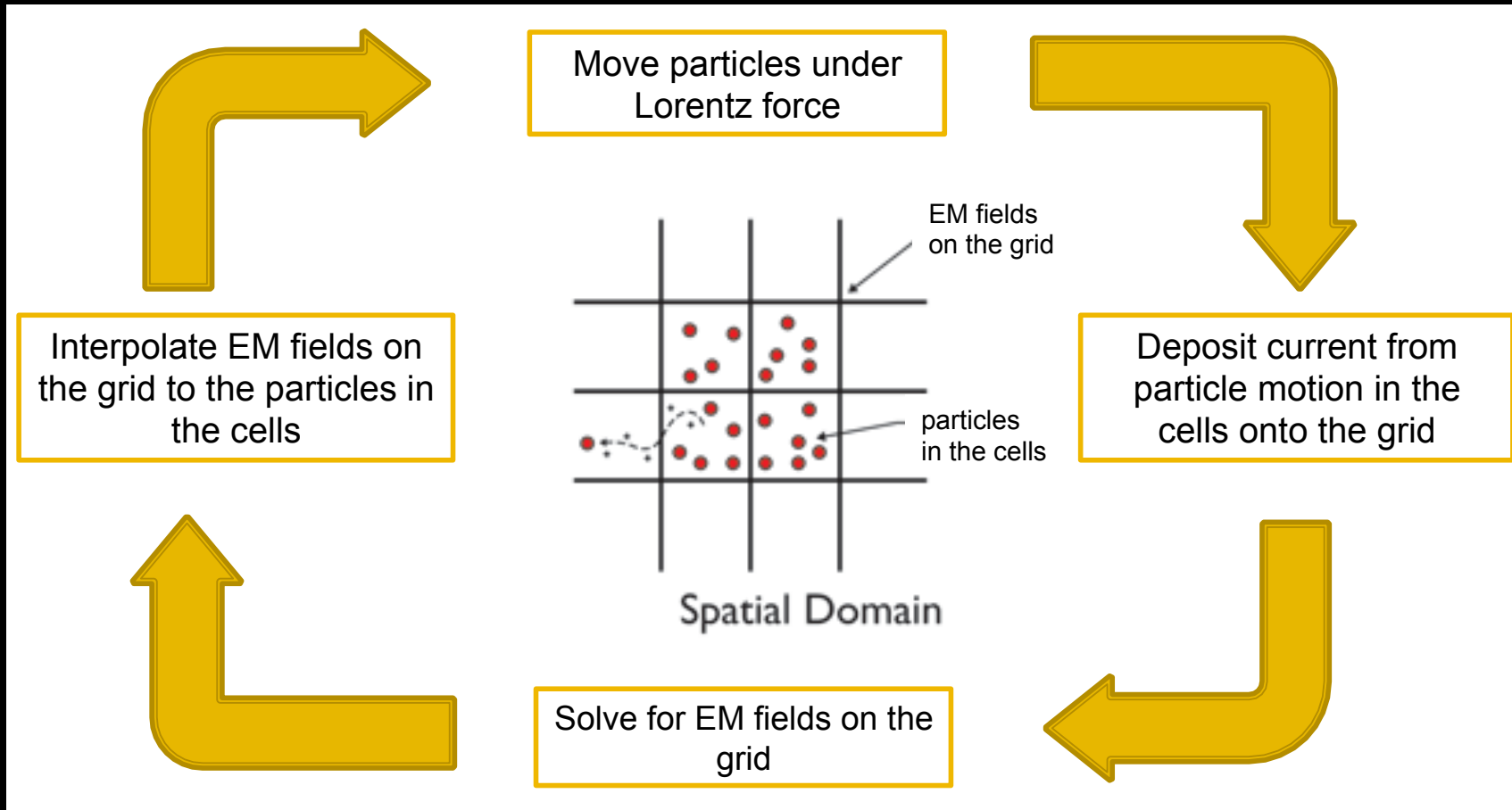
Magnetically-dominated  
(aka "relativistic"):

$$\sigma = \frac{B_0^2}{4\pi\rho c^2} \gg 1 \quad v_A \sim c$$

# The PIC method

Particle-in-Cell (PIC) method:

It is the most fundamental way of capturing the interplay of charged particles and e.m. fields.



The computational challenge:

The *microscopic* scales resolved by PIC simulations are much smaller than *astronomical* scales.

Typical length ( $c/\omega_p$ ) and time ( $1/\omega_p$ ) scales are:

$$\frac{c}{\omega_p} \simeq 5.5 \times 10^5 \left( \frac{n}{1 \text{ cm}^{-3}} \right)^{-1/2} \text{ cm} \quad \frac{1}{\omega_p} \simeq 1.8 \times 10^{-5} \left( \frac{n}{1 \text{ cm}^{-3}} \right)^{-1/2} \text{ s}$$

$$\omega_p = \omega_{pe} \quad ; \quad \omega_{pi} = \omega_{pe} \sqrt{m_e/m_i}$$

# Shock-driven reconnection in spider pulsars

Reconnection



Shocks

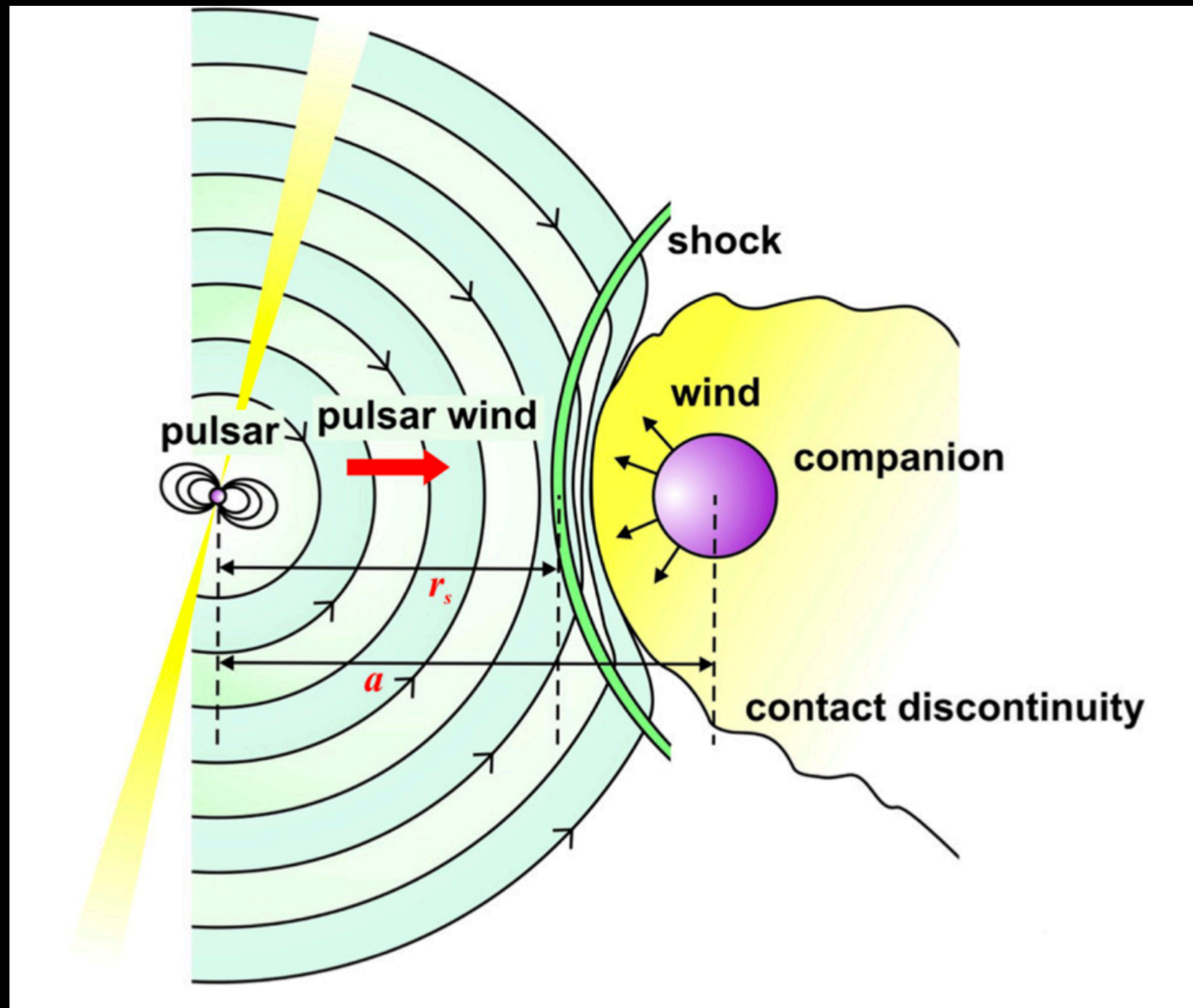
with J. Cortes



Cortes & LS 2022, arXiv:2203.00023

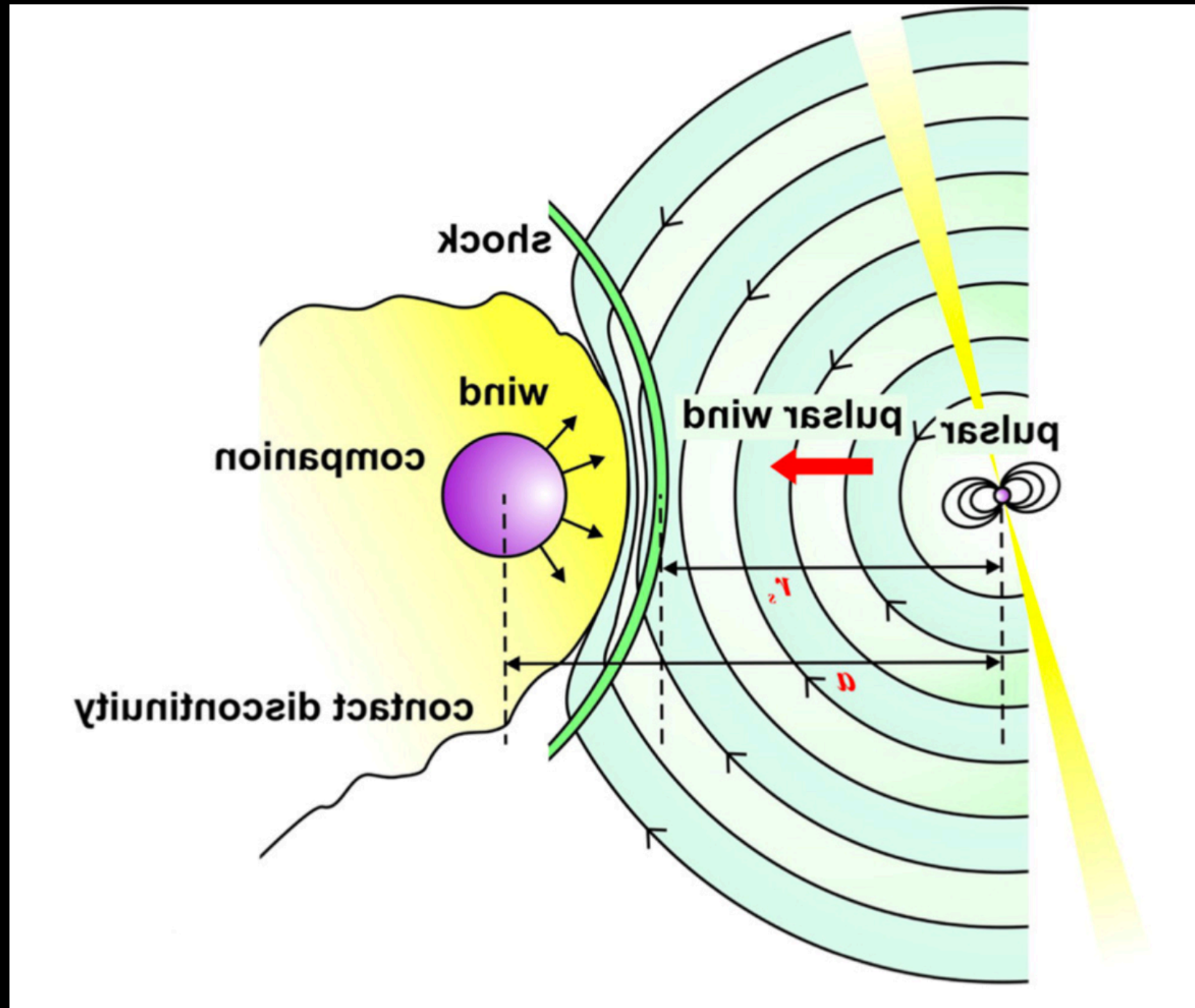
# What are spider pulsars?

- Millisecond pulsars in tight binary orbits with a degenerate (black widows) or non-degenerate (redbacks) companion.
- The pulsar wind evaporates (devours) the companion.



# What are spider pulsars?

- Millisecond pulsars in tight binary orbits with a degenerate (black widows) or non-degenerate (redbacks) companion.
- The pulsar wind evaporates (devours) the companion.

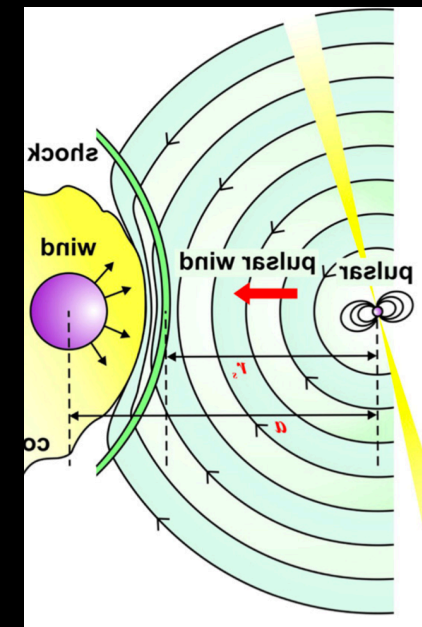
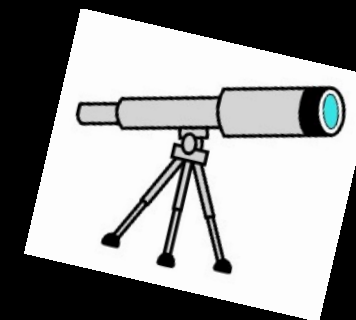
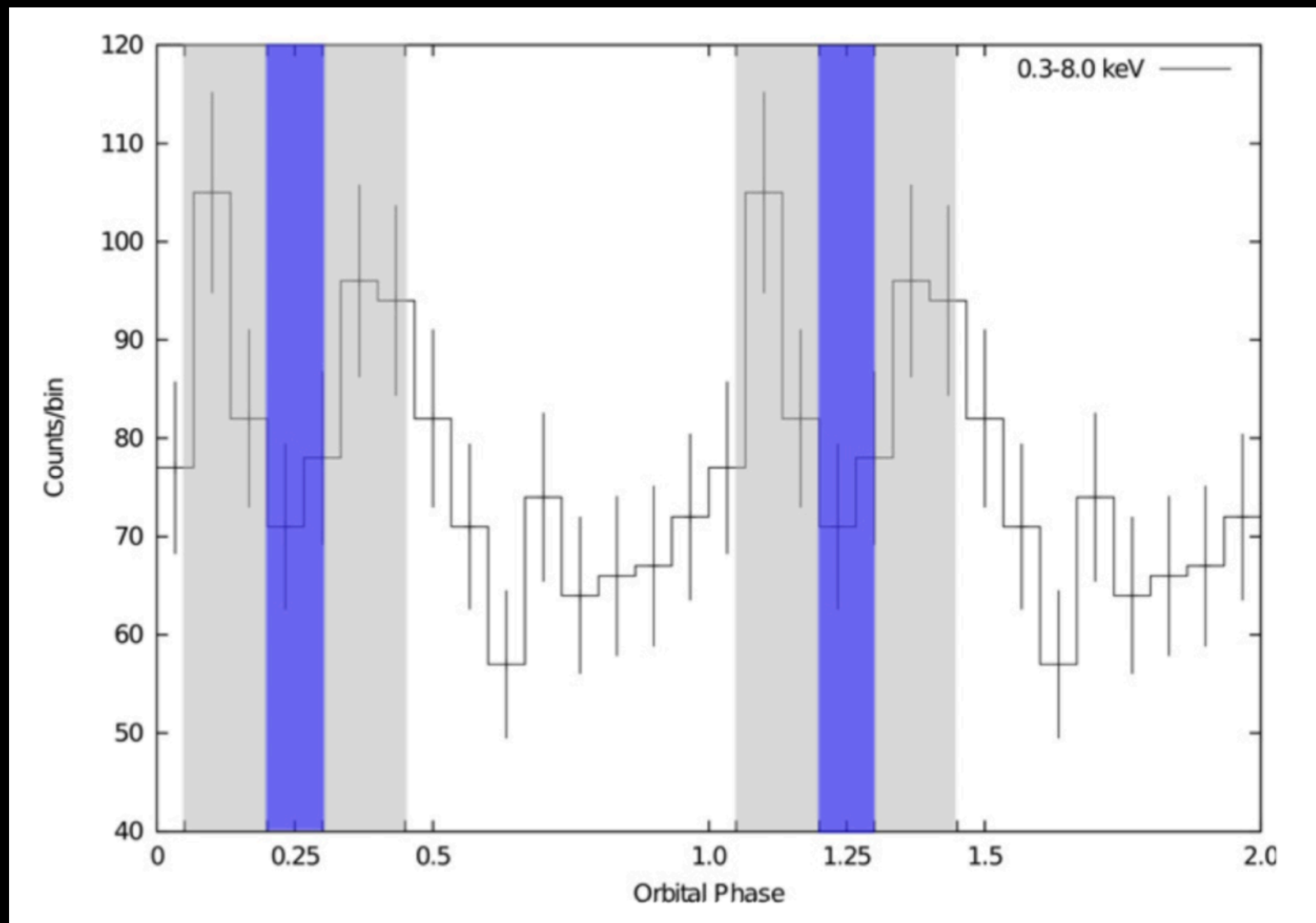


# Spectra and lightcurves

- The X-ray spectrum is hard, requiring an electron spectrum with hard slope.

$$\frac{dn}{d\gamma} \propto \gamma^{-p}$$

$$p = -d \log N / d \log \gamma \approx 1 - 2$$

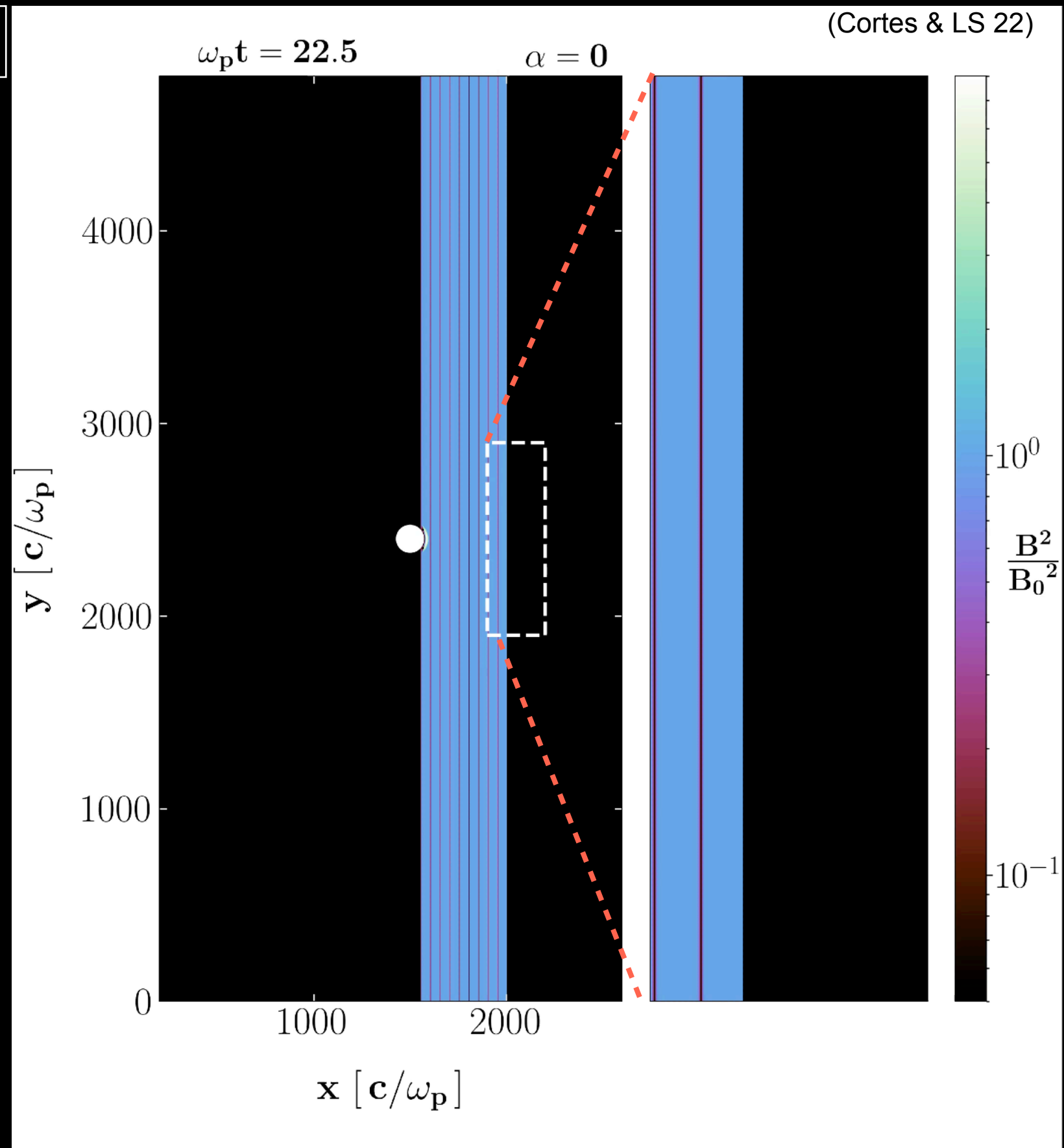


- The X-ray lightcurve has two peaks, just before and after the pulsar eclipse.

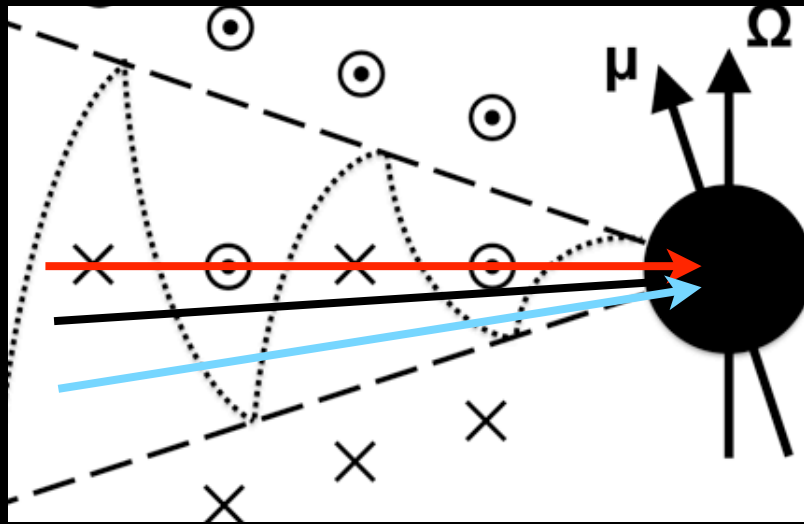
# Flow dynamics from a global PIC sim

$\sigma=10$

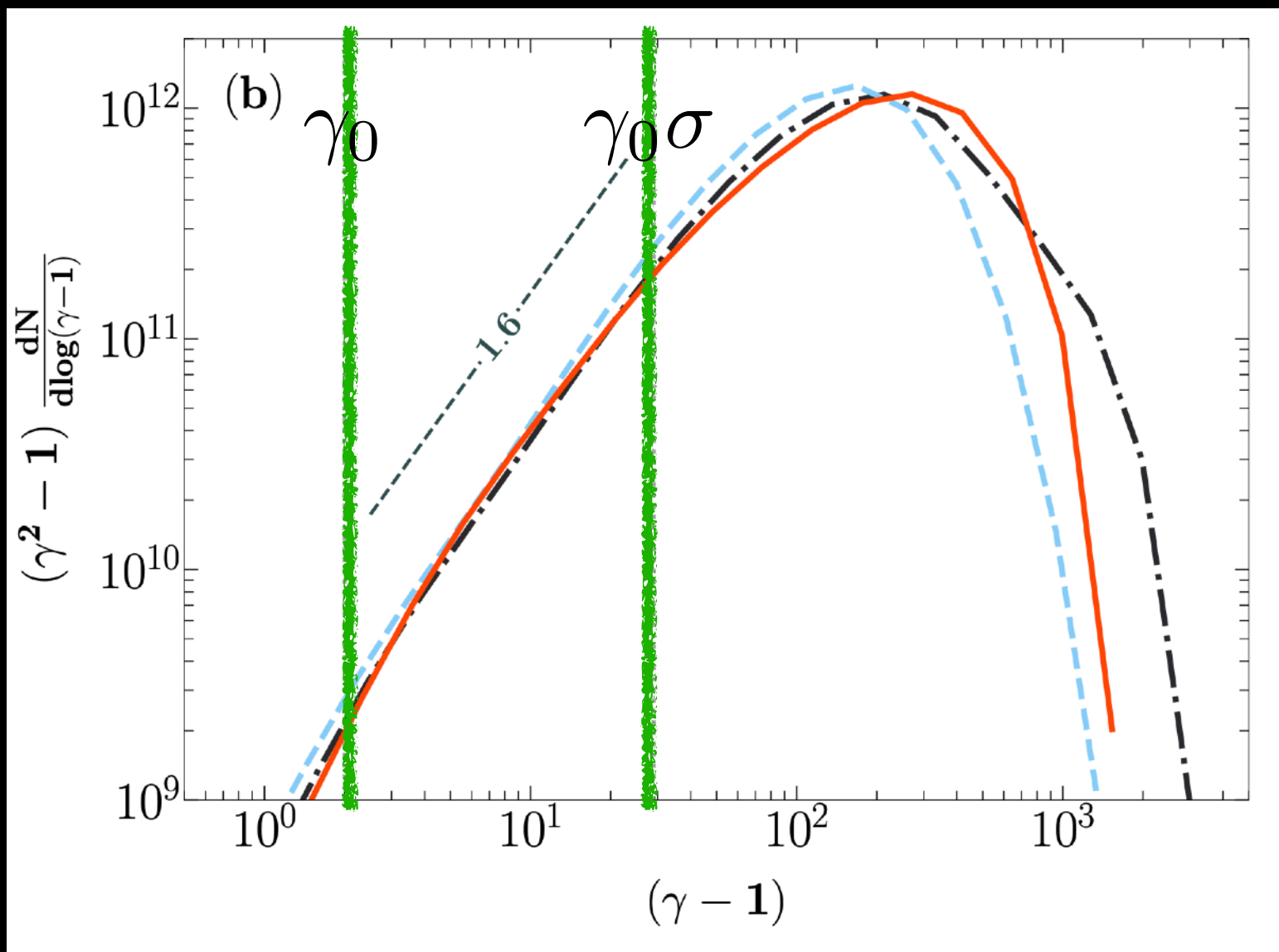
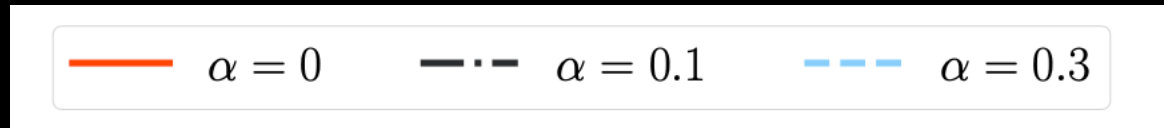
- The pulsar wind is terminated at a relativistic shock that wraps around the companion.
- Shock-driven reconnection dissipates the magnetic stripes.



# Particle spectrum



We explore the whole range of latitudes where the wind is striped ( $\alpha$  from 0 to 1)

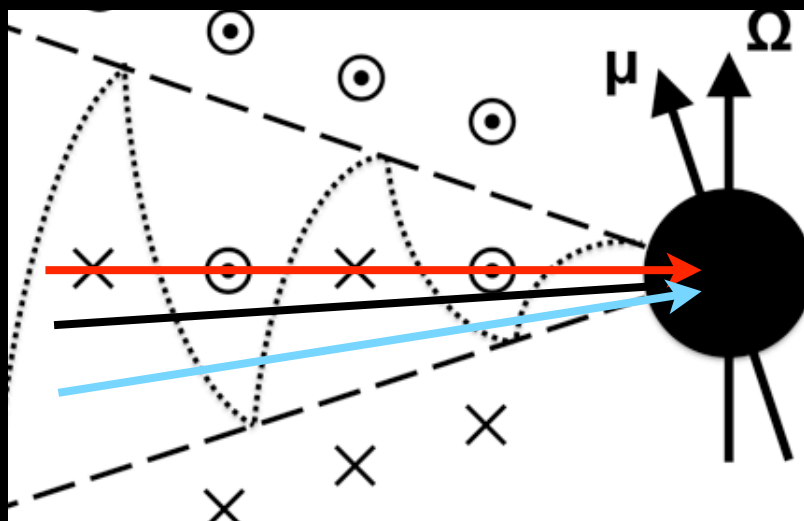


- The particle spectrum is hard, with  $p \sim 1.4$ , in the range

$$\gamma_0 \lesssim \gamma \lesssim \gamma_0\sigma$$

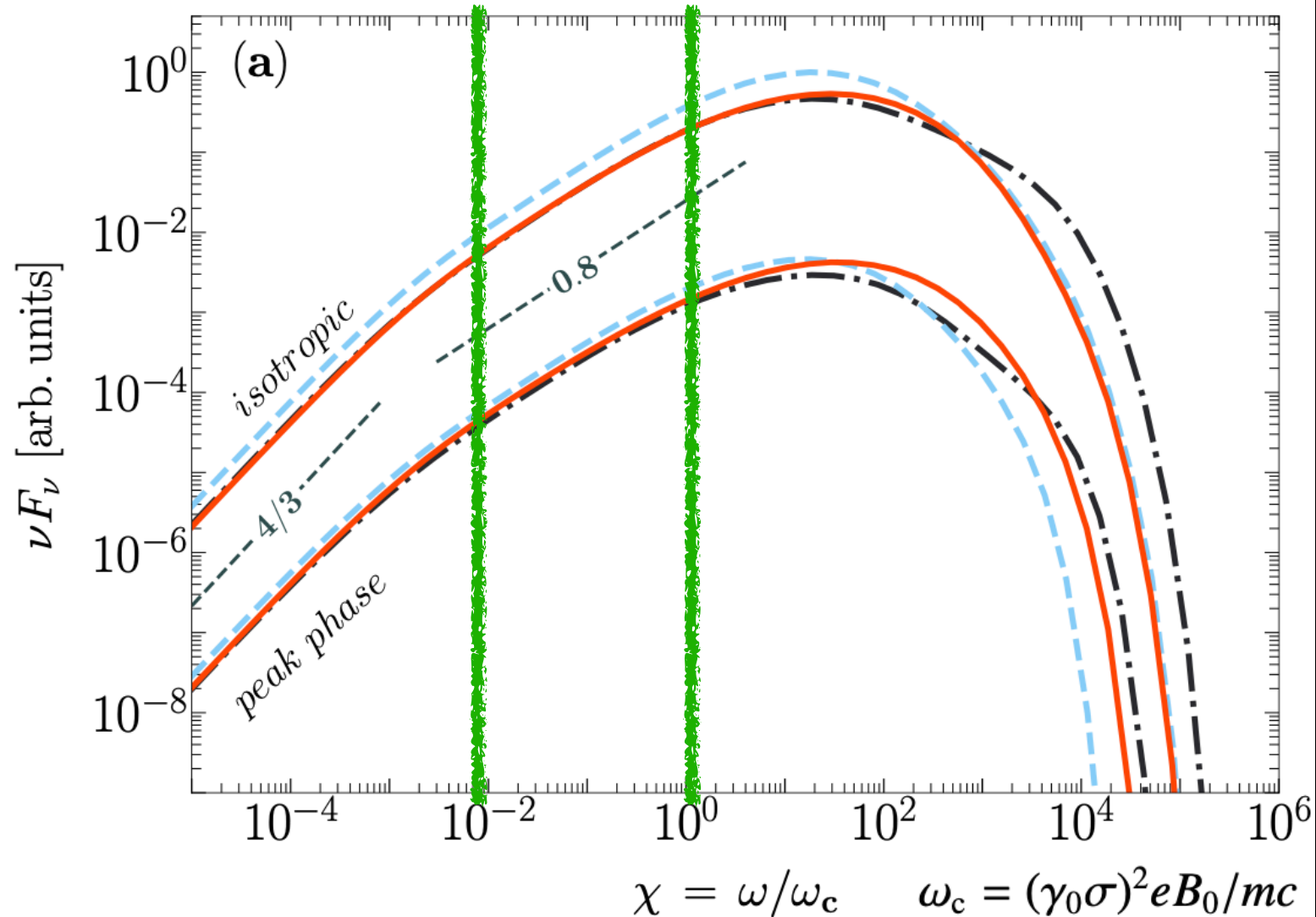
as a result of shock-driven reconnection.

# Synchrotron spectrum



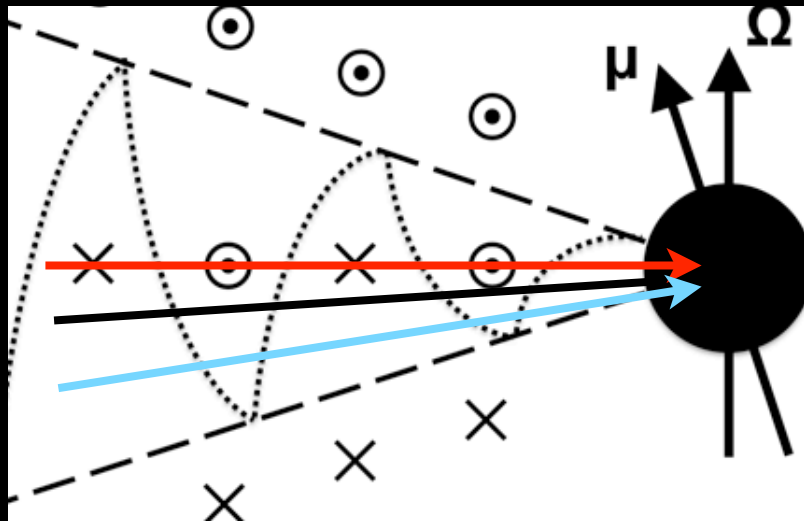
We explore the whole range of latitudes where the wind is striped ( $\alpha$  from 0 to 1)

—  $\alpha = 0$     - · -  $\alpha = 0.1$     - - -  $\alpha = 0.3$

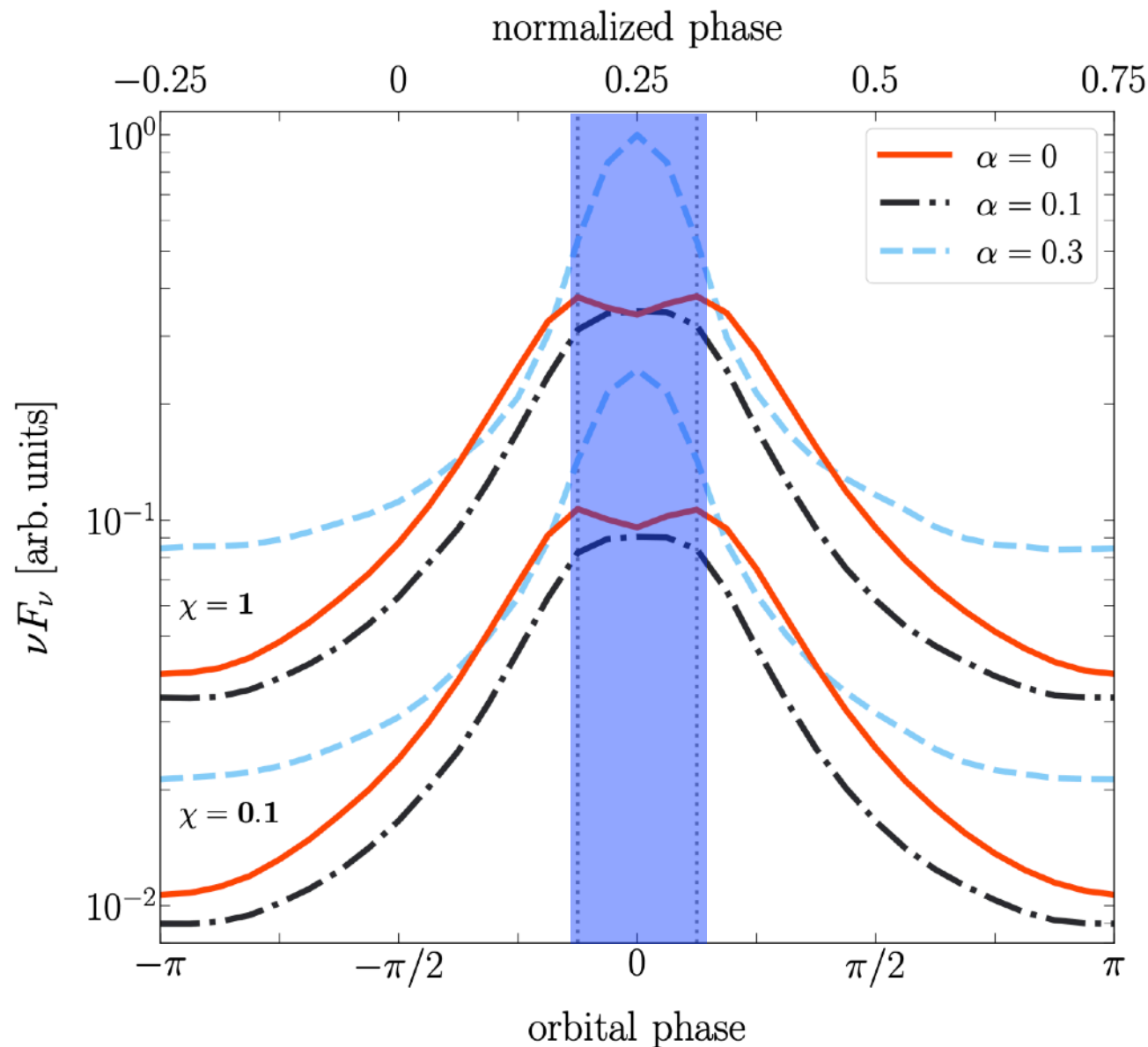
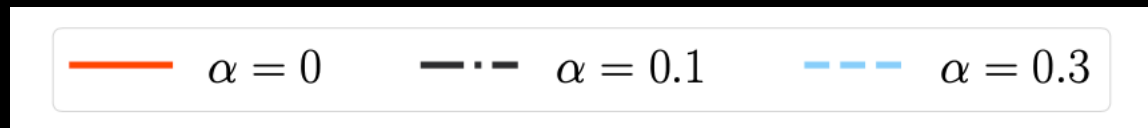


- In the corresponding frequency range, the synchrotron spectrum is hard, with a slope consistent with X-ray observations.

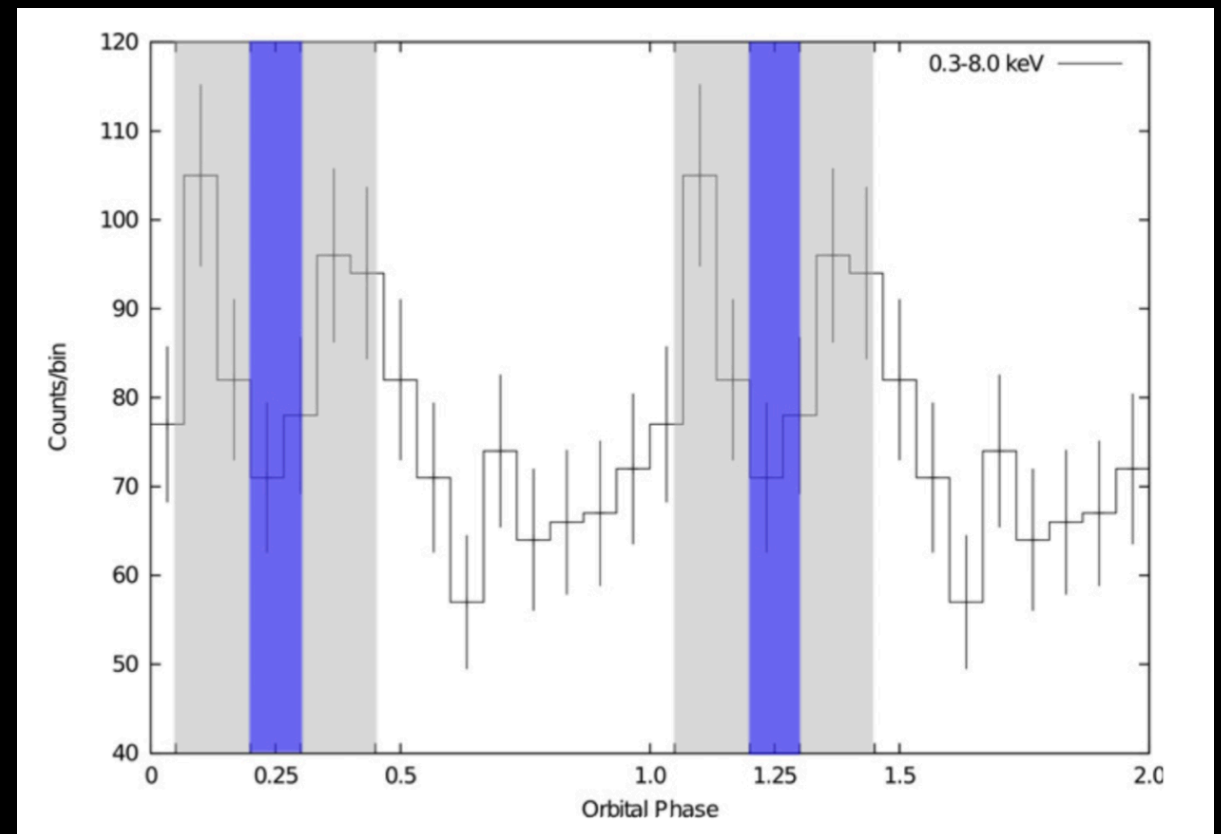
# Lightcurve



We explore the whole range of latitudes where the wind is striped ( $\alpha$  from 0 to 1)

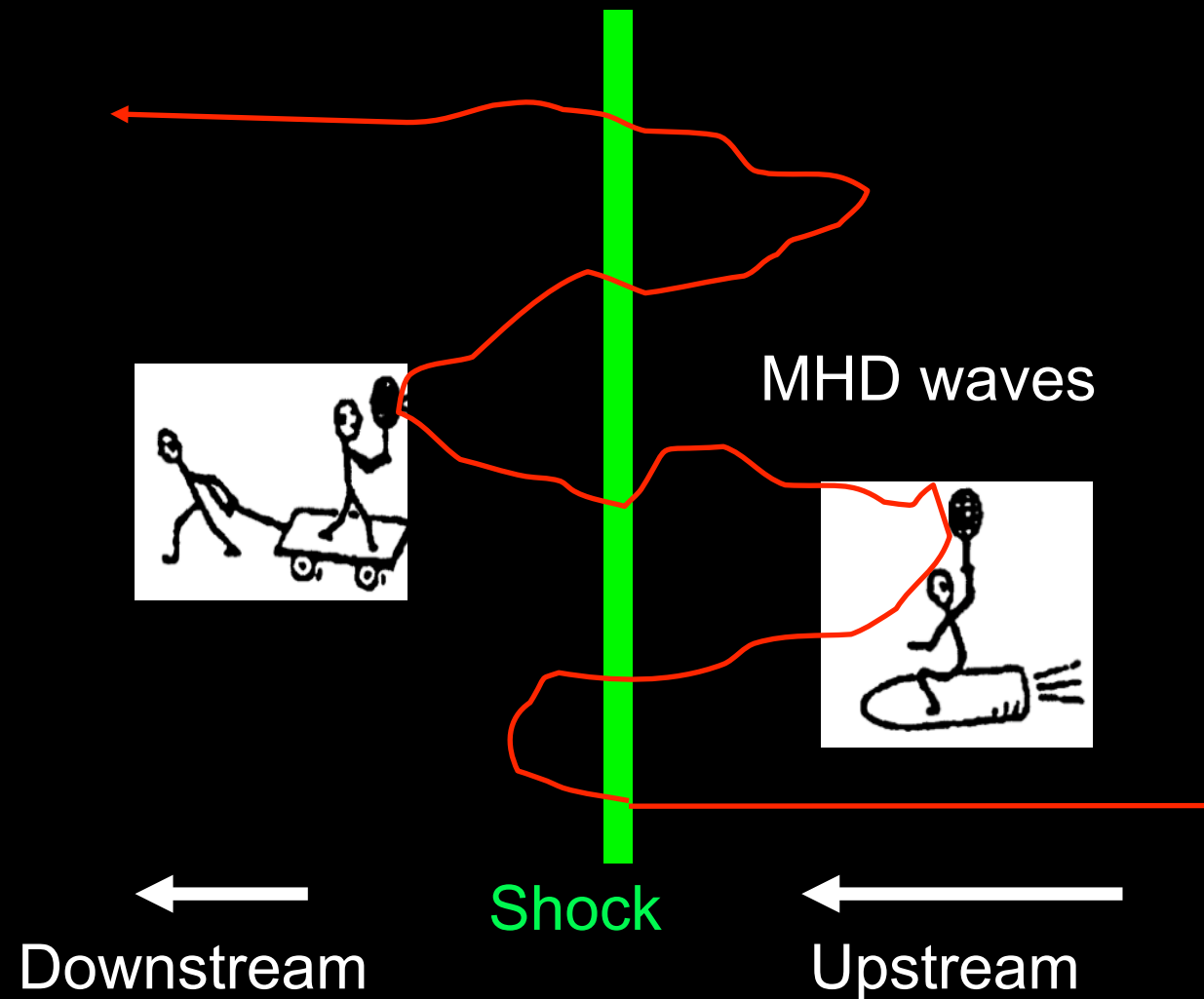


- For  $\alpha \sim 0$ , the lightcurve shows two peaks, just before and after the pulsar eclipse.

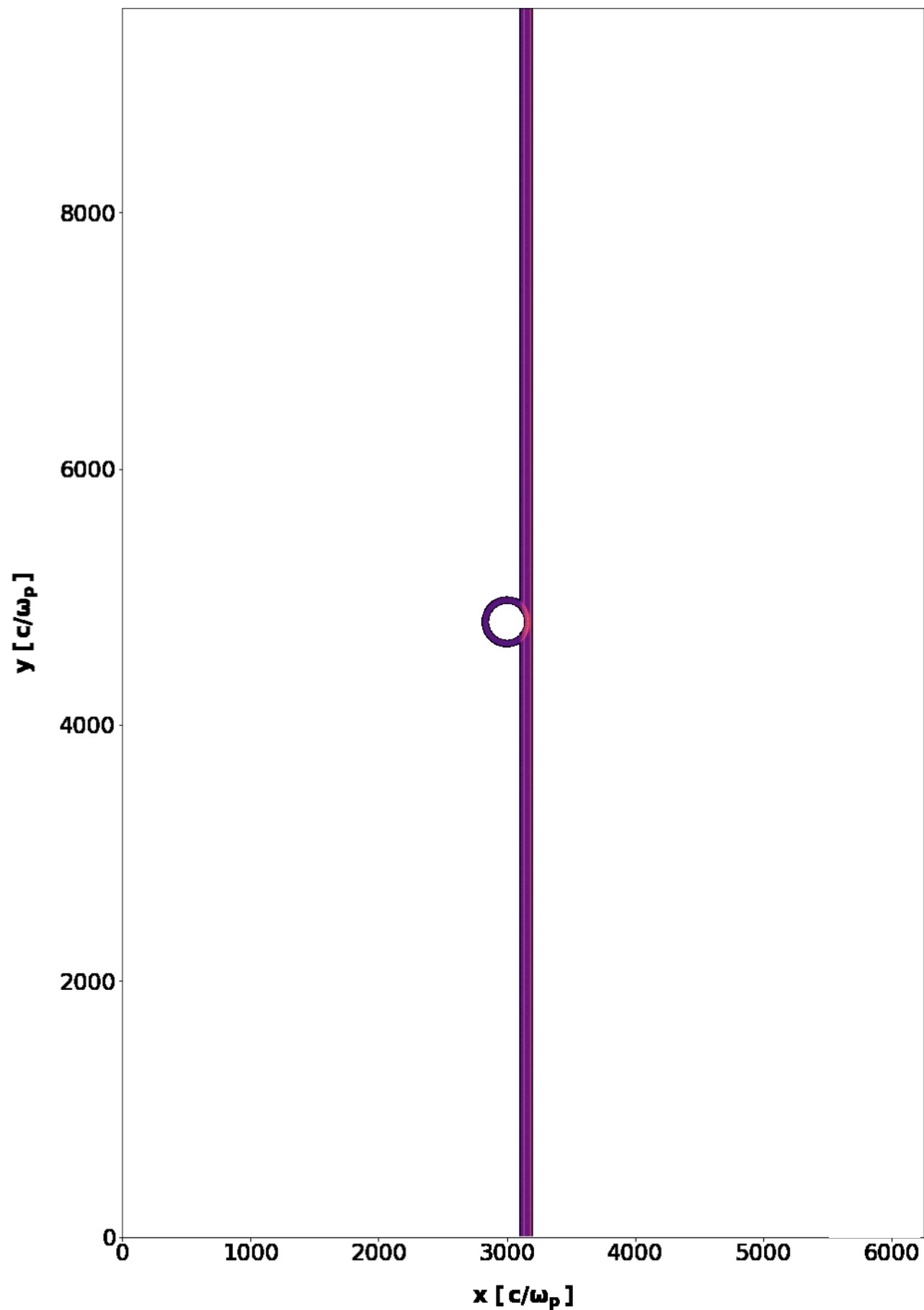


# Fermi acceleration

- For  $\alpha \sim 0$ , particles accelerated by shock-driven reconnection can be injected in the good old Fermi process at the termination shock.



# Fermi acceleration



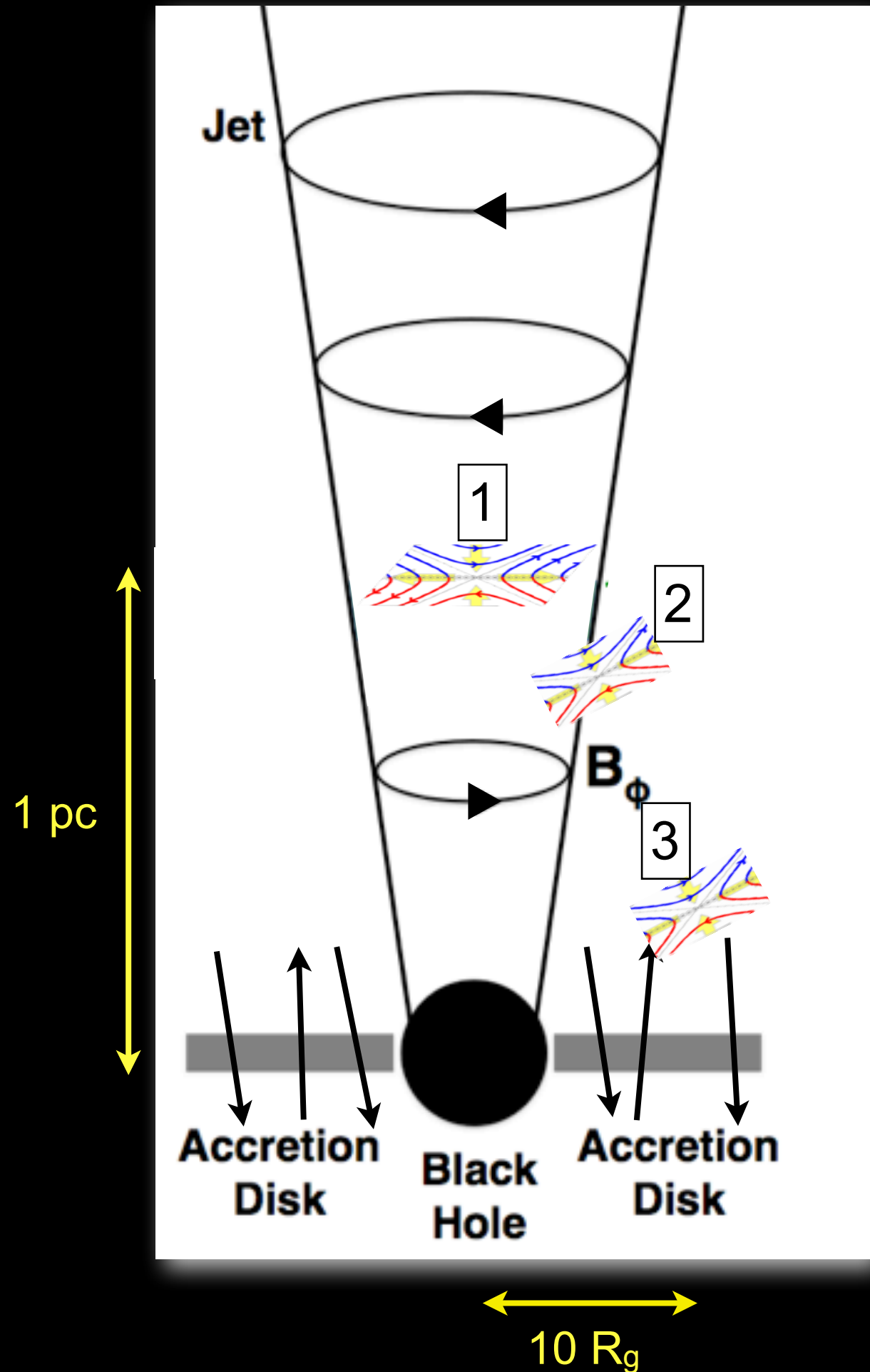
- For  $\alpha \sim 0$ , particles accelerated by shock-driven reconnection can be injected in the *Fermi process* at the termination shock.

# Overarching summary

## Relativistic reconnection can:

- efficiently dissipate magnetic energy (at rate  $\sim 0.1 c$ ).
- produce non-thermal particles with hard power-law slopes.
- **serve as injection process for subsequent (non-reconnection) acceleration:**  
**e.g., Fermi acceleration at shocks**, stochastic acceleration in turbulence, shear acceleration at jet boundaries.
- imprint strong pitch-angle anisotropy.
- produce trans-relativistic bulk motions.

# Reconnection-powered emission in jets and black hole coronae



### (1) Blazars and AGN jets.

- Can reconnection explain the multi-wavelength and multi-timescale blazar emission?

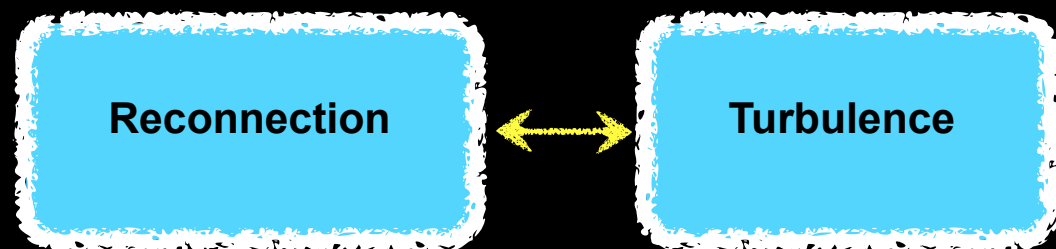
### (2) Boundary layers of relativistic jets.

- Can reconnection explain the limb-brightened appearance of AGN jets?

### (3) Magnetized coronae of highly accreting BHs in X-ray binaries.

- Can radiative reconnection explain the hard-state X-ray emission?

# 1. Relativistic reconnection in blazar jets



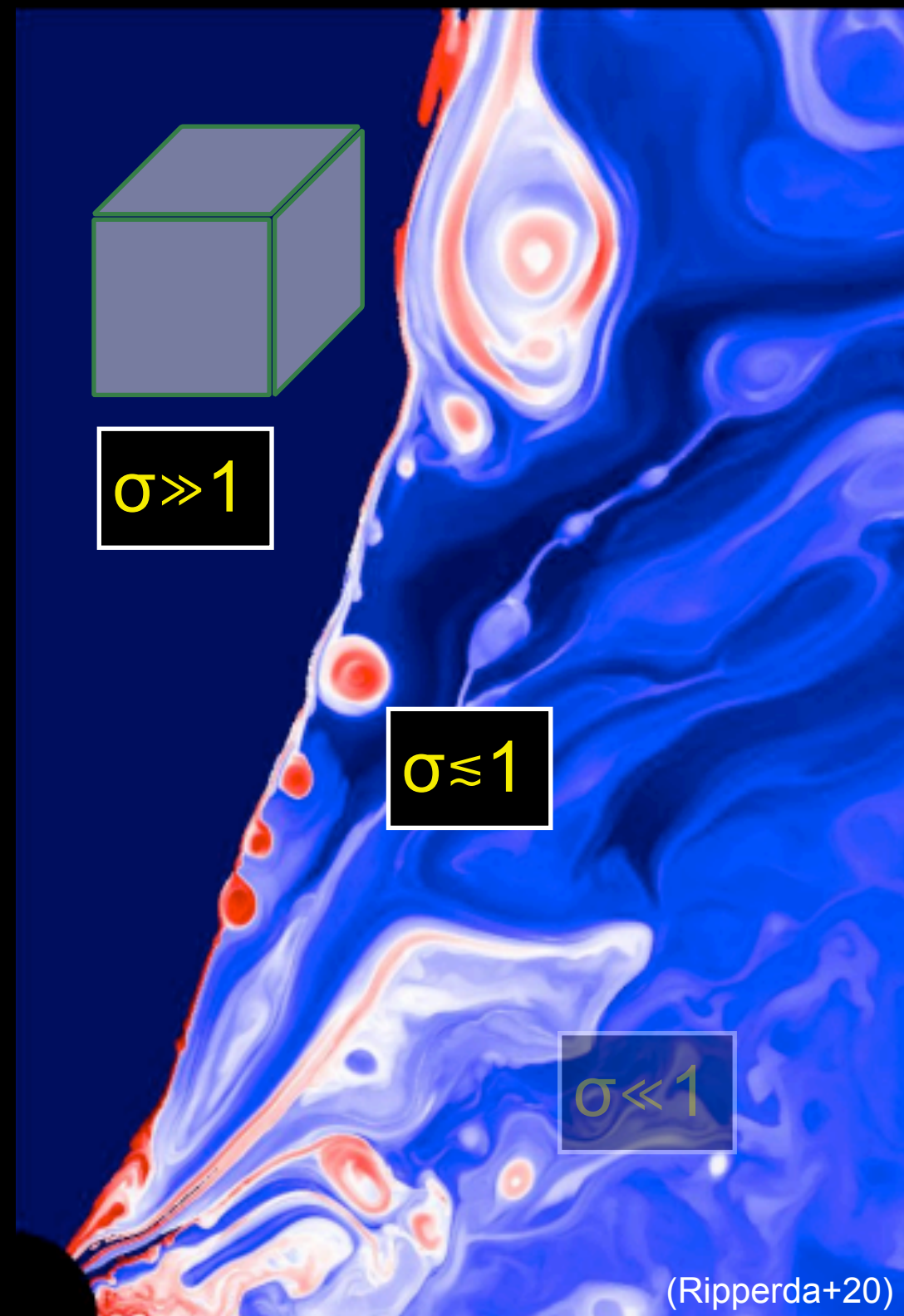
with L. Comisso, E. Sobacchi and J. Nättilä



Comisso & LS 2018, PRL, 121, 255101

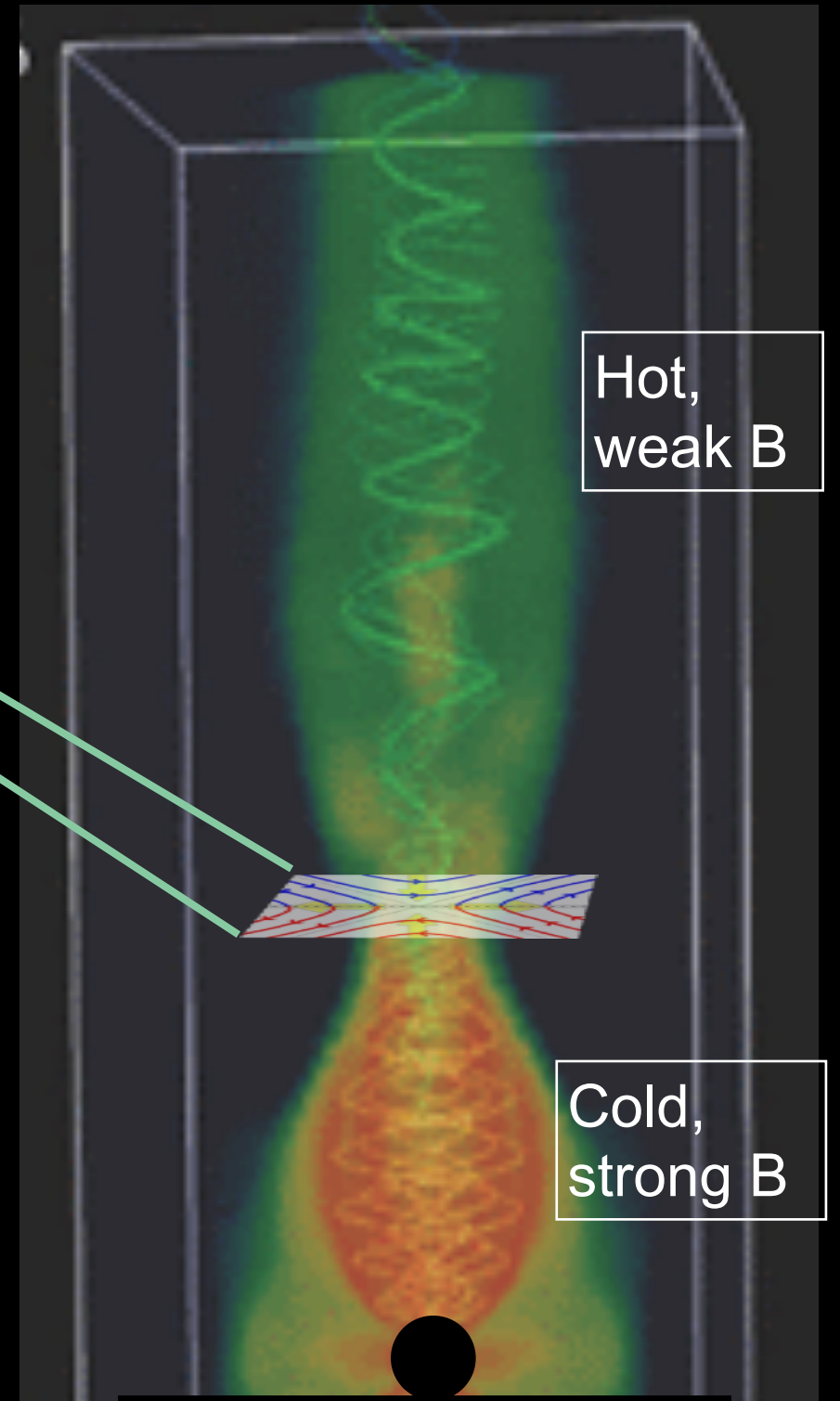
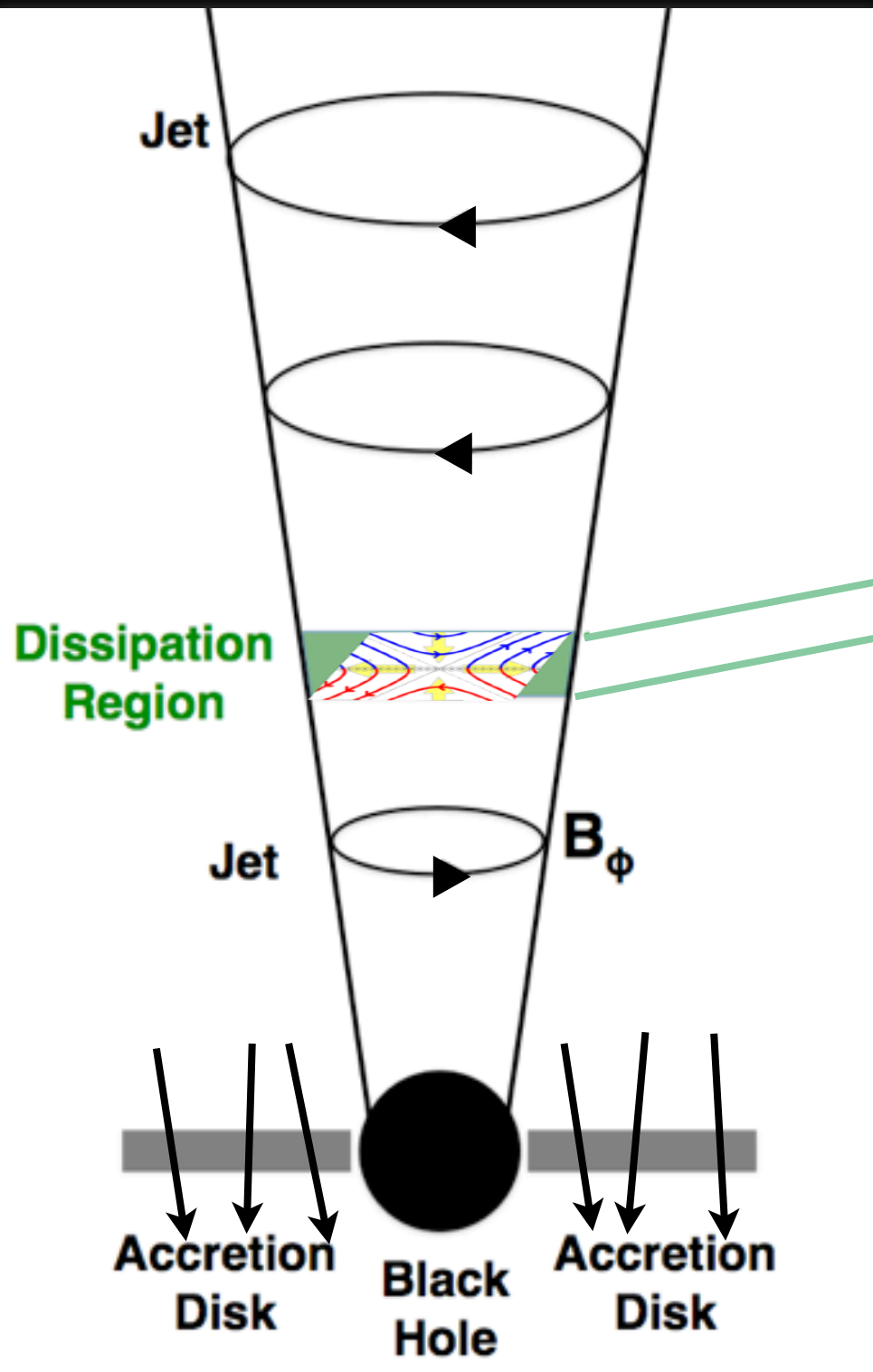
Comisso & LS 2019, ApJ, 886, 122

Sobacchi, Nattila & LS 2021, MNRAS,  
503, 688



# Why does reconnection occur?

M87



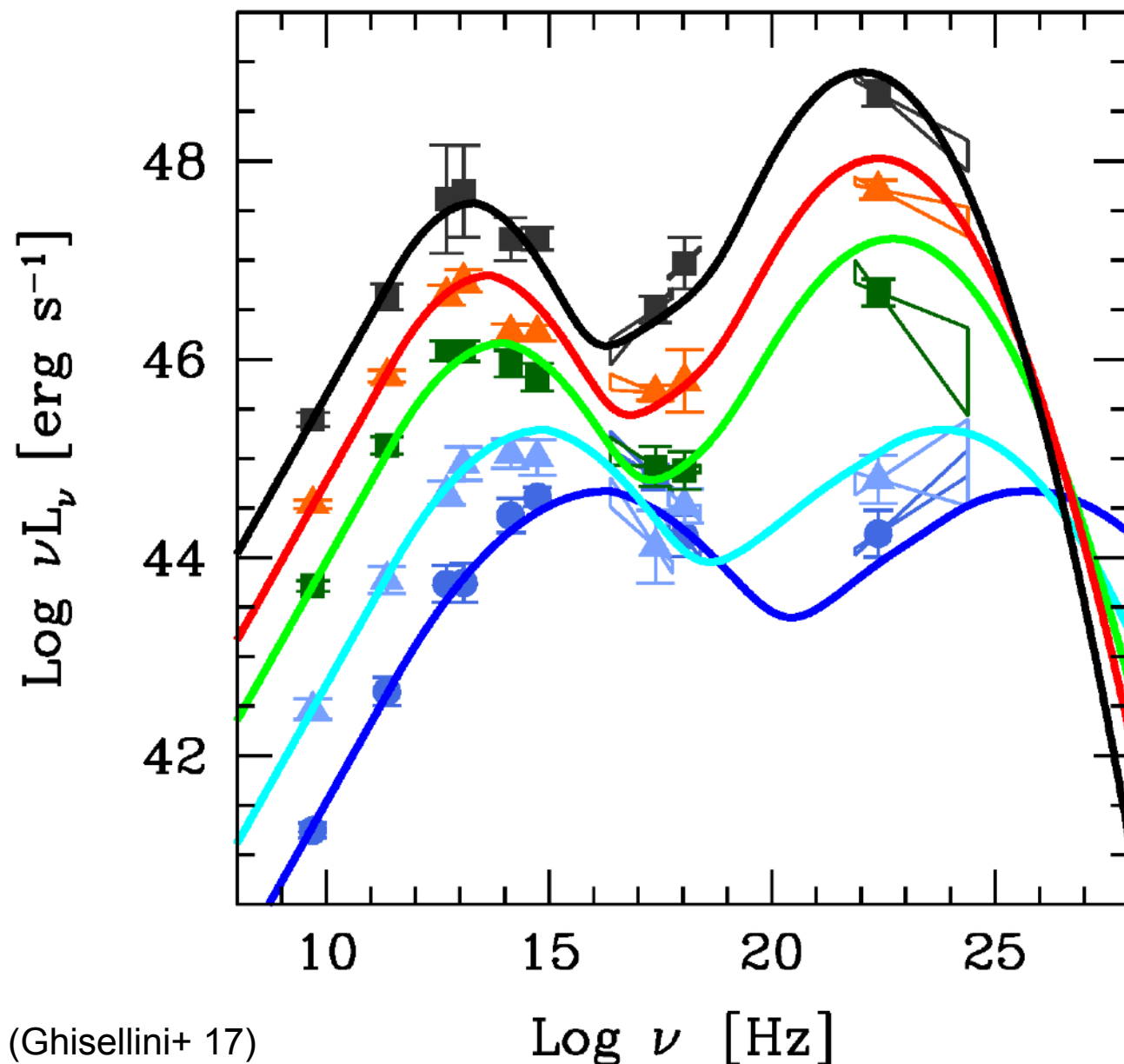
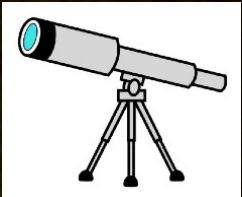
(Bromberg & Tchekhovskoy 15)

# Blazar jets

Blazars: jets from Active Galactic Nuclei pointing along our line of sight

$10^8 M_{\odot}$  BH

relativistic jet



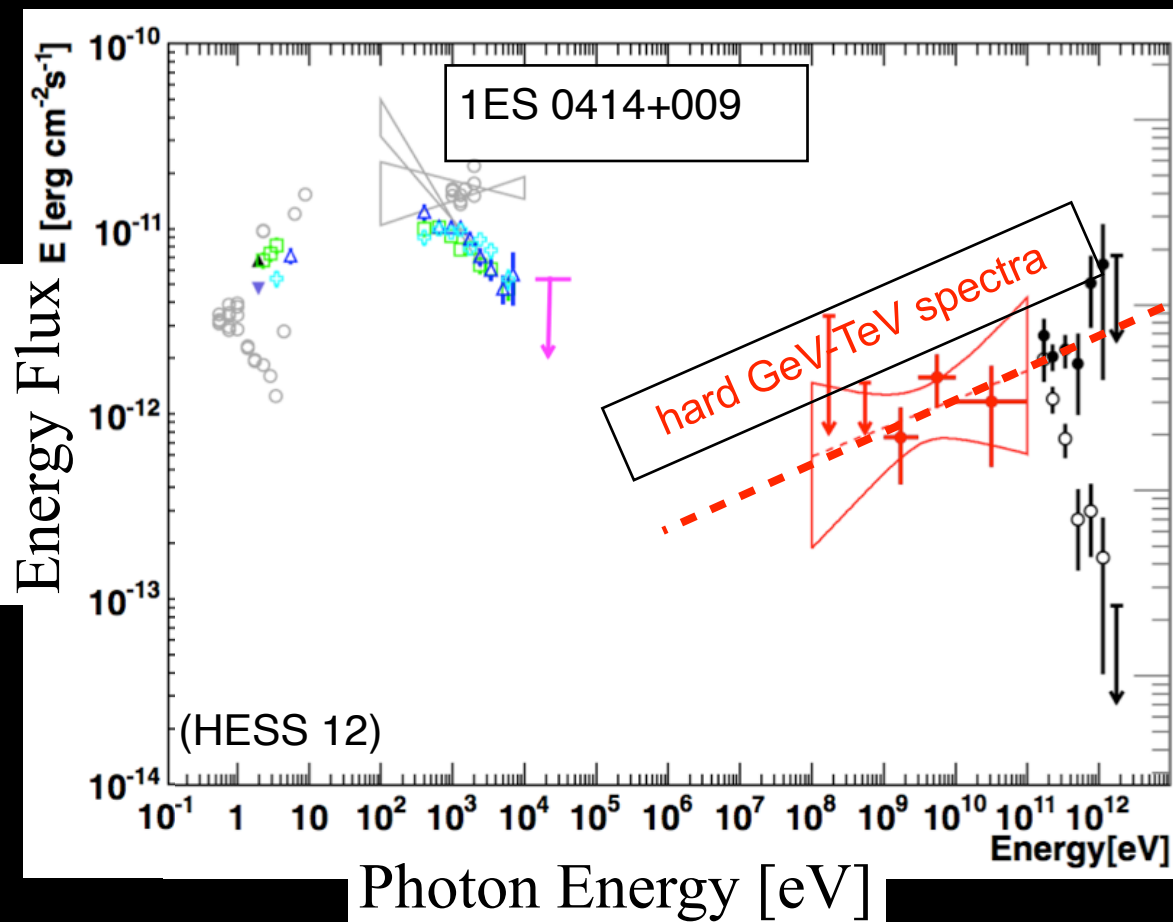
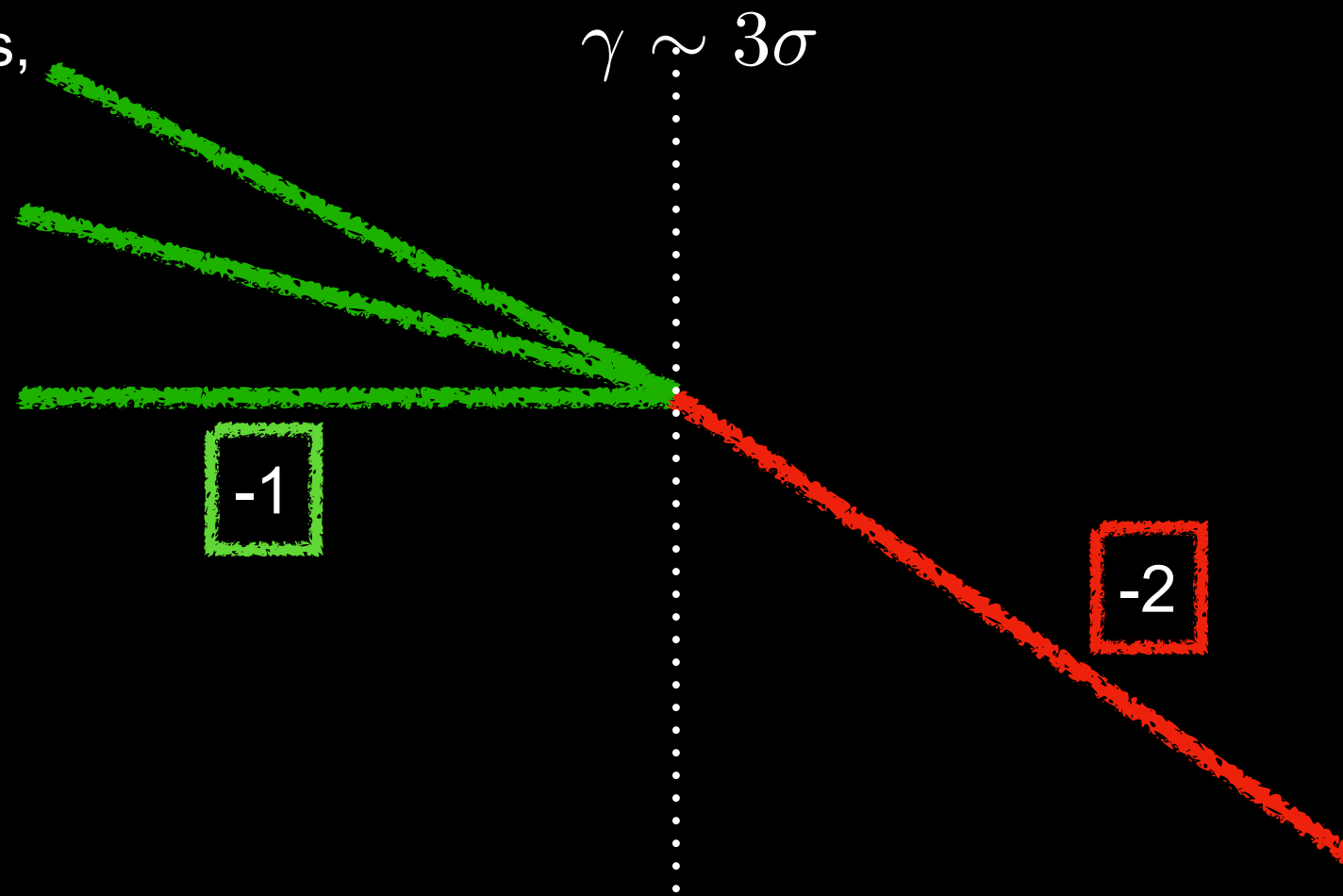
- broadband spectrum, from radio to  $\gamma$ -rays (and even TeV energies)
- low-energy synchrotron + high-energy inverse Compton (IC)
- high degree of radio and optical polarization

# Blazar emission

(A) power-law spectra of the emitting particles, often with hard slope

$$\frac{dn}{d\gamma} \propto \gamma^{-p}$$

$$p \lesssim 2$$

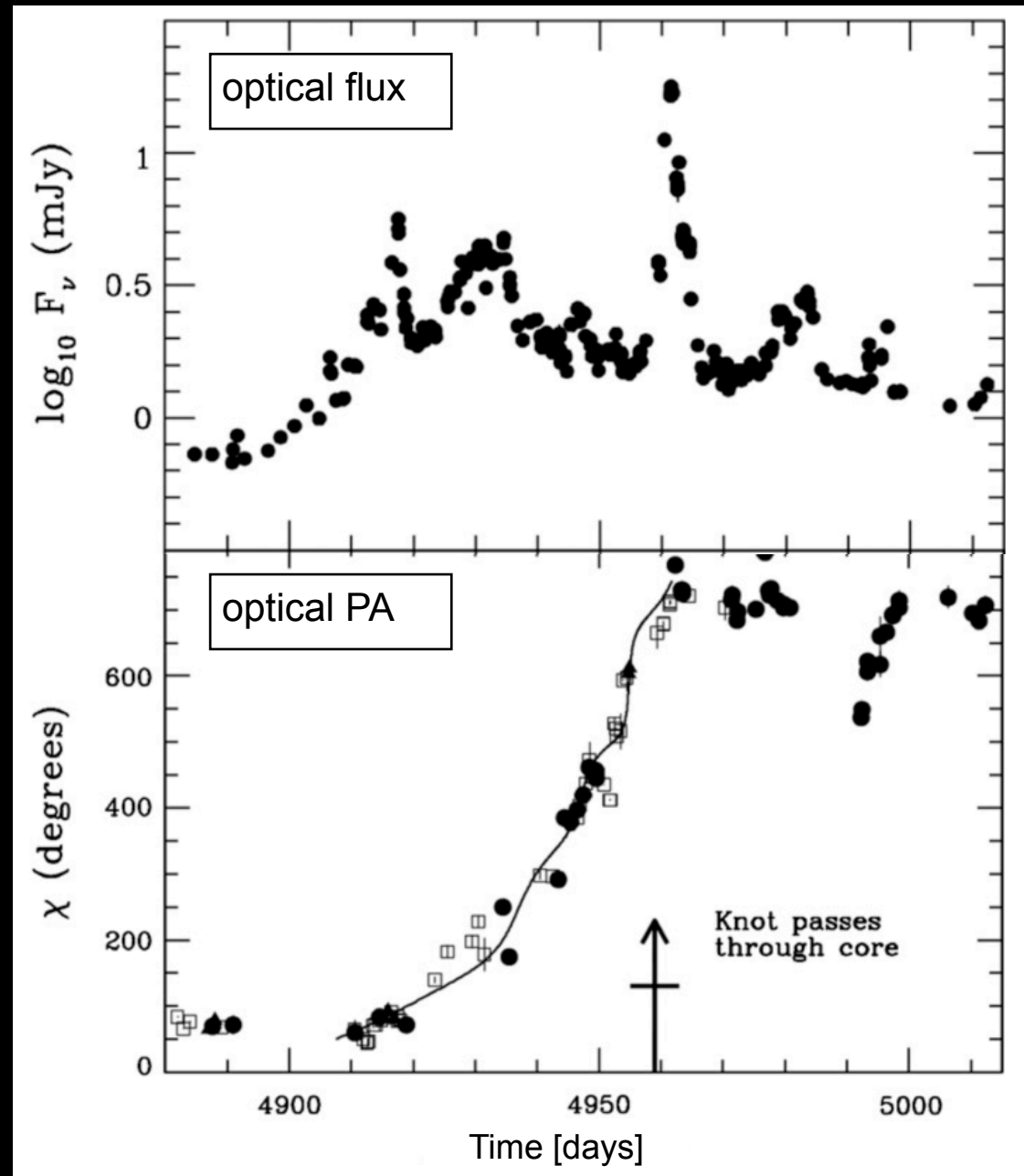


At  $\gamma \lesssim 3\sigma$  injection in reconnection leads to  $\sigma$ -dependent slopes, as hard as  $p=1$ .

At  $\gamma \gtrsim 3\sigma$  3D reconnection leads to a  $\sigma$ -independent slope of  $p=2$ .

# Blazar emission

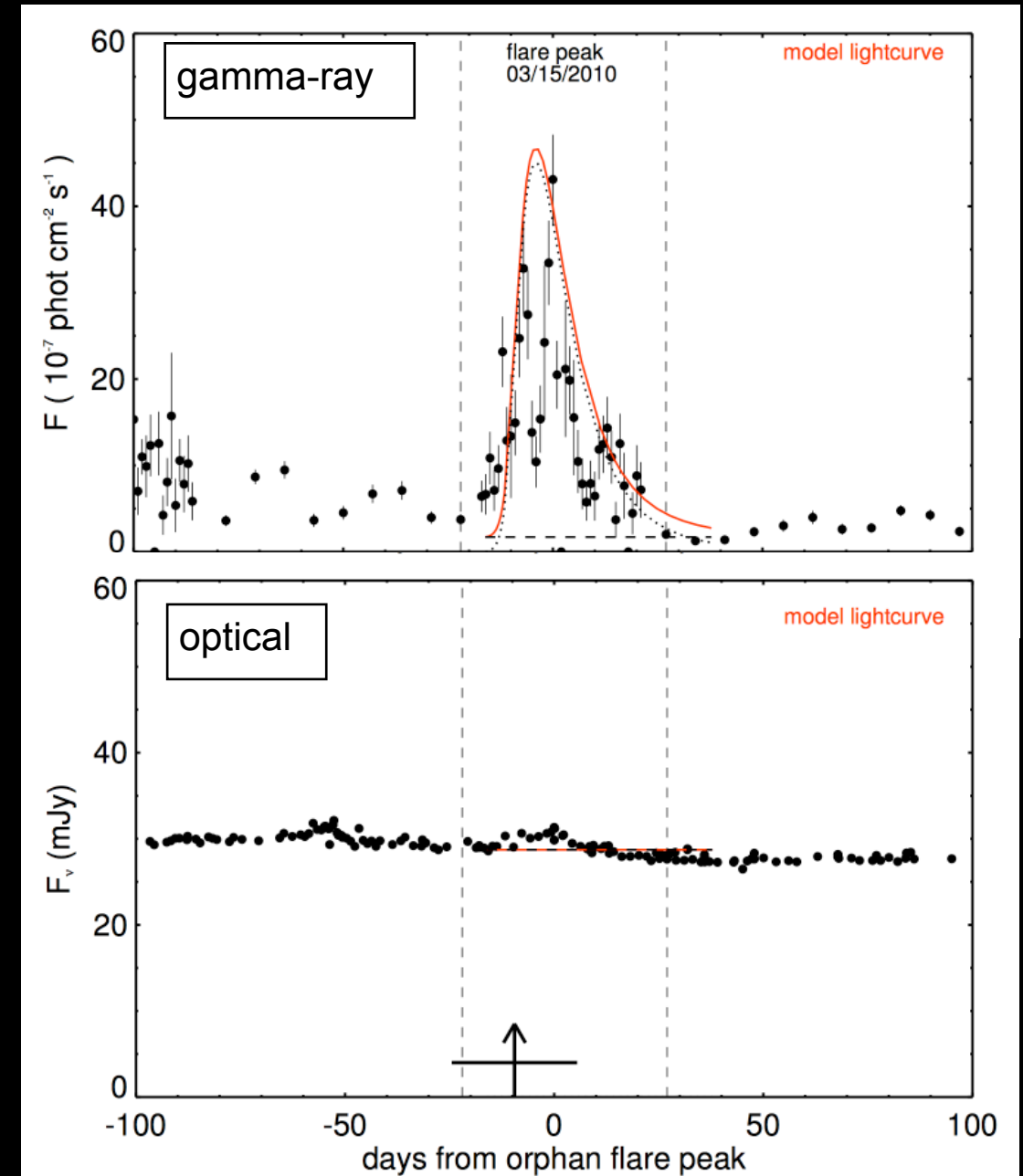
(B) optical polarization rotations



(Marscher+2010)

Large-angle polarization rotations during optical day-long flares.

(C) “orphan” gamma-ray flares



(MacDonald+2017)

Gamma-ray flares with no optical counterpart.

# (C) “orphan” gamma-ray flares

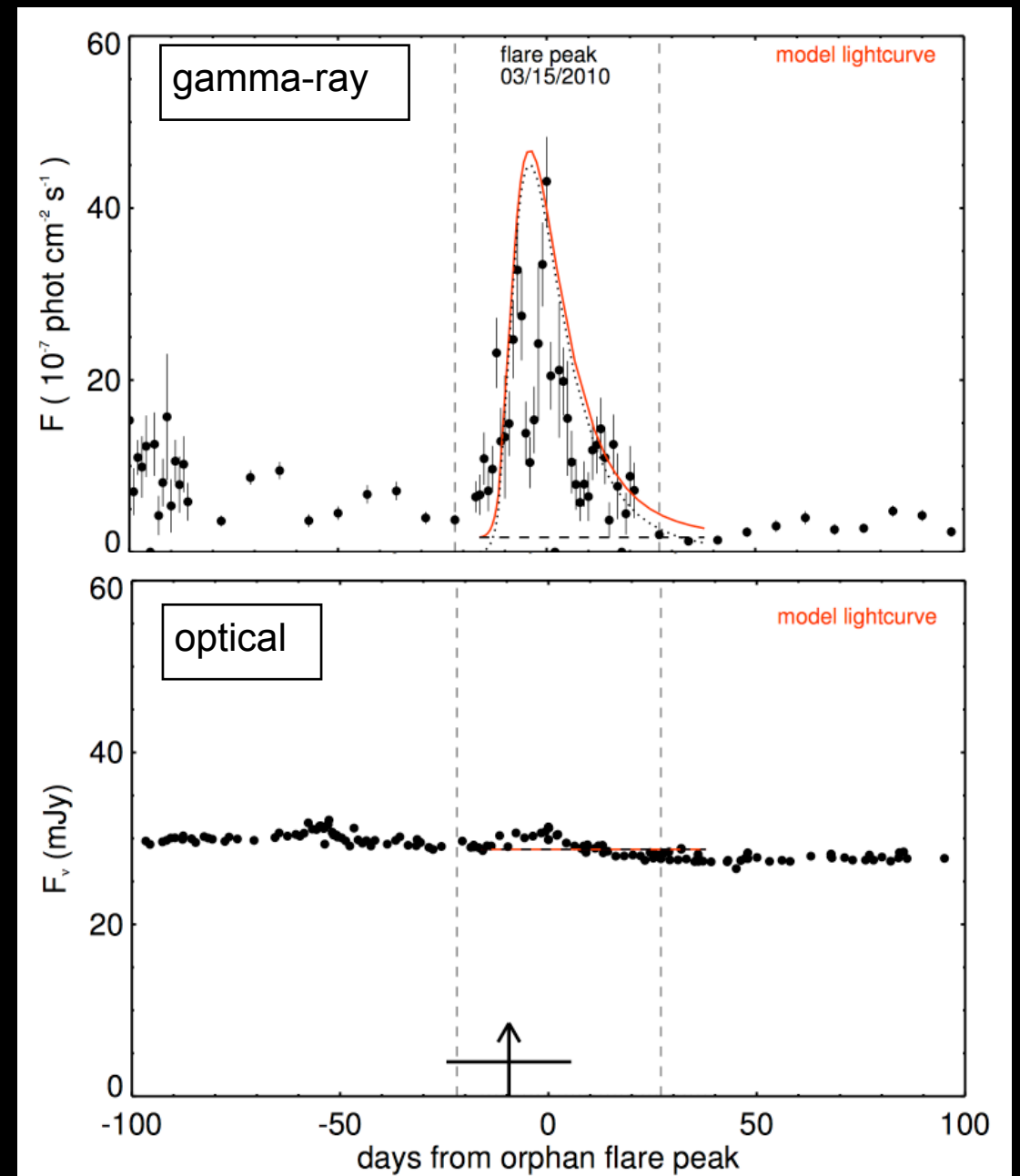
with L. Comisso, E. Sobacchi and J. Nättilä



Comisso & LS 2018, PRL, 121, 255101

Comisso & LS 2019, ApJ, 886, 122

Sobacchi, Nattila & LS 2021, MNRAS,  
503, 688

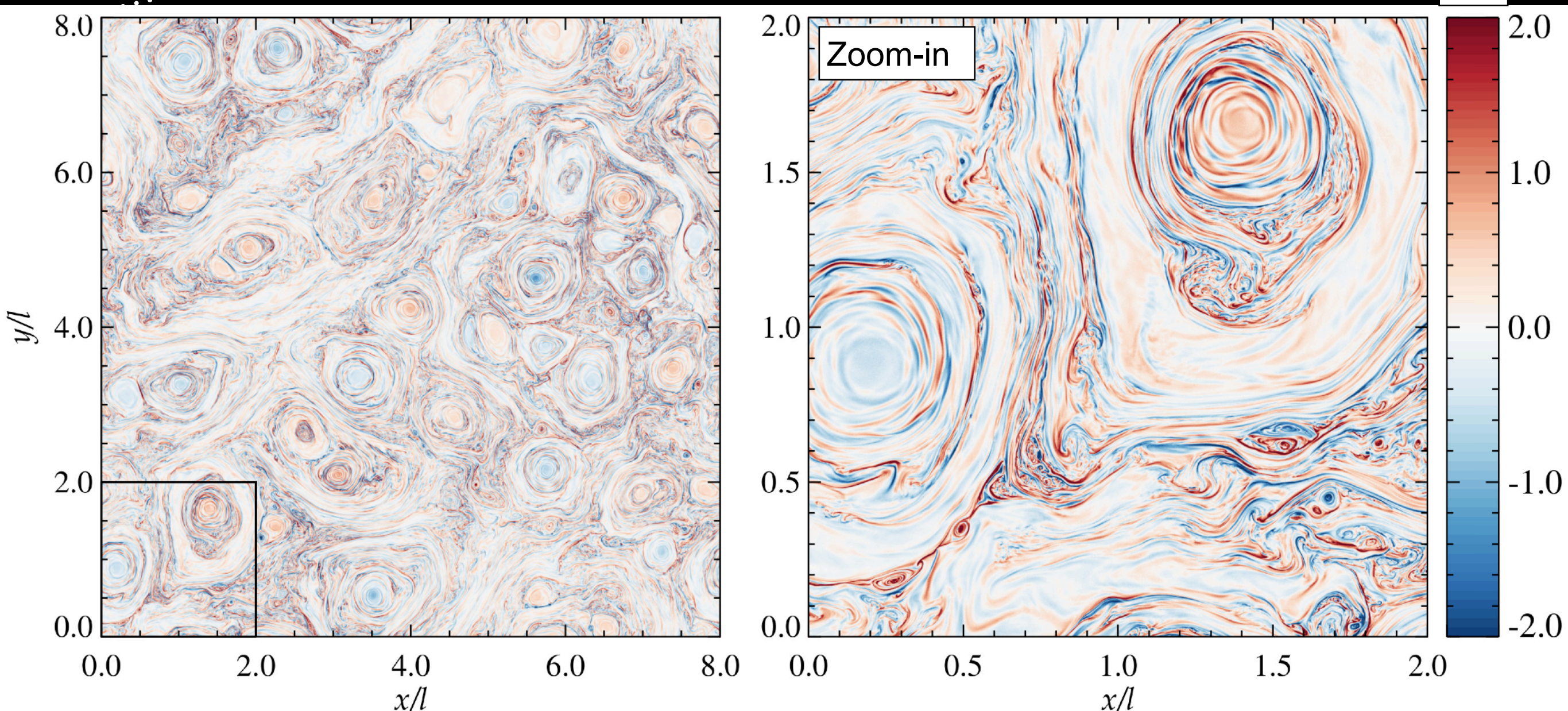


(MacDonald+2017)

Gamma-ray flares with no optical counterpart.

# Reconnection within turbulence

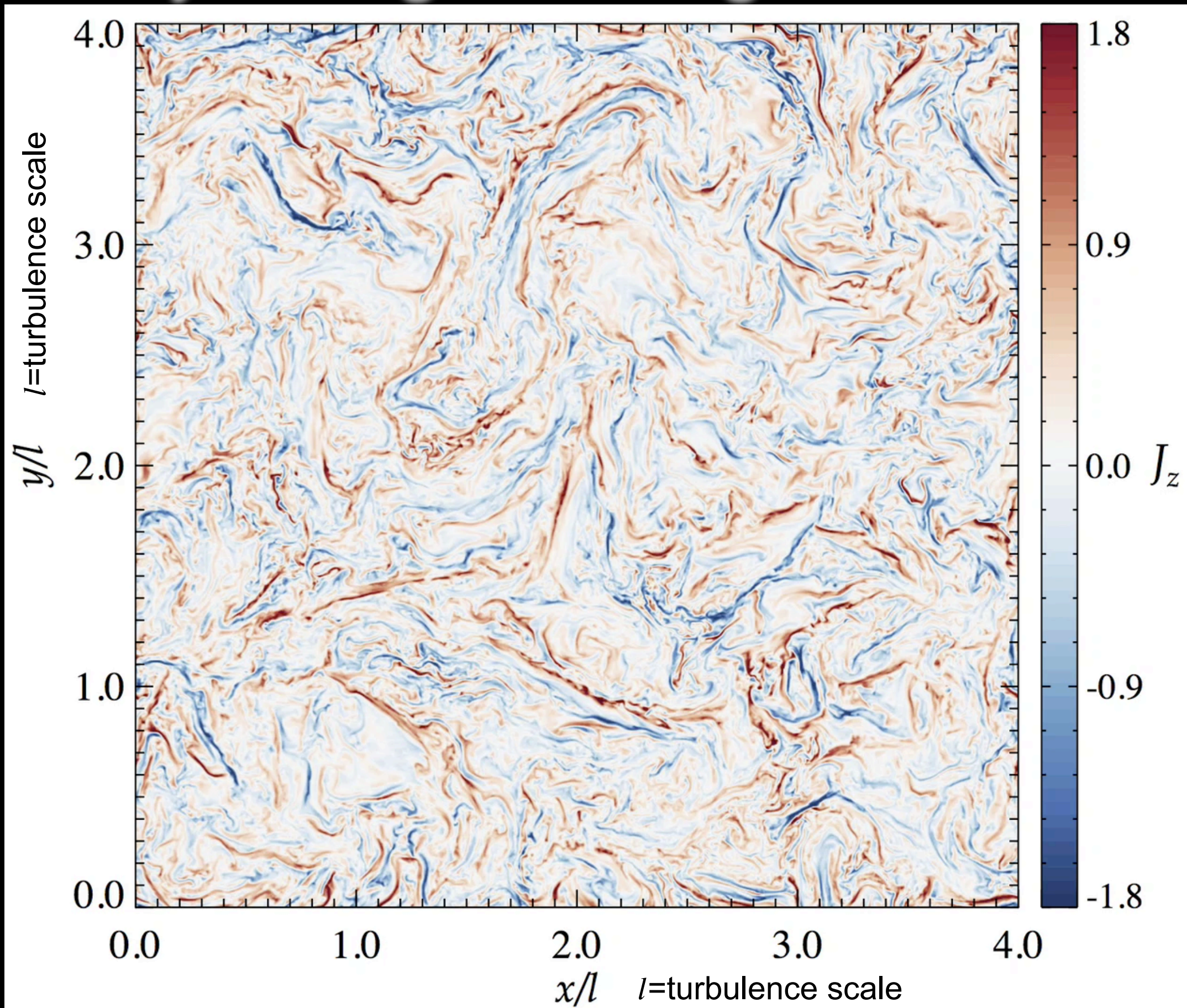
Reconnection is a natural by-product of magnetically-dominated turbulence



$l$ =turbulence outer scale

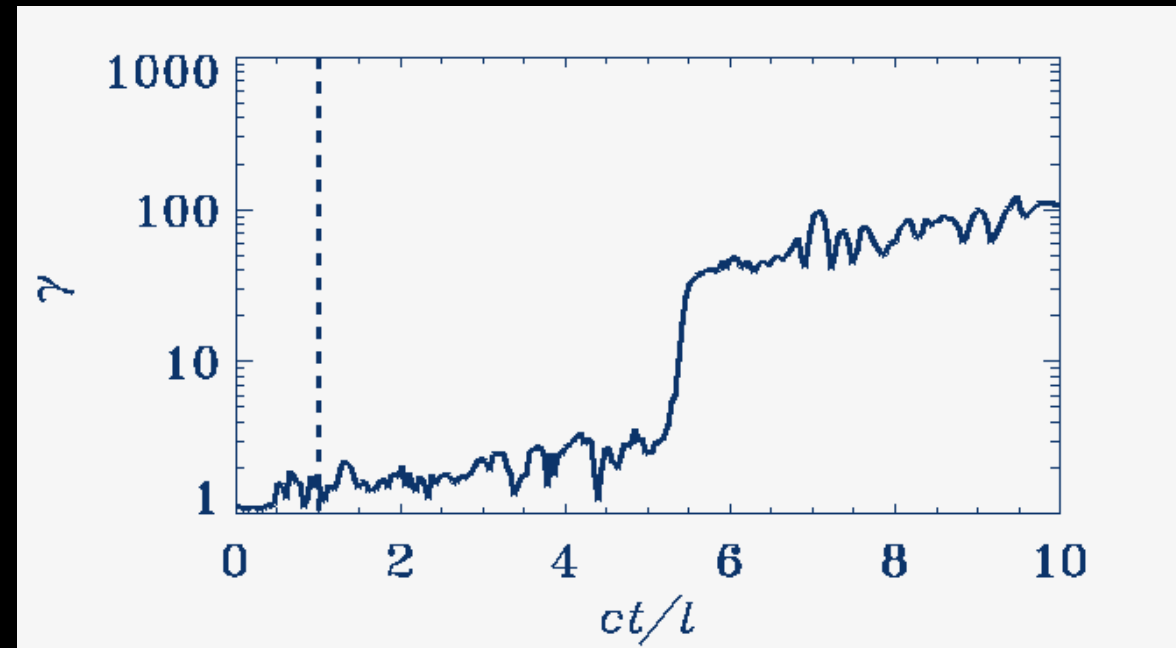
(Comisso & LS 18,19)

# Fly-through $J_z$ along $z$ direction

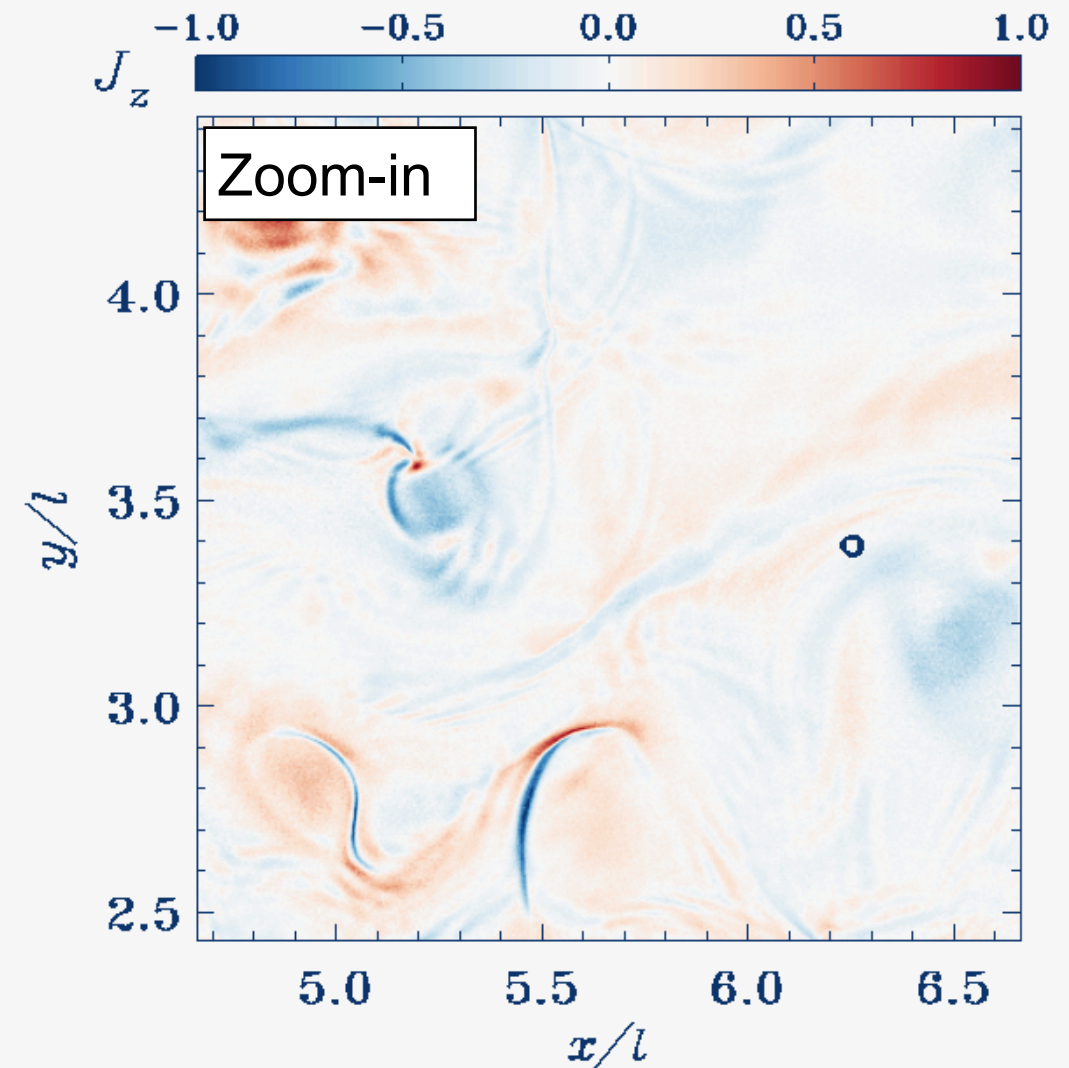
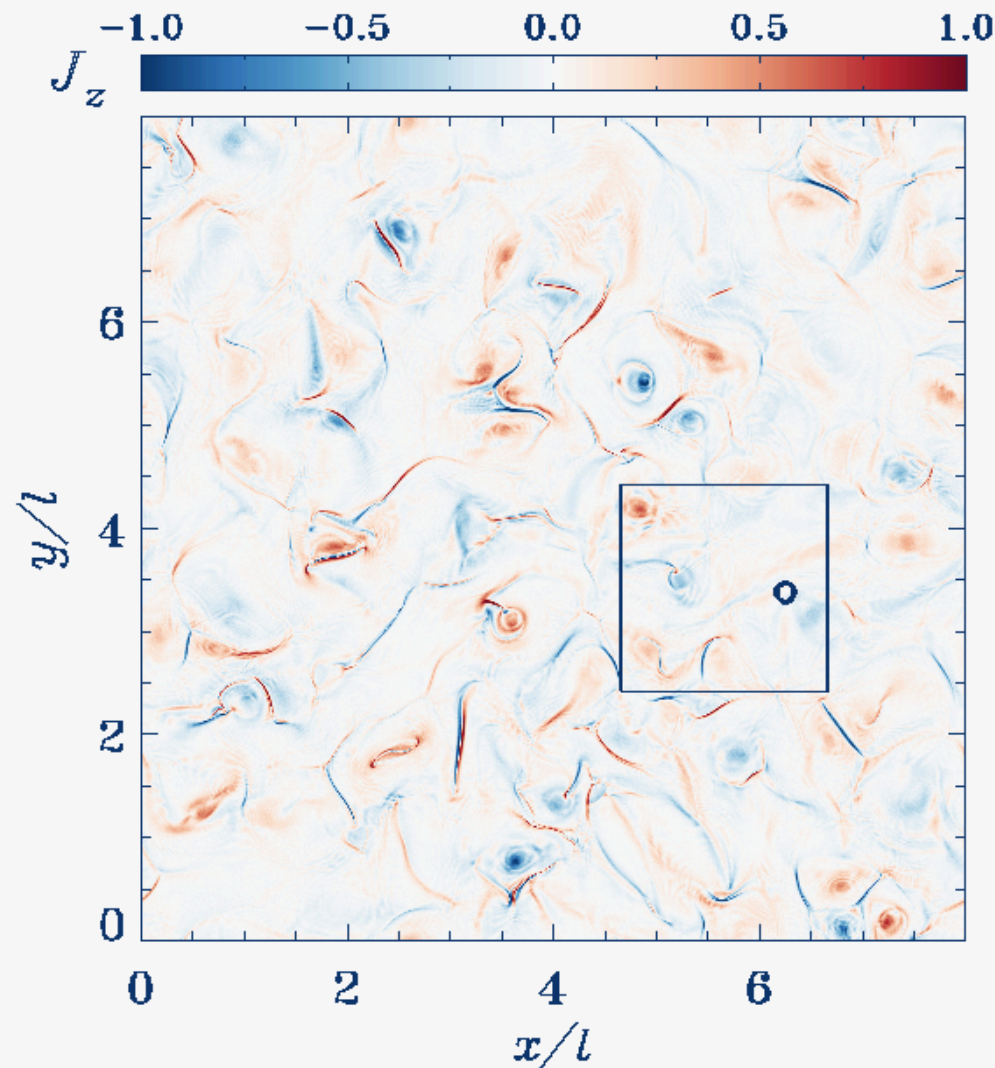


# A representative high-energy particle

Two stages of acceleration

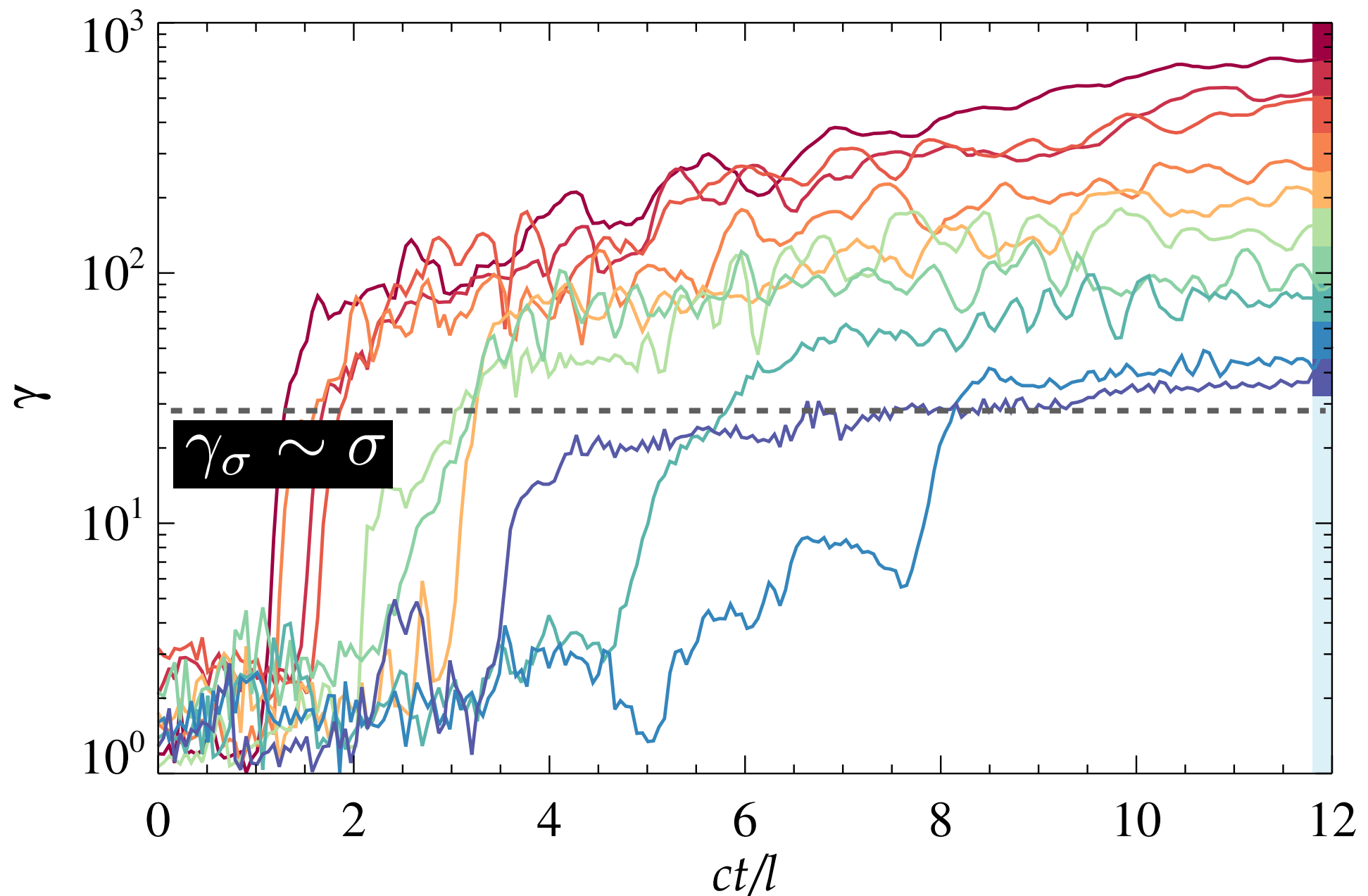


2D  
no cooling



# Particle acceleration: a two-stage process

3D  
no cooling

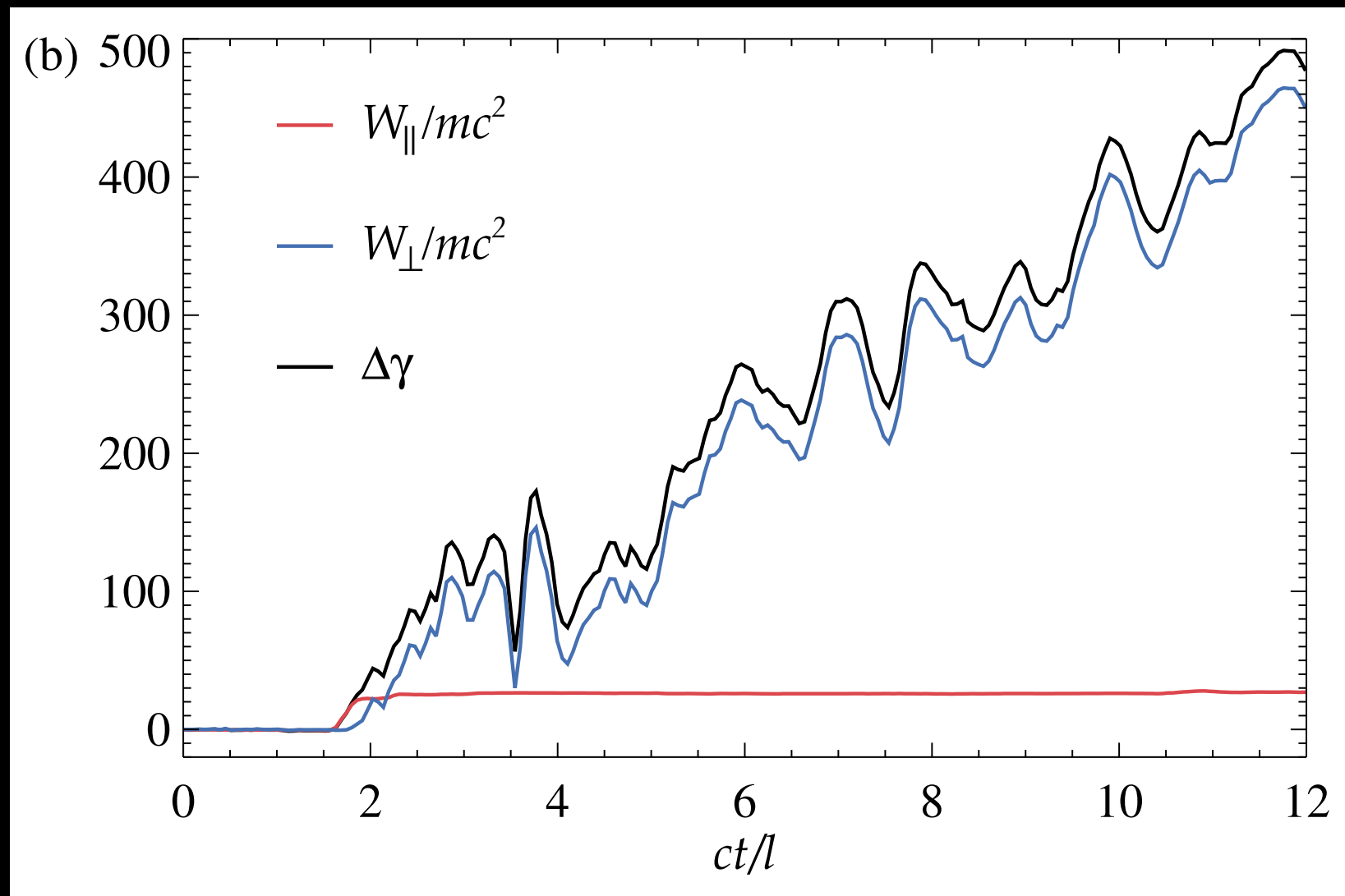


(Comisso & LS 19)

- Particle injection occurs quickly ( $t_{\text{inj}} \sim 10/\omega_d$ ), at reconnection layers.
- This is followed by further acceleration (but slower,  $t_{\text{scatt}} \sim l/c$ ) by scattering off the turbulent fluctuations.

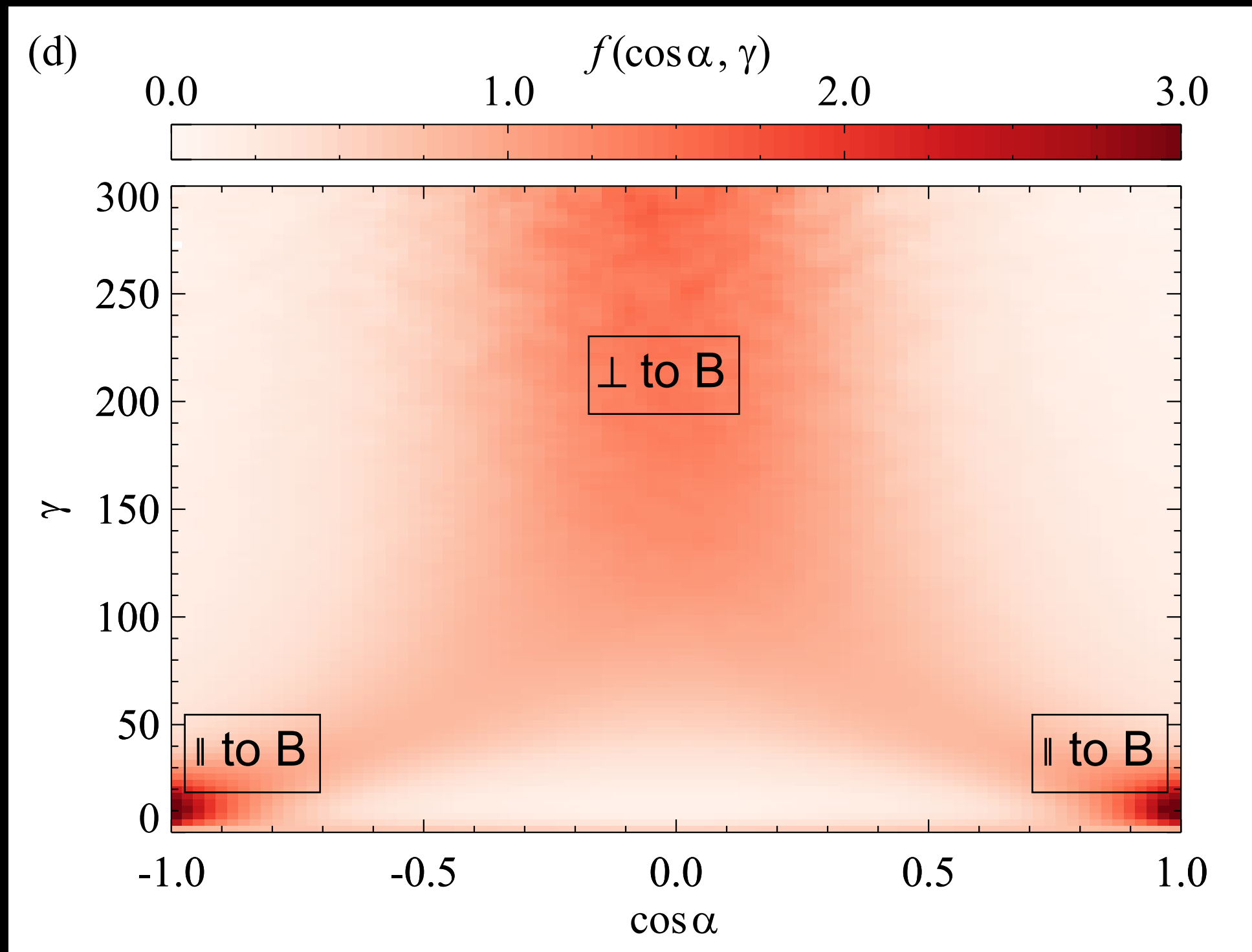
# The two stages of acceleration

Work by parallel and perp E field:  $W_{\parallel,\perp}(t) = q \int_0^t \mathbf{E}_{\parallel,\perp}(t') \cdot \mathbf{v}(t') dt'$



- Injection by  $\mathbf{E}_{\parallel}$  in reconnection layers.
- Then, acceleration by  $\mathbf{E}_{\perp}$  via scattering off turbulent fluctuations.

# Particle anisotropy



$$\cos \alpha = \frac{\mathbf{v} \cdot \mathbf{B}}{|\mathbf{v}| |\mathbf{B}|}$$

(Comisso & LS 19)

- Lower energy particles (near injection) are mostly aligned with B field.
- Higher energy particles lie mostly in a plane perp to B.

# IC cooling in blazar jets

We parameterize IC cooling losses via a critical Lorentz factor  $\gamma_{\text{cr}}$  (balancing acceleration with IC losses):

$$eE_{\text{rec}} = \frac{4}{3}\sigma_{\text{T}}\gamma_{\text{cr}}^2 U_{\text{rad}}$$

$$E_{\text{rec}} = \eta_{\text{rec}} B_0 \quad (\eta_{\text{rec}} \sim 0.1)$$

## In blazar jets

1.  $\gamma_{\sigma} \sim \sigma \sim 10^2 - 10^3$
2.  $\gamma_{\text{cr}} \gg \gamma_{\sigma}$
3.  $\gamma_{\text{cool}} \sim 0.01 - 0.1\gamma_{\sigma}$

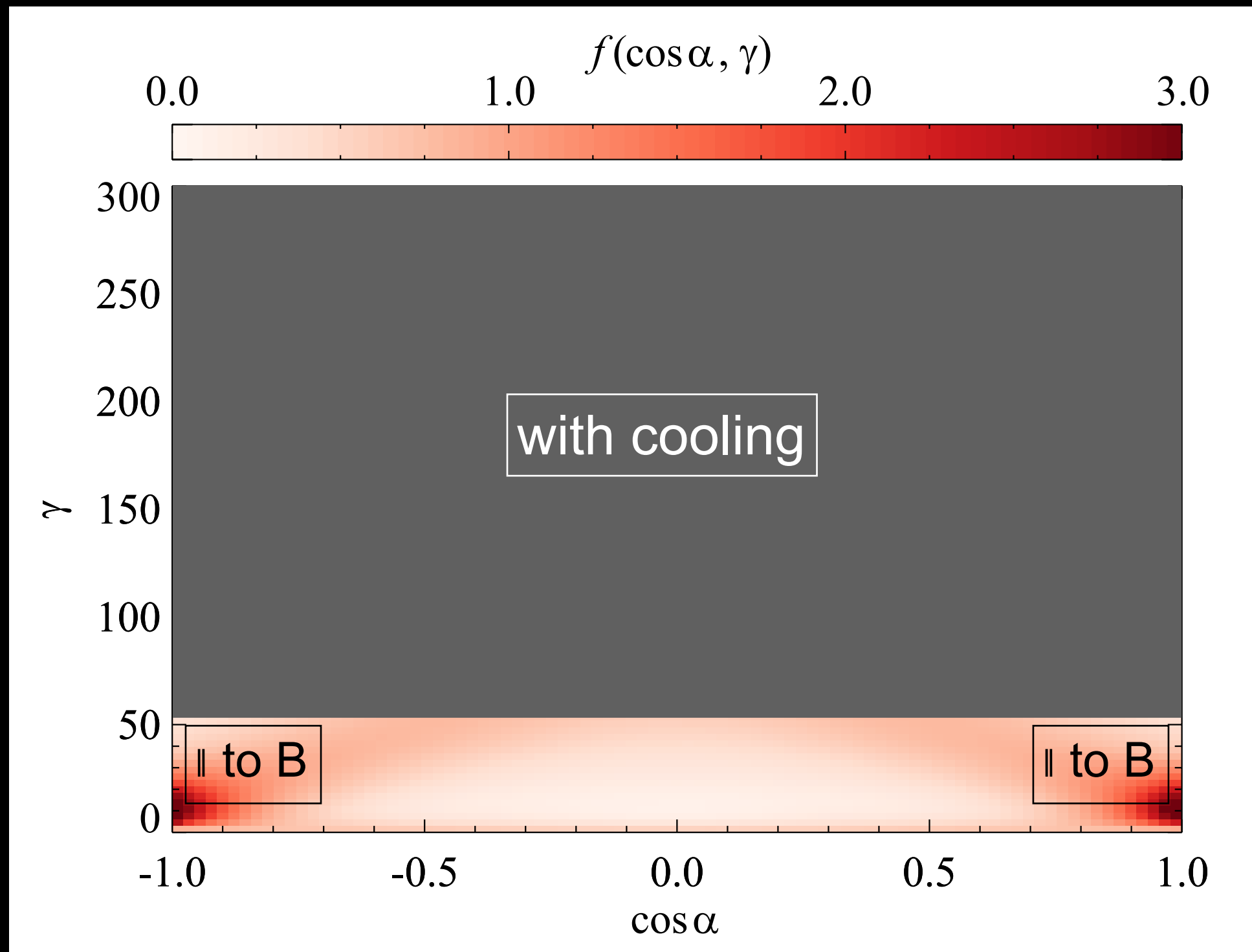
## In our simulations

1.  $\gamma_{\sigma} \sim \sigma = 160$
2.  $\gamma_{\text{cr}} \gtrsim \gamma_{\sigma}$
3.  $\gamma_{\text{cool}} \sim 0.01\gamma_{\sigma}$

→ injection up to  $\gamma_{\sigma}$  is unaffected by cooling since  $t_{\text{inj}} \ll t_{\text{cool}}$

→ acceleration to  $\gg \gamma_{\sigma}$  is prohibited by cooling since  $t_{\text{scatt}} \gg t_{\text{cool}}$

# Particle anisotropy

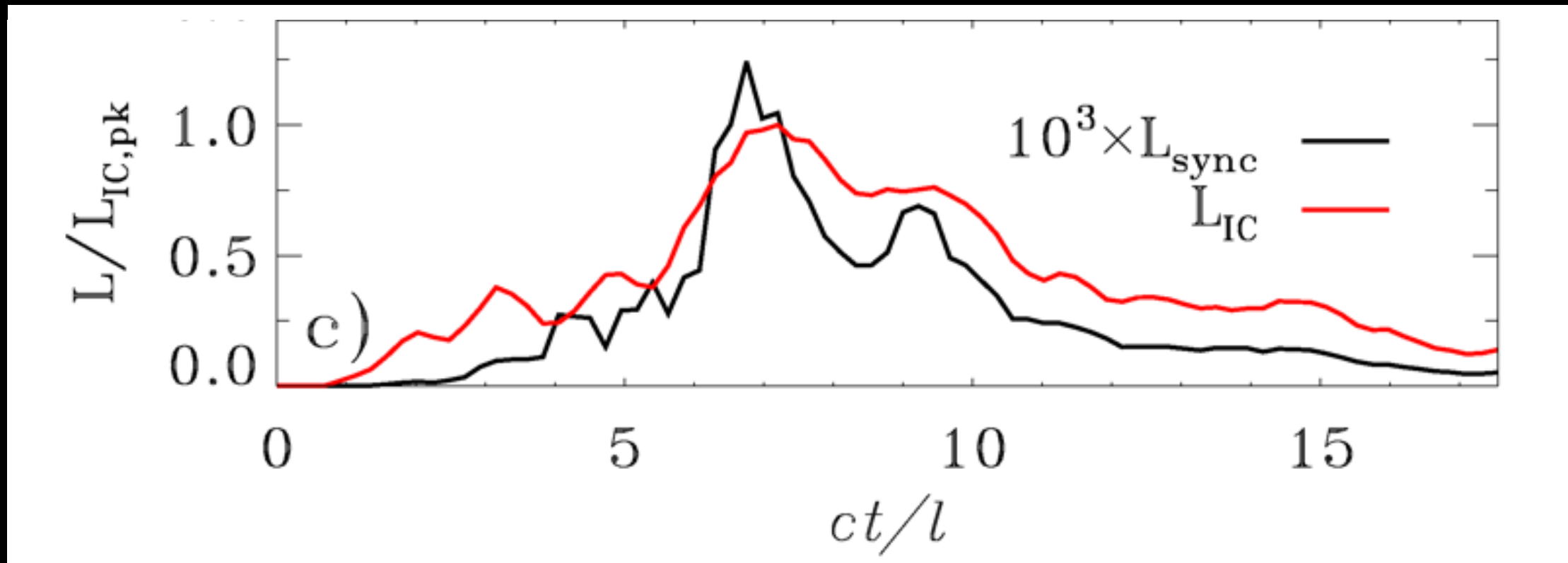


(Comisso & LS 19)

- Lower energy particles (near injection) are mostly aligned with B field.
- Higher energy particles lie mostly in a plane perp to B.

# Synchrotron and IC emission

- Small pitch angles suppress the synchrotron emission,  $P_{\text{sync}} \propto \sin^2 \alpha$



(Sobacchi + 21)

- Even though  $U_B/U_{\text{rad}} \sim 1$ , we find that  $L_{\text{sync}}/L_{\text{IC}} \sim 10^{-3}$ .  
→ a first-principles explanation for orphan gamma-ray flares!

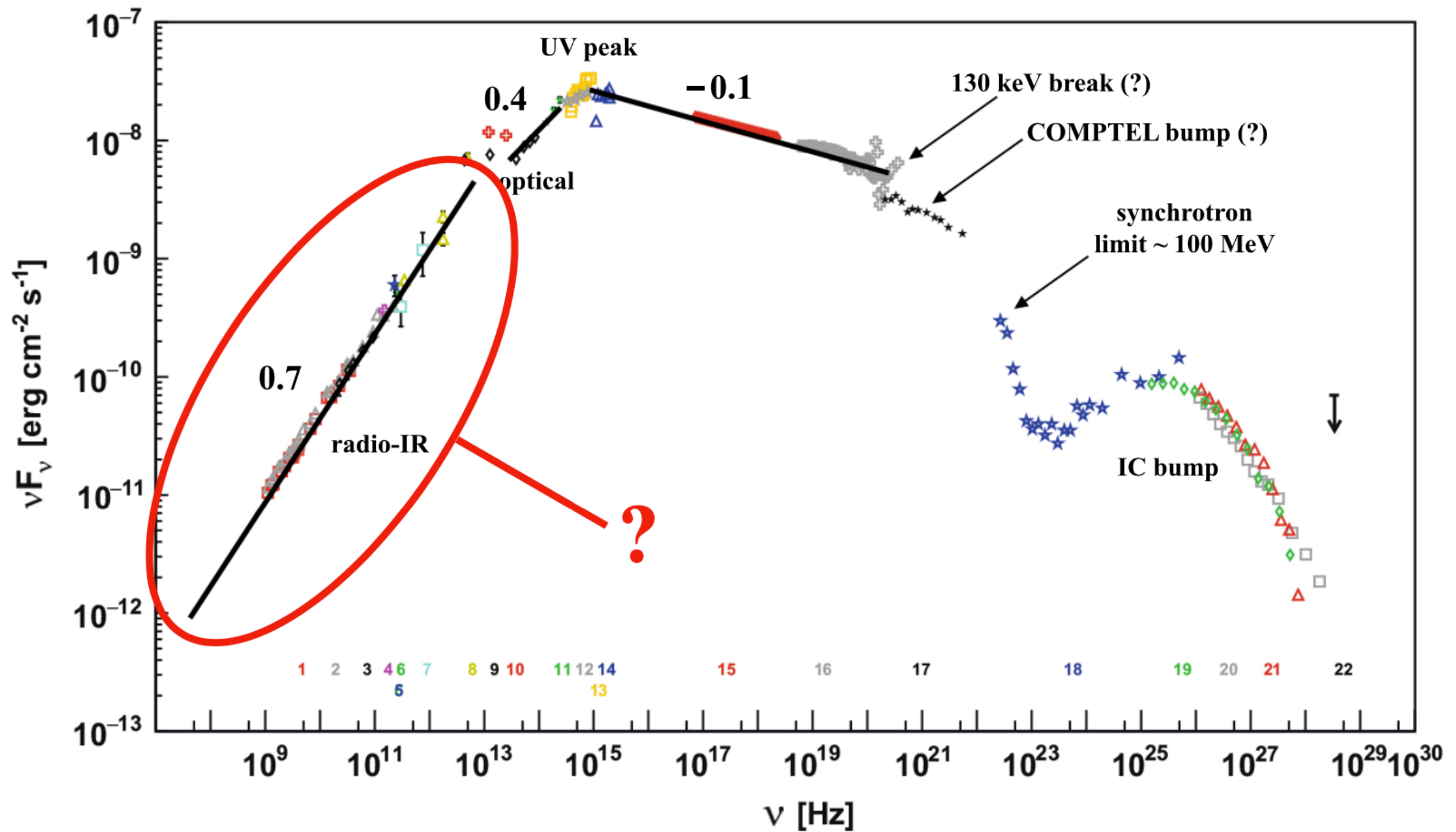
# Overarching summary

## Relativistic reconnection can:

- efficiently dissipate magnetic energy (at rate  $\sim 0.1 c$ ).
- produce non-thermal particles with hard power-law slopes.
- **serve as injection process for subsequent (non-reconnection) acceleration:**  
e.g., Fermi acceleration at shocks, **stochastic acceleration in turbulence**,  
shear acceleration at jet boundaries.
- **imprint strong pitch-angle anisotropy.**
- produce trans-relativistic bulk motions.

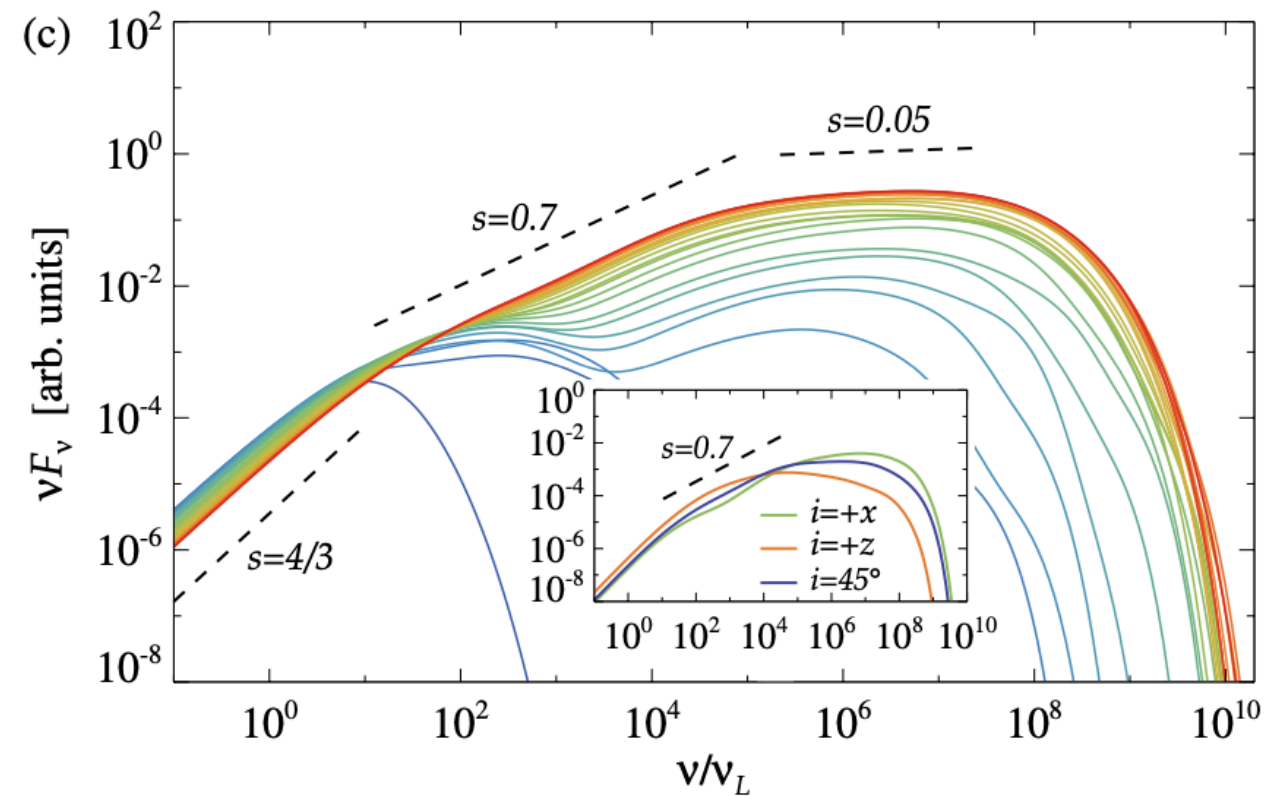
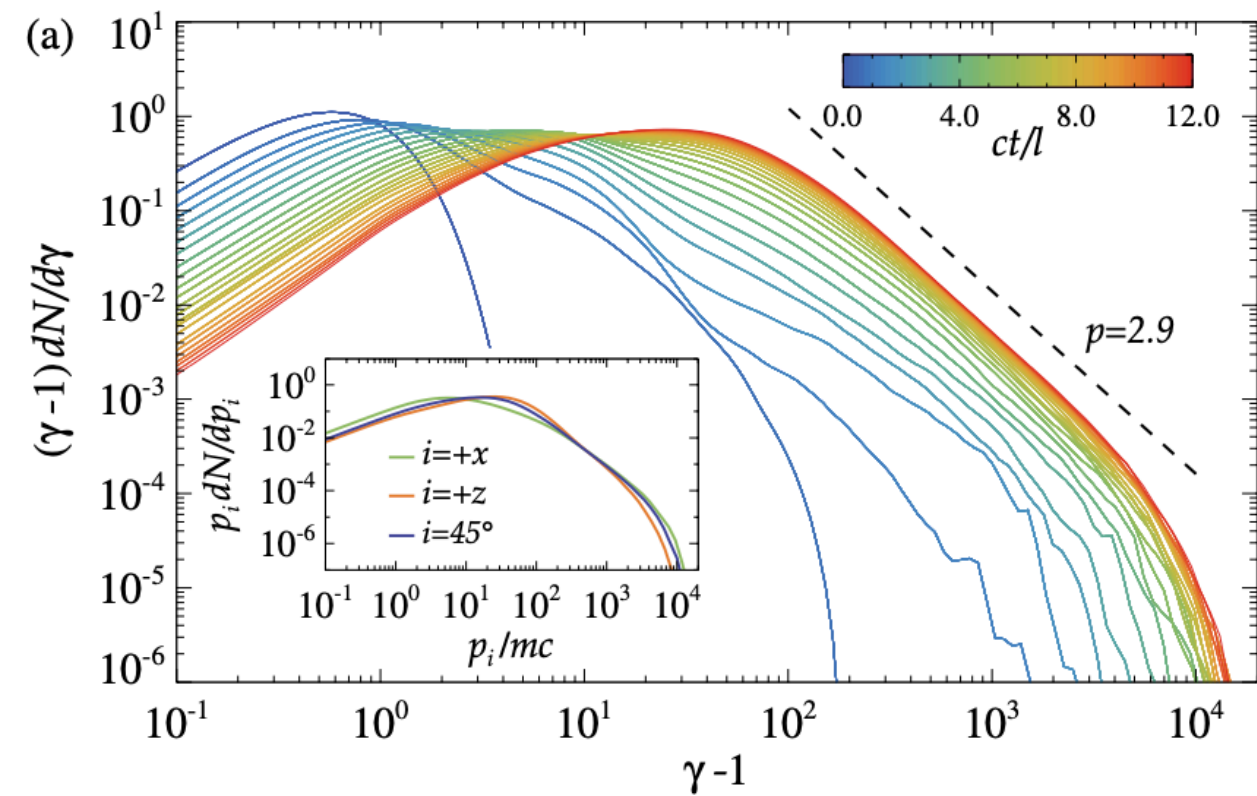
- A system with high-sigma reconnection has field  $B$  and size  $L$ . What is the max energy of a synchrotron photon in this system? Account for the effect of the particle anisotropy.
- A striped pulsar wind has magnetic field  $B$  and wavelength  $\lambda$ . What is the minimum energy that shock-driven reconnection should provide, so that particles can be injected into Fermi acceleration?
- Propose an alternative explanation for orphan flares in blazars.

# The Crab Nebula radio spectrum



Zanin 2017, Lyutikov *et al.* 2019

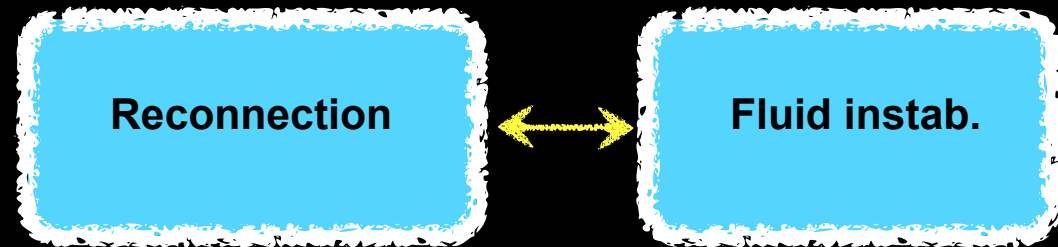
# The role of pitch angle anisotropy



► Low frequencies:  
 $\nu F_\nu \propto \nu^{4/3}$

► High frequencies:  
 $\nu F_\nu \propto \nu^{(3-p)/2}$

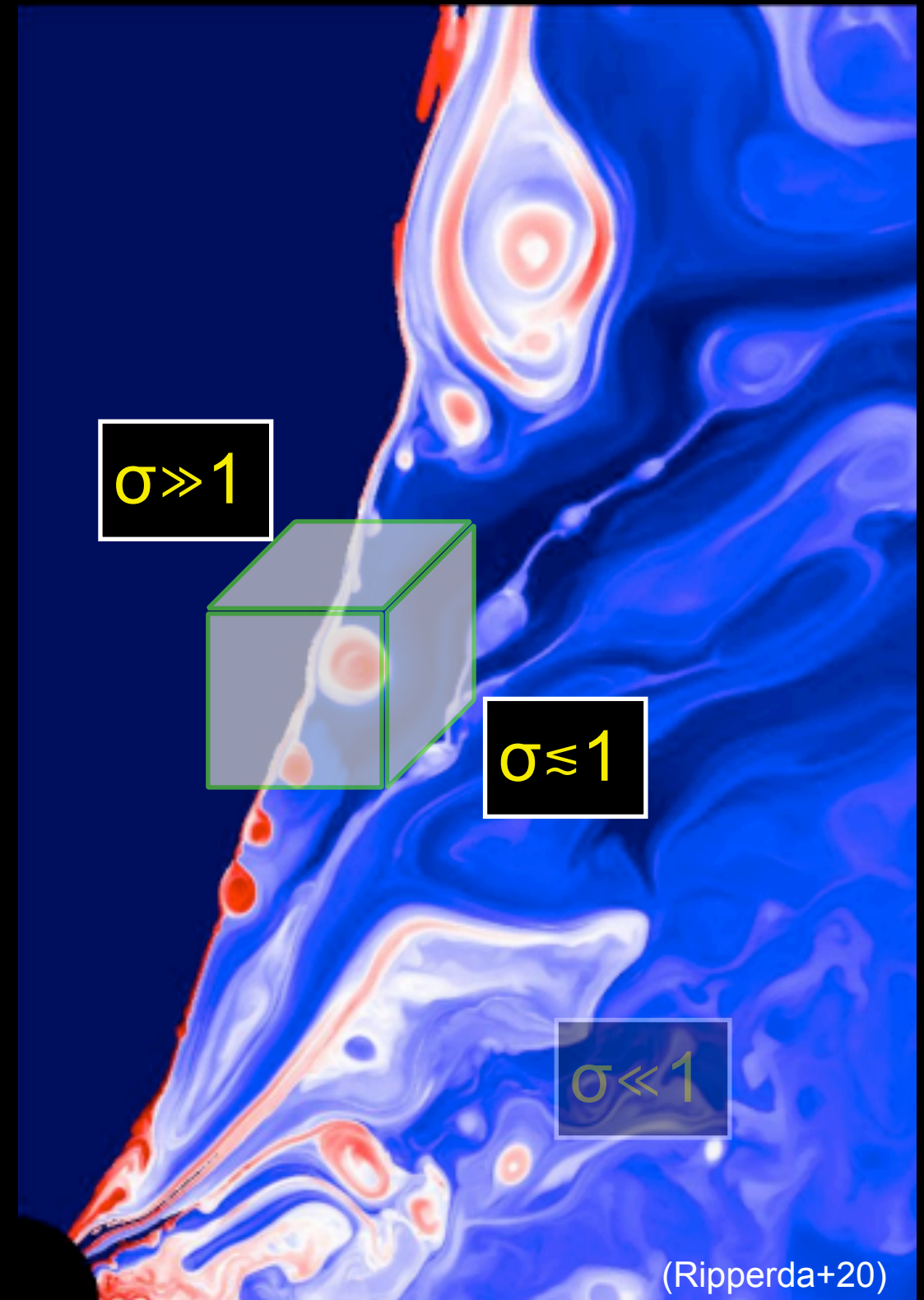
# 2. KH-driven relativistic reconnection at jet boundaries



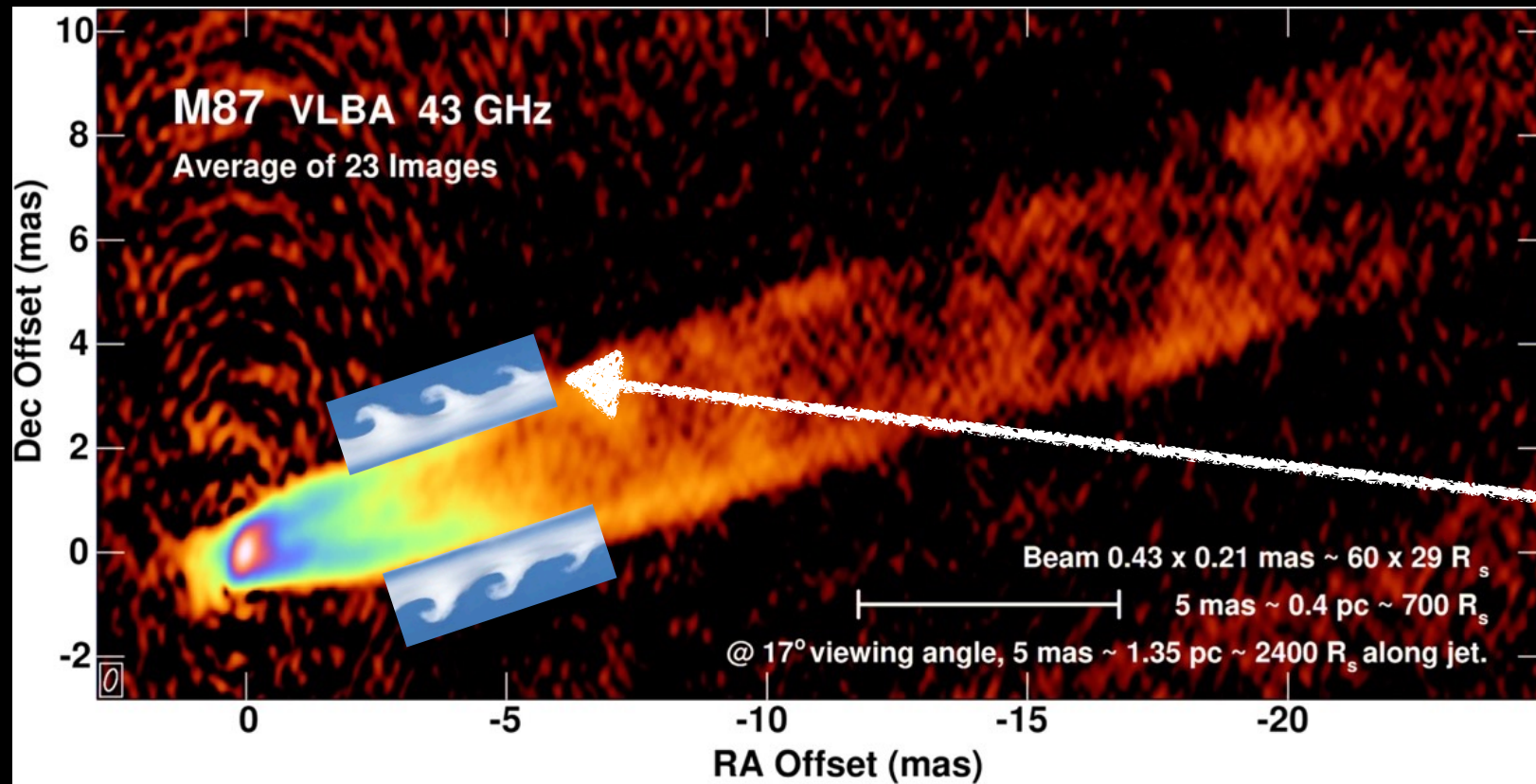
with M. Rowan and R. Narayan



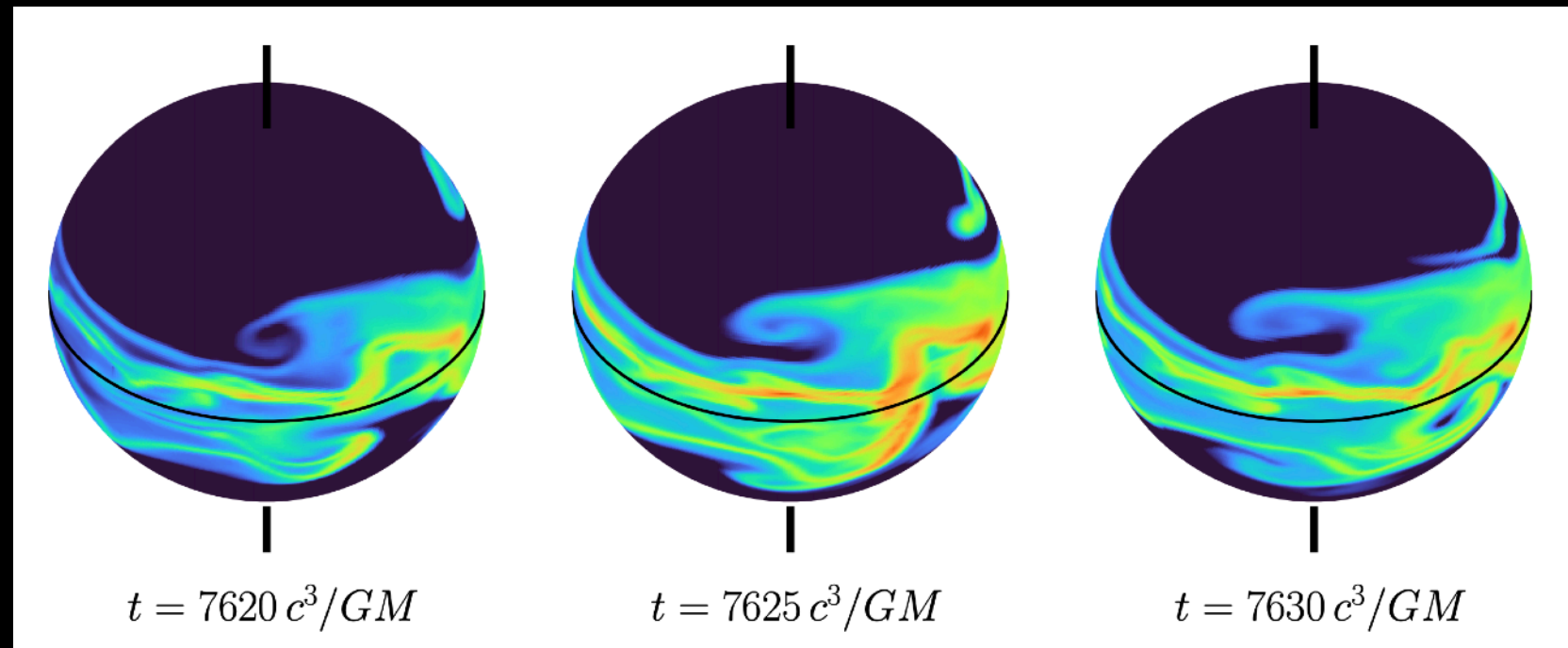
LS et al. 2021, ApJL, 907, L44



# The boundary of M87 jet



Kelvin-Helmholtz (KH) instability at the jet boundary

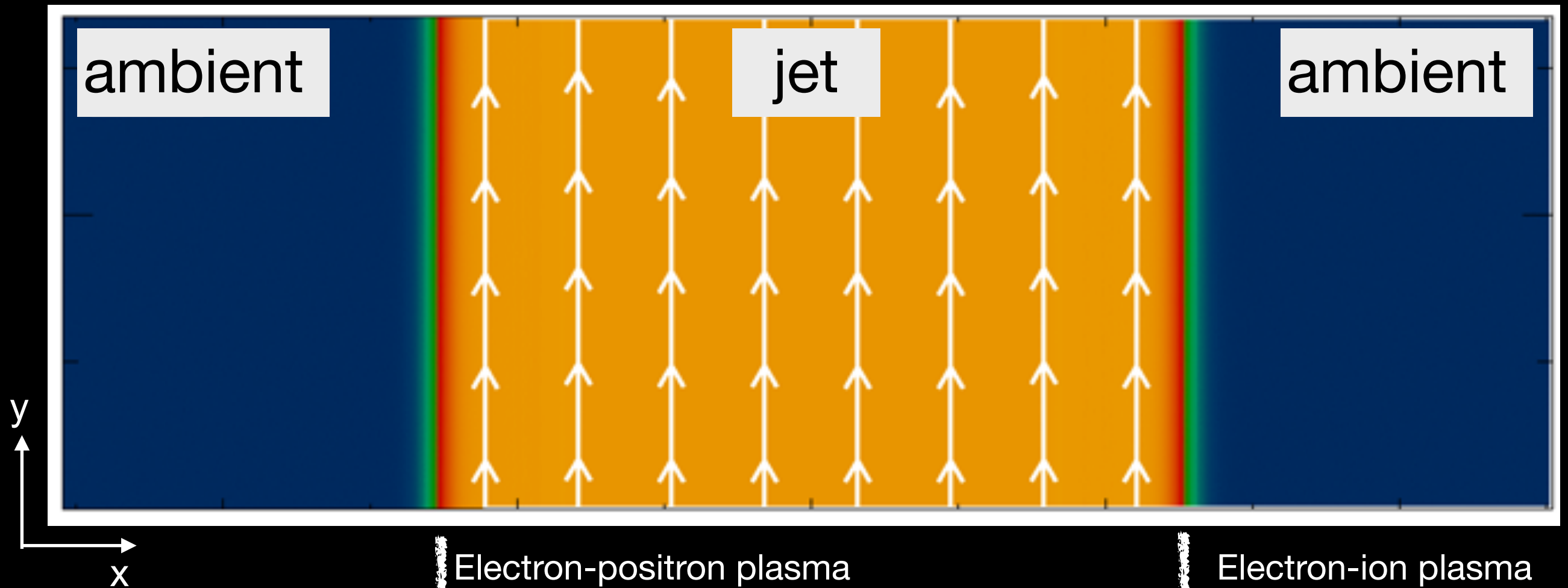


(Wong+21; see also Chatterjee+19)

What is the nonlinear outcome of KH at the jet boundary?

# The jet / ambient system

2D PIC with TRISTAN-MP (Spitkovsky 2005)



Electron-positron plasma

Relativistic bulk motion:

$$\Gamma_0 \beta_0 = 1.3$$

Dominant  $B_y$  (poloidal) and  $B_z$  (toroidal)

$$\sigma_{j,y} = B_{j,y}^2 / (4\pi n_0 m_e c^2) = 6.7$$

Field obliquity

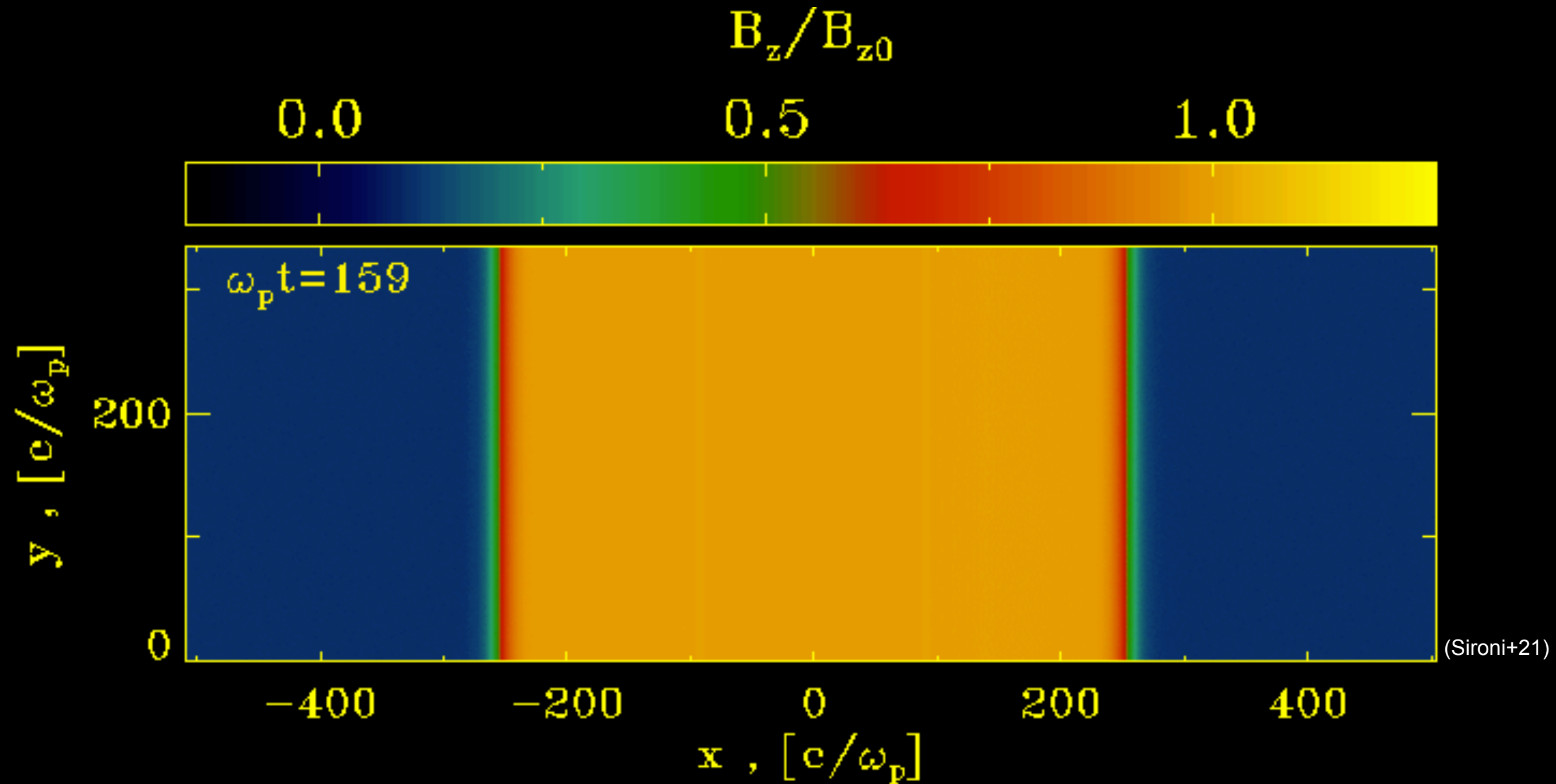
$$\theta = 75^\circ$$

Electron-ion plasma

Stationary

Plasma-pressure dominated, weak  $B_z$

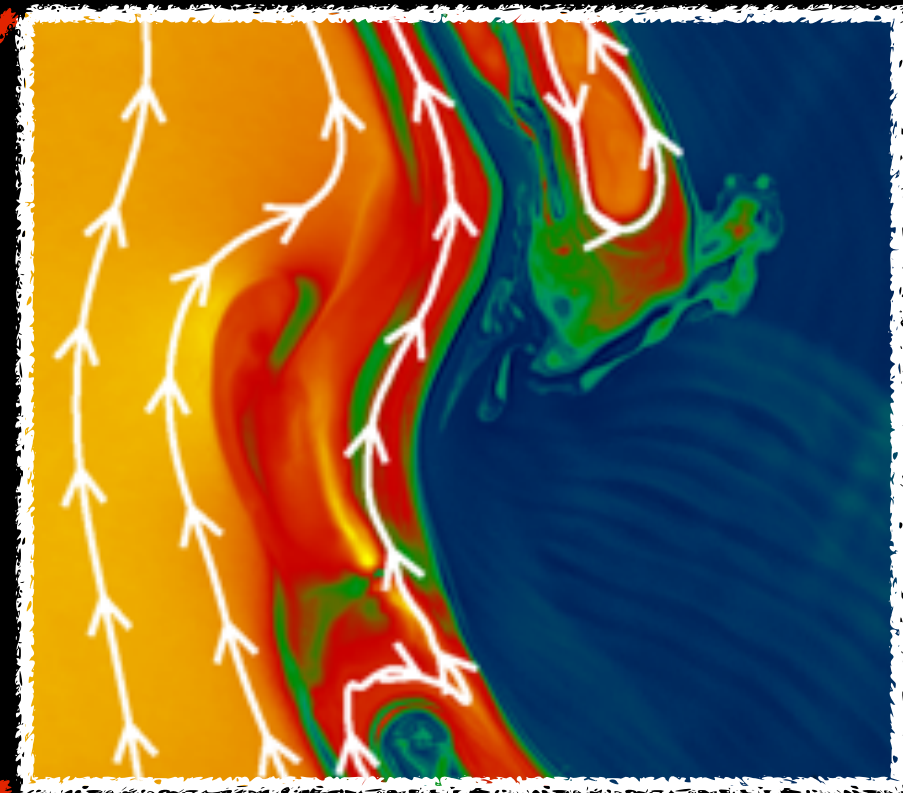
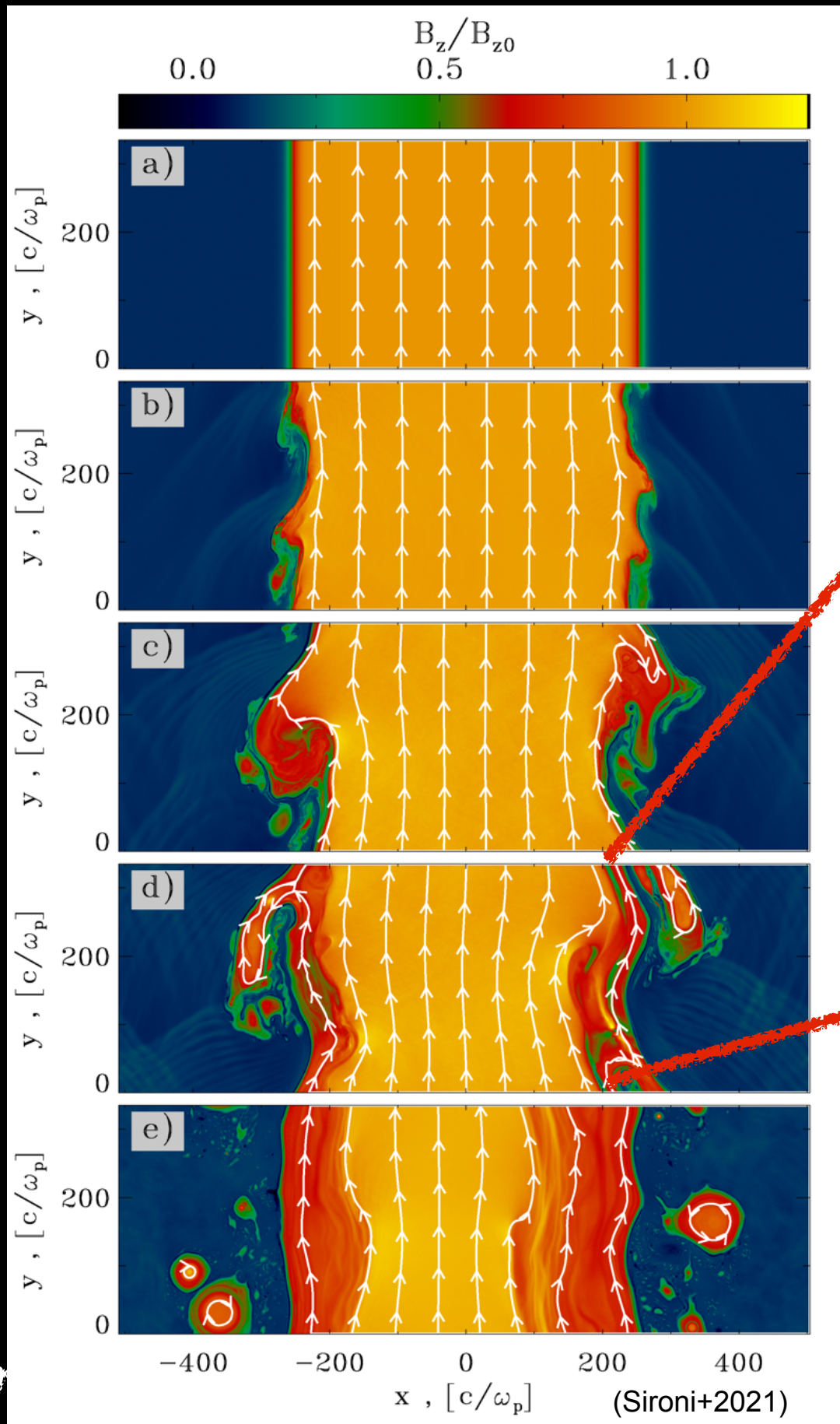
# Kelvin-Helmholtz (KH) instability



- For realistic jet and ambient plasma conditions, the interface is KH unstable.
- The KH growth rate matches well with MHD expectations [which confirms that we start from  $\sim$  MHD-scale initial conditions]

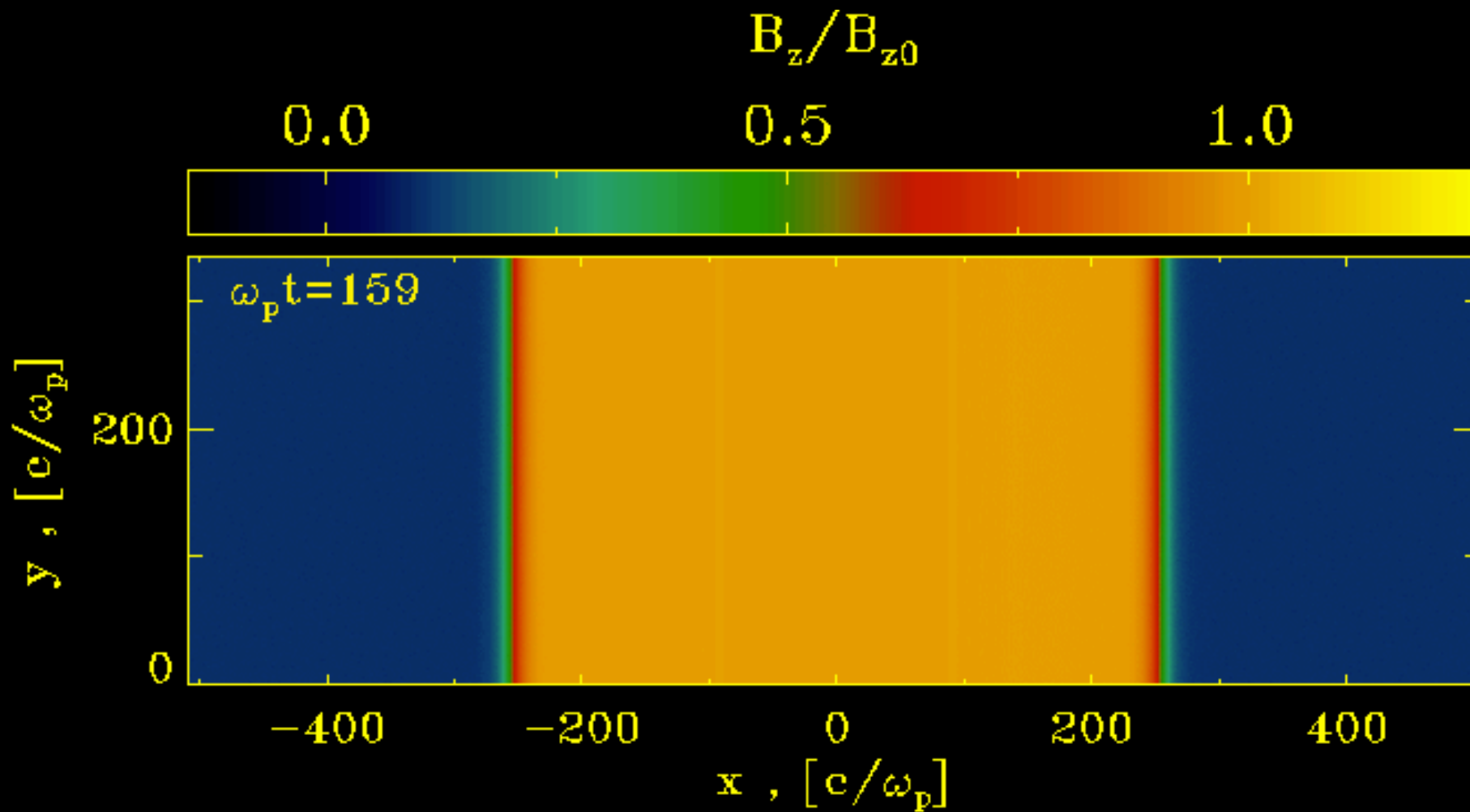
# KH $\rightarrow$ reconnection

Time

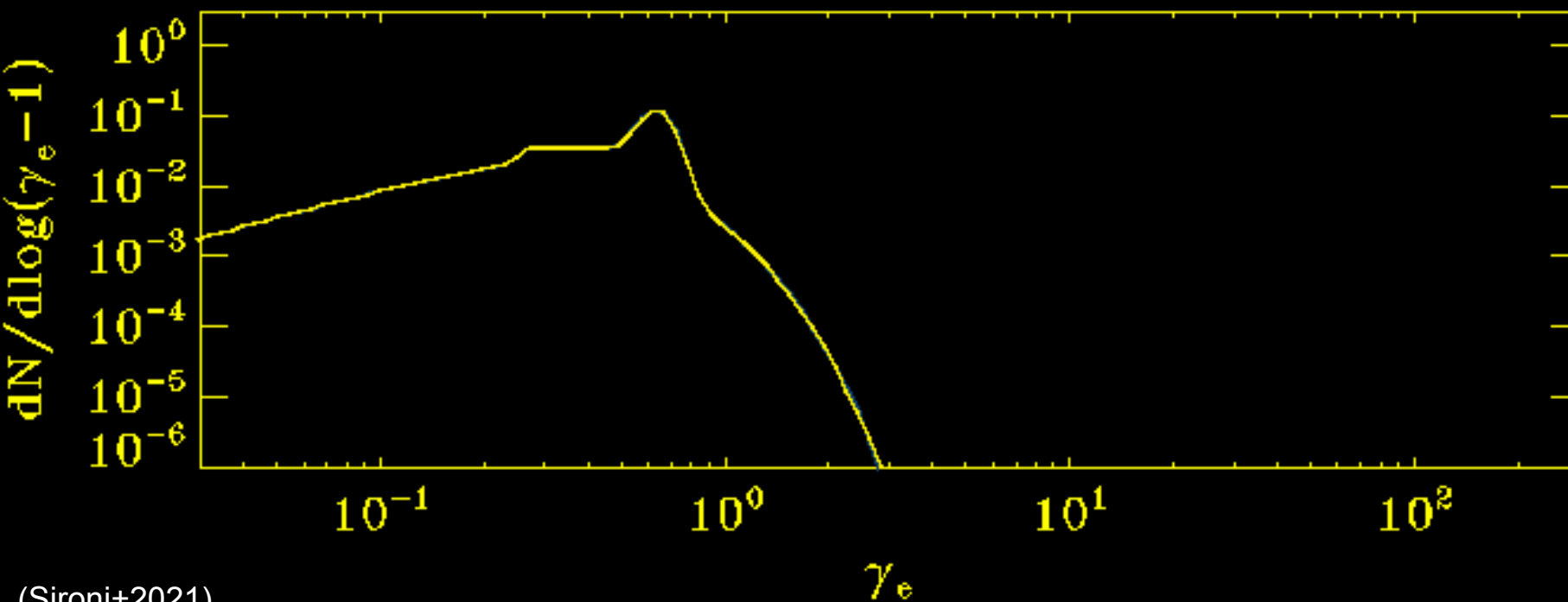


Magnetic reconnection is a natural by-product of the nonlinear KH evolution.

# KH $\rightarrow$ reconnection $\rightarrow$ particle acceleration

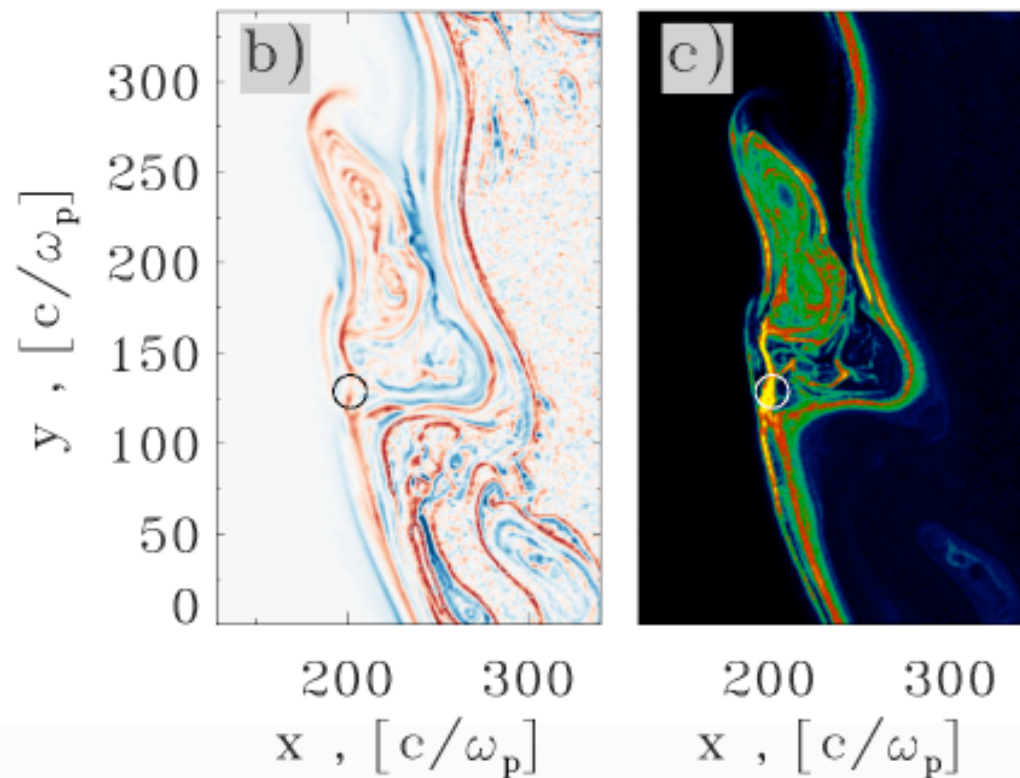
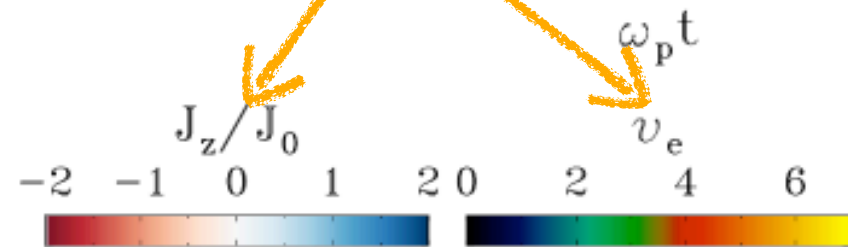
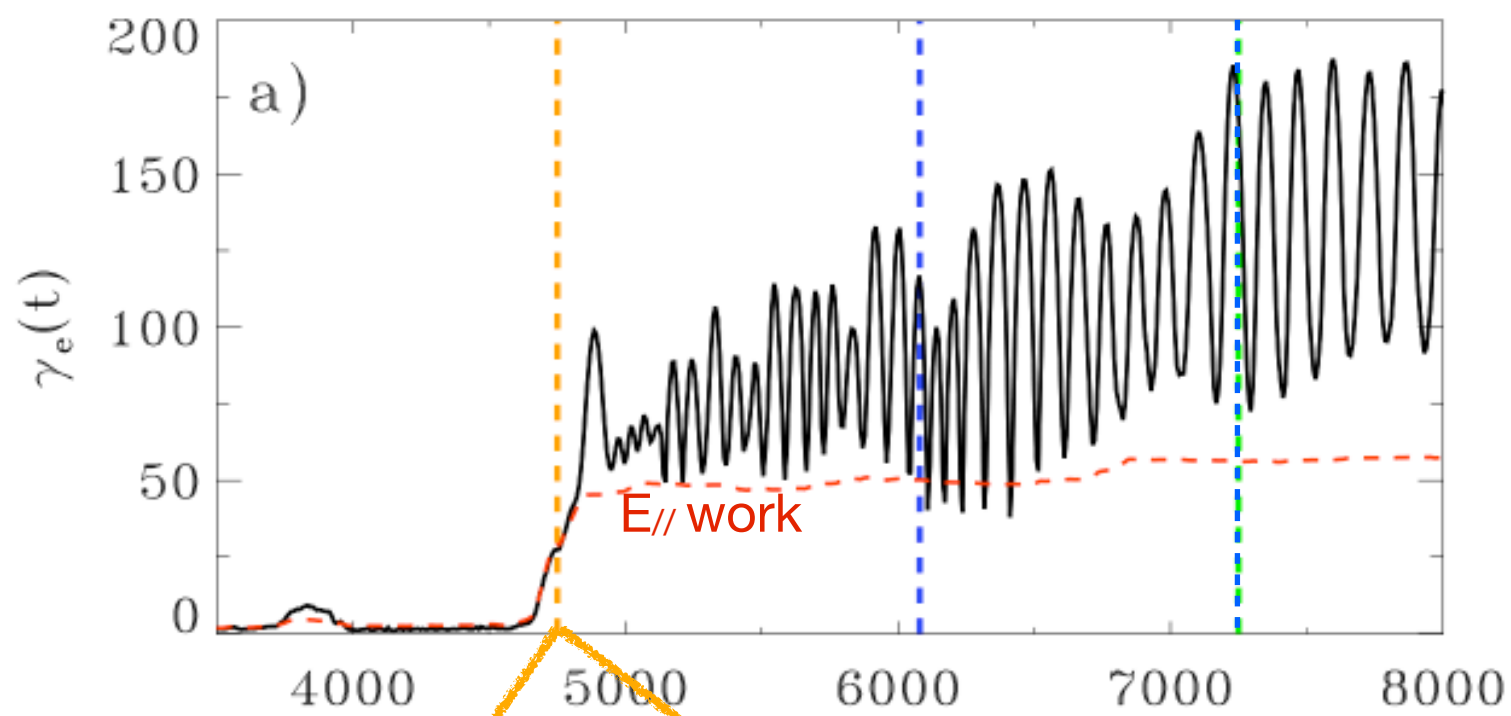


KH-driven reconnection leads to efficient acceleration of jet particles.



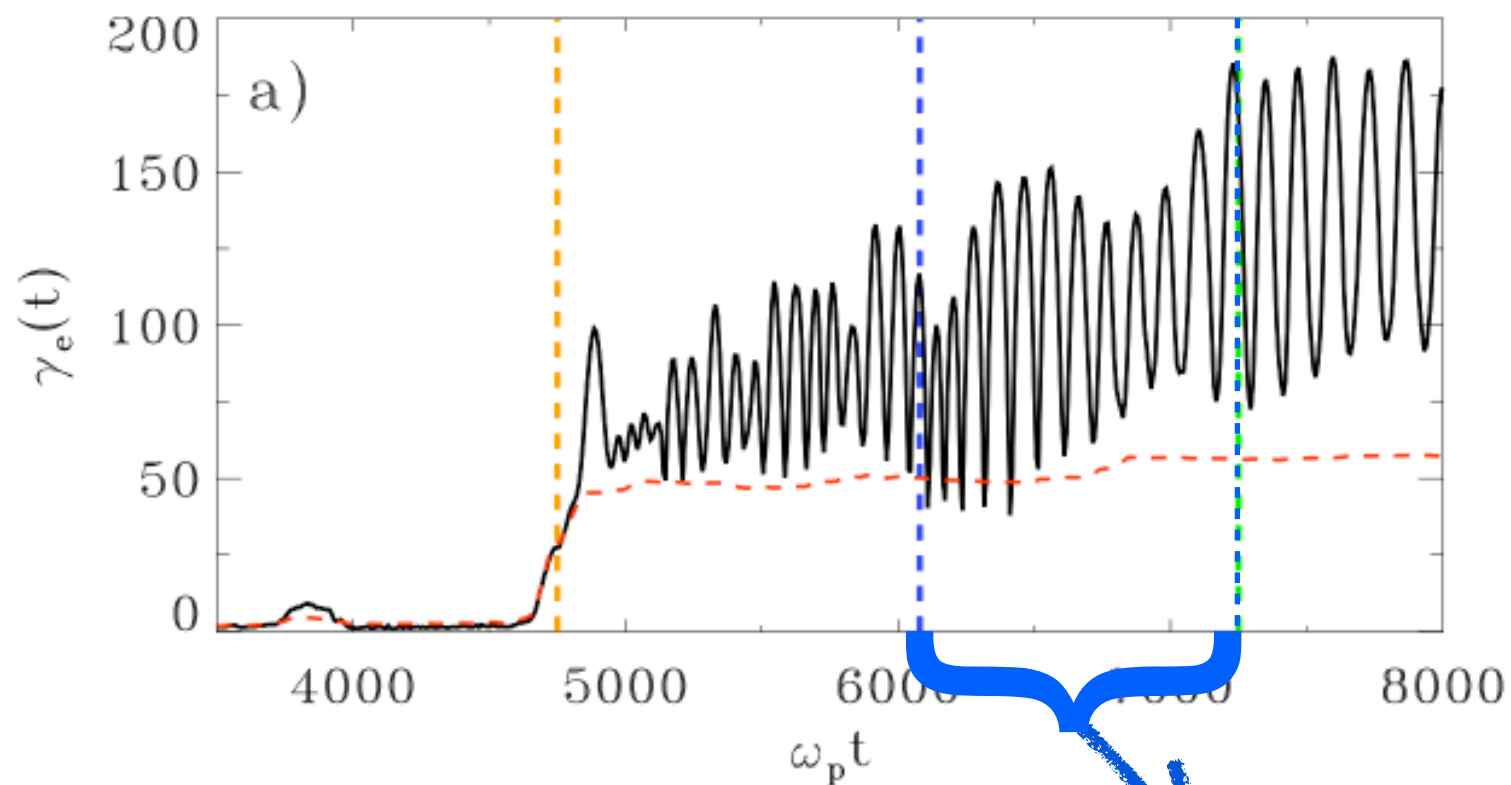
The high-energy cutoff increases at every nonlinear stage of KH evolution.

# The acceleration mechanism



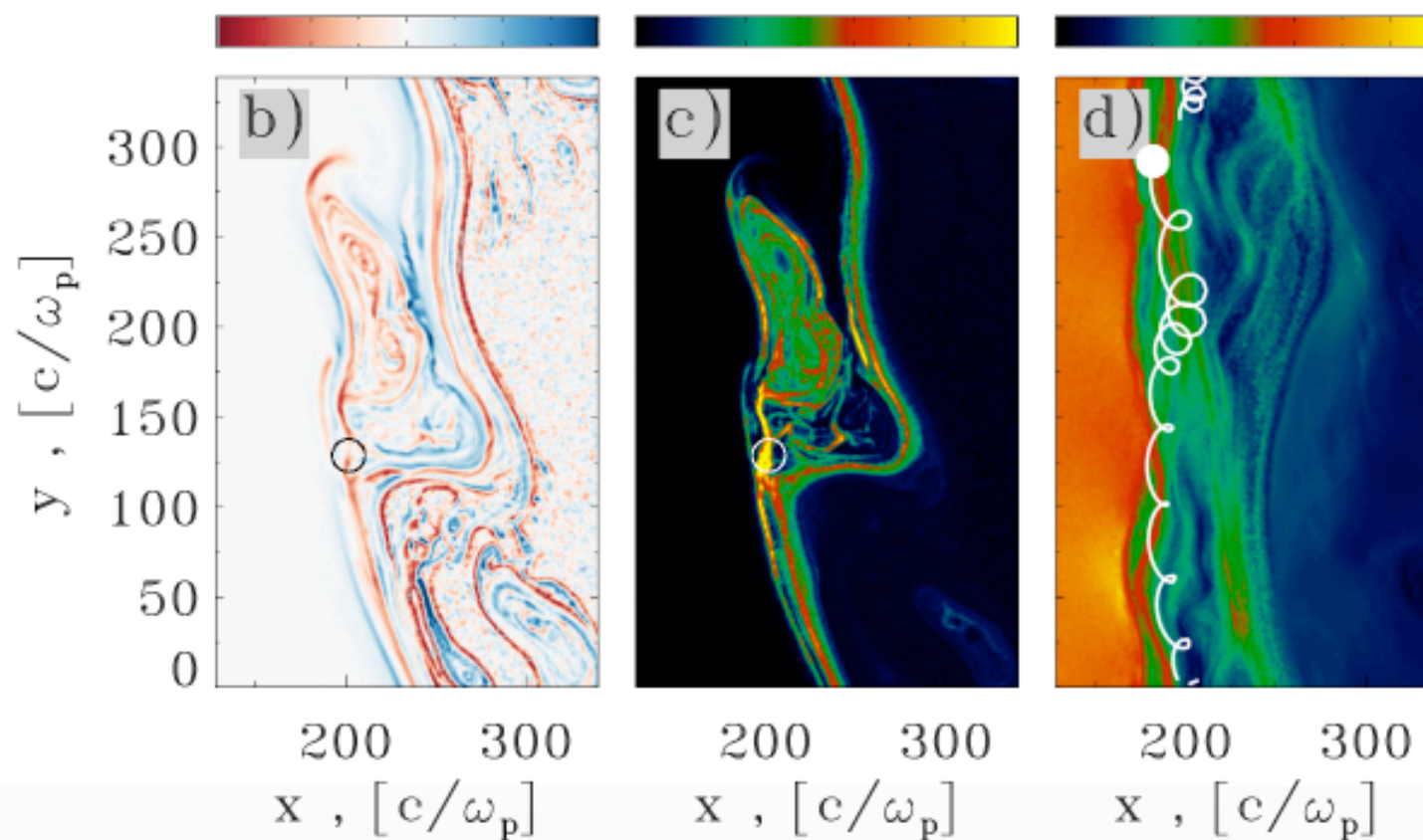
(1) The early acceleration stages (injection) are powered by  $E_{//}$  at reconnection layers.

# The acceleration mechanism



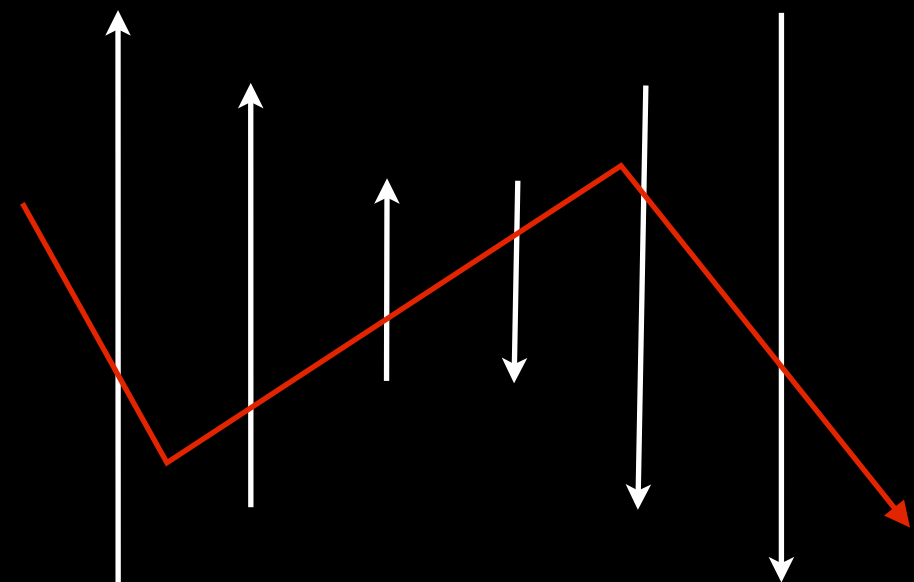
$J_z/J_0$        $v_e$        $\Gamma\beta_y$

-2 -1 0 1 2 0 2 4 6 0.0 0.5 1.0 1.5



(1) The early acceleration stages (injection) are powered by  $E_{\parallel}$  at reconnection layers.

(2) Reconnection-accelerated particles then experience shear-driven acceleration.



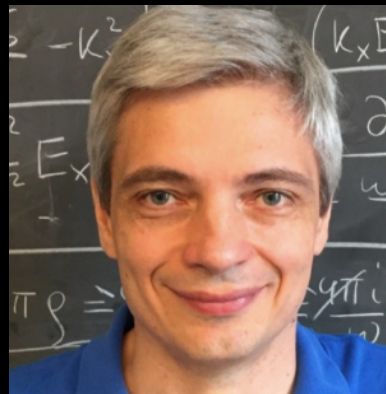
# Overarching summary

Relativistic reconnection can:

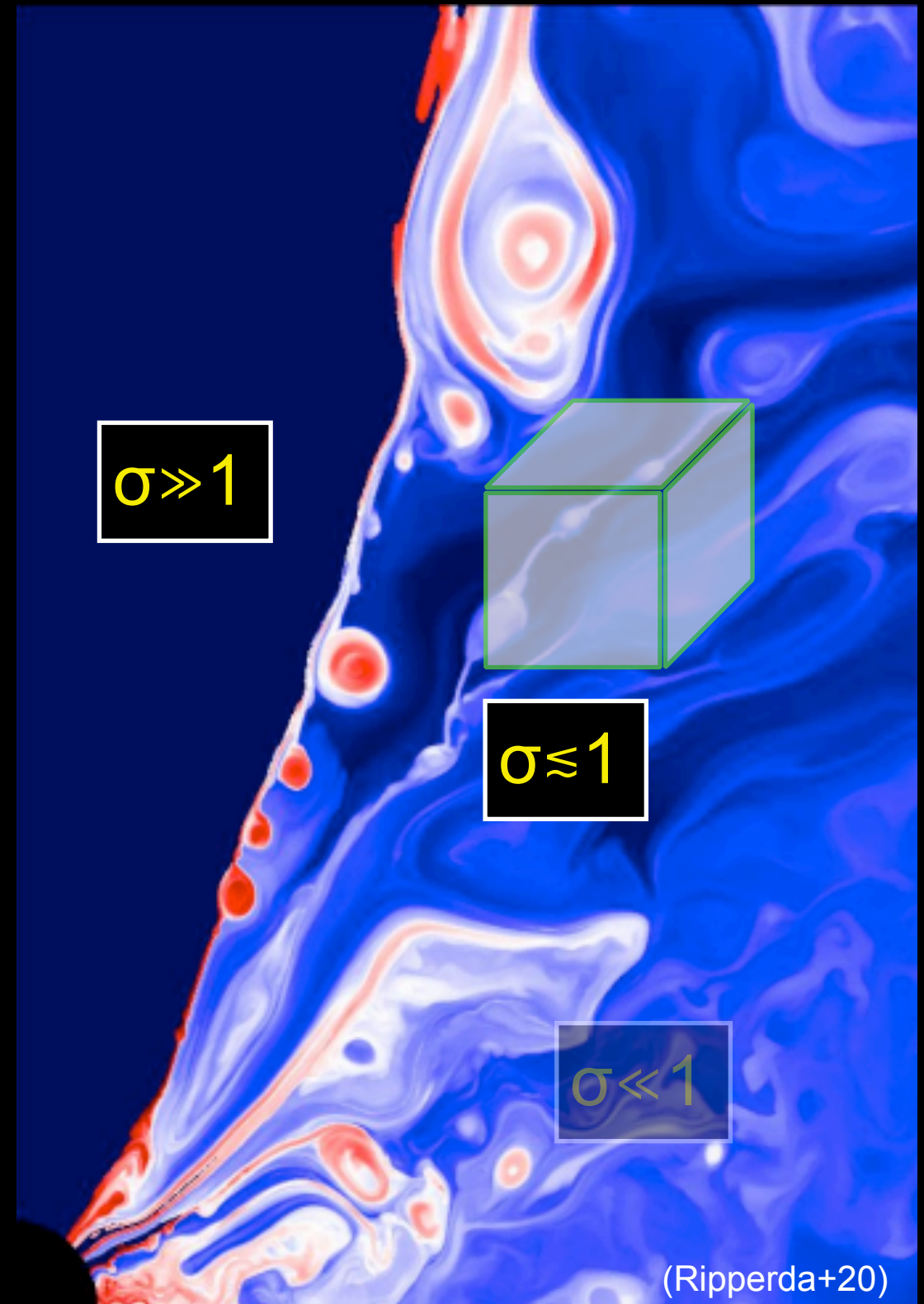
- efficiently dissipate magnetic energy (at rate  $\sim 0.1 c$ ).
- produce non-thermal particles with hard power-law slopes.
- **serve as injection process for subsequent (non-reconnection) acceleration:**  
e.g., Fermi acceleration at shocks, stochastic acceleration in turbulence,  
**shear acceleration at jet boundaries.**
- imprint strong pitch-angle anisotropy.
- produce trans-relativistic bulk motions.

# 3. Radiative relativistic reconnection in black hole X-ray coronae

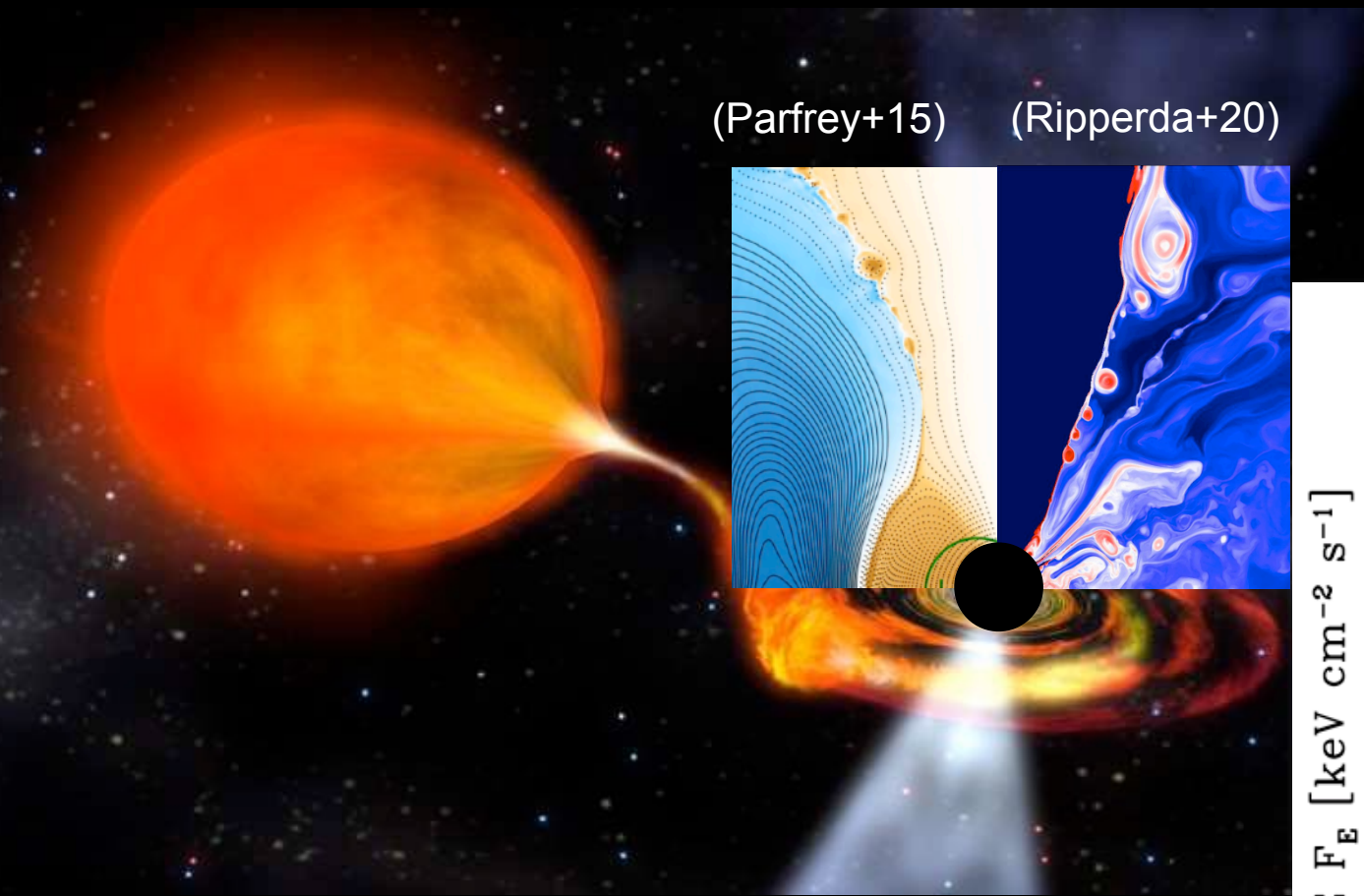
with N. Sridhar and A. Beloborodov



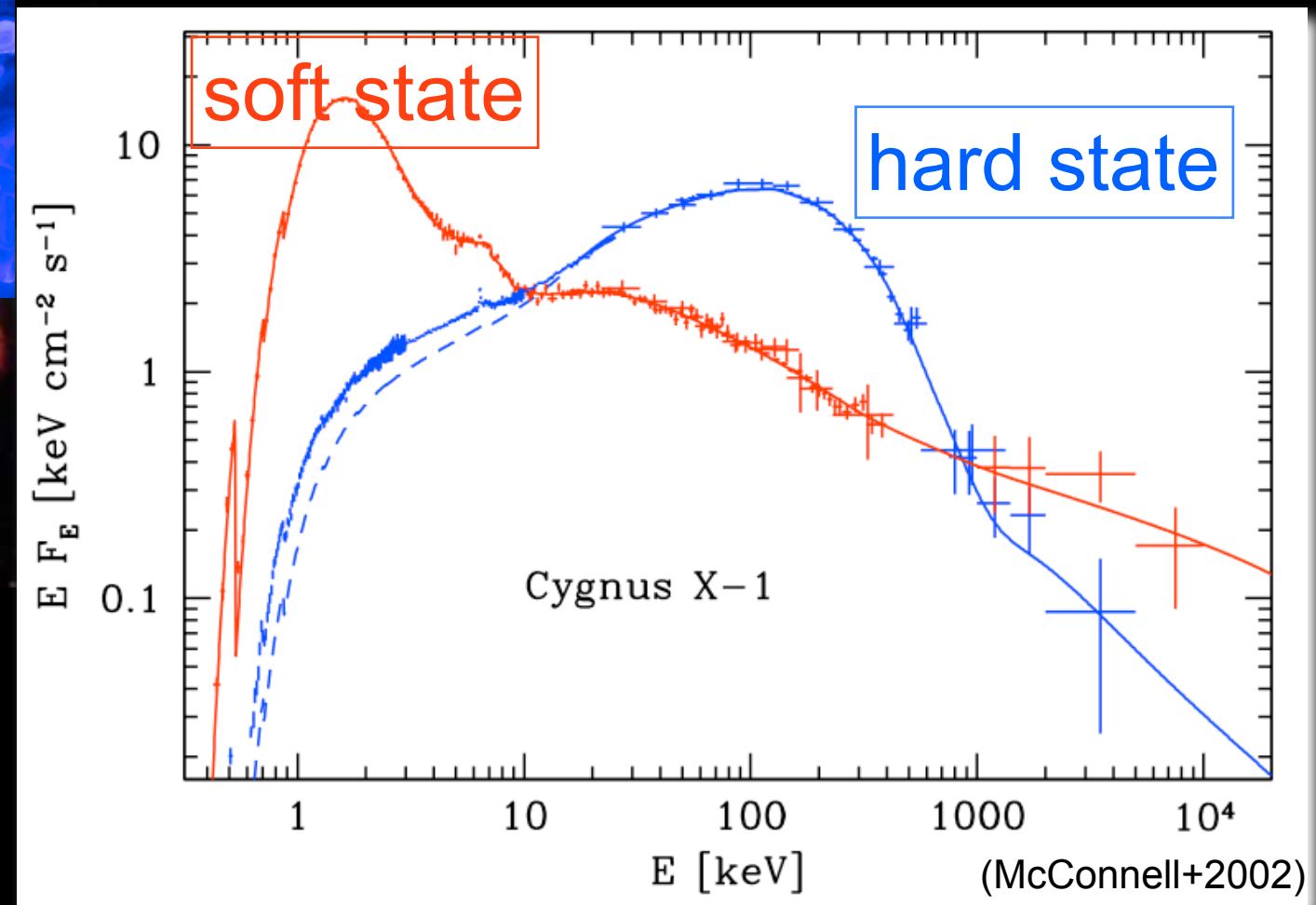
- Sridhar, LS et al. 2022, arXiv:2203.02856
- Sridhar, LS et al. 2021, MNRAS, 507, 5625
- LS & Beloborodov 2020, ApJ, 899, 52



# The hard state of X-ray binaries



Hard state: interpreted as thermal Comptonization by “coronal” plasma with electron temperature  $\sim 100$  keV.



But: how can the electrons stay hot?

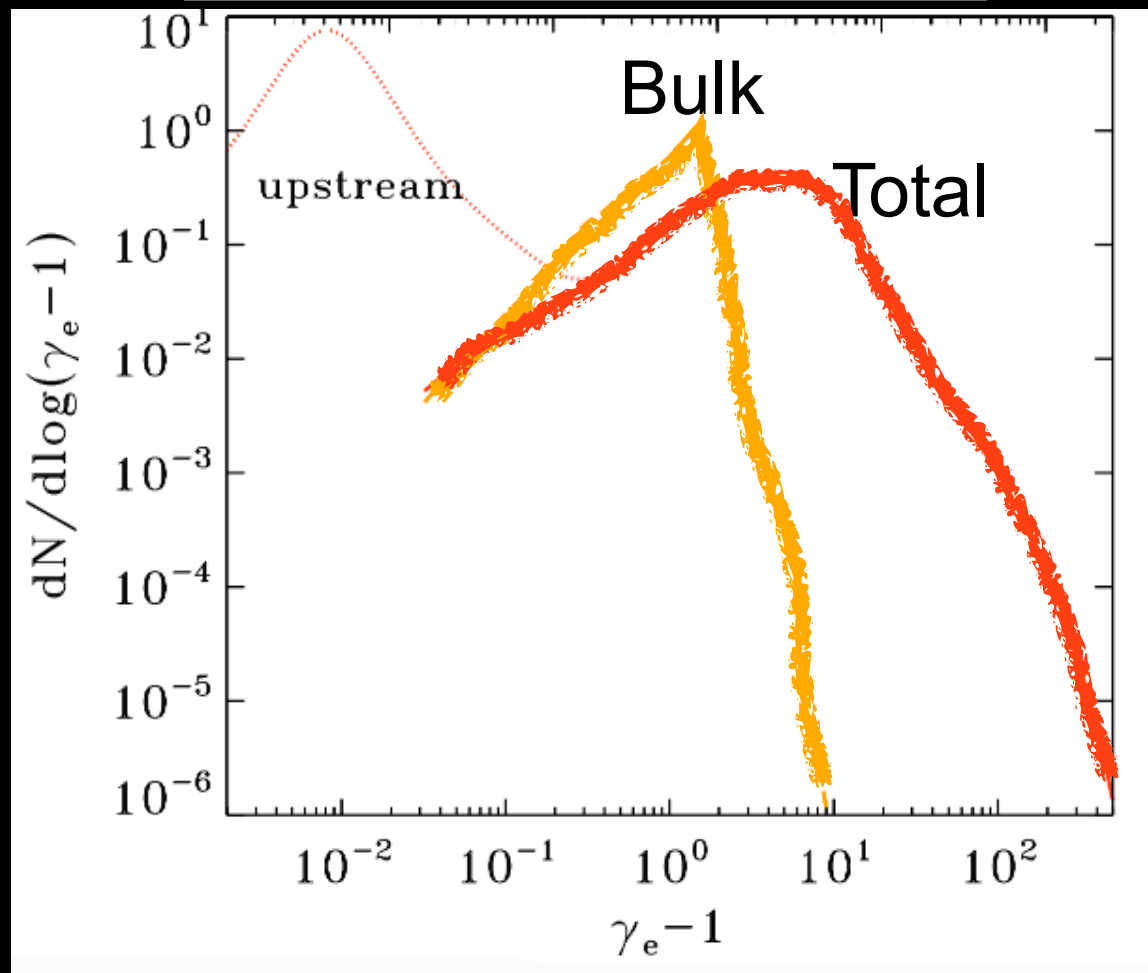
# Radiative reconnection

We parameterize IC cooling via a critical Lorentz factor  $\gamma_{\text{cr}}$  (balancing acceleration with IC losses):

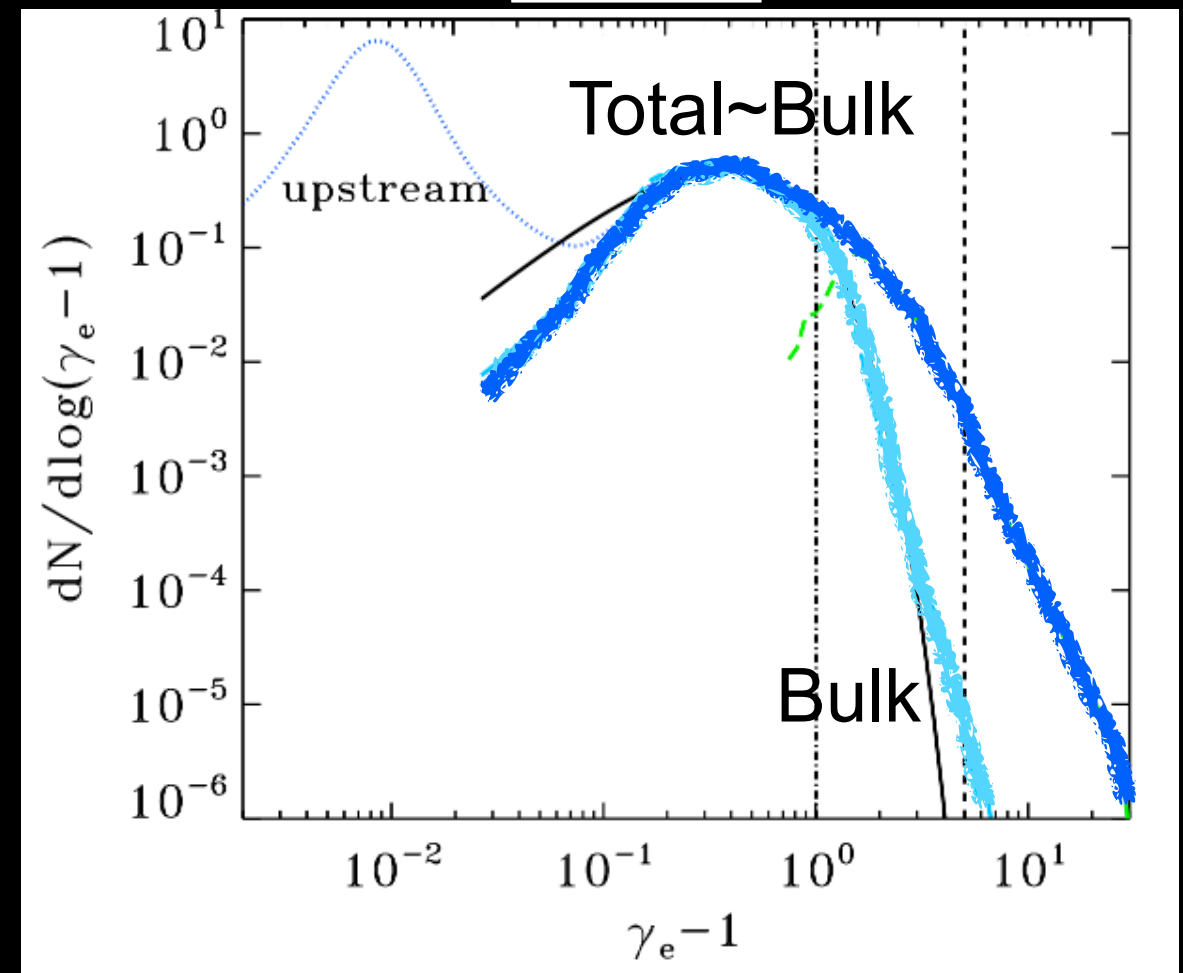
$$eE_{\text{rec}} = \frac{4}{3}\sigma_{\text{T}}\gamma_{\text{cr}}^2 U_{\text{rad}}$$

$$E_{\text{rec}} \simeq 0.1B_0$$

$\gamma_{\text{cr}} = \infty$  [uncooled]



$\gamma_{\text{cr}} = 16$



(LS & Beloborodov 20;  
see also Werner+19)

- Strong IC cooling suppresses particle acceleration.
- For strong cooling, the particle spectrum is dominated by plasmoid bulk motions.

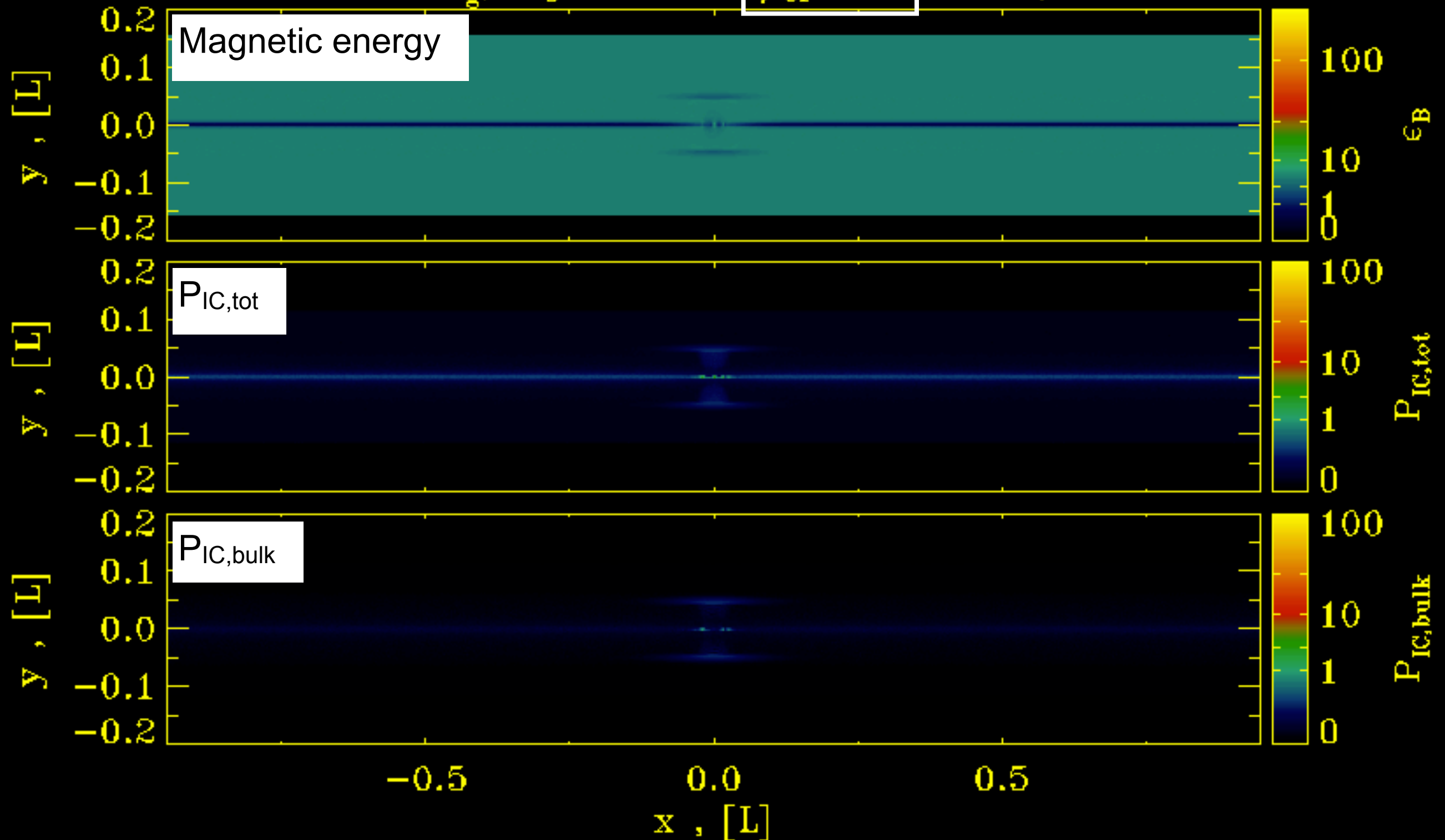
# The radiative plasmoid chain

$\sigma=10$

$B_g/B_0=0.1$

$\gamma_{cr}=16$

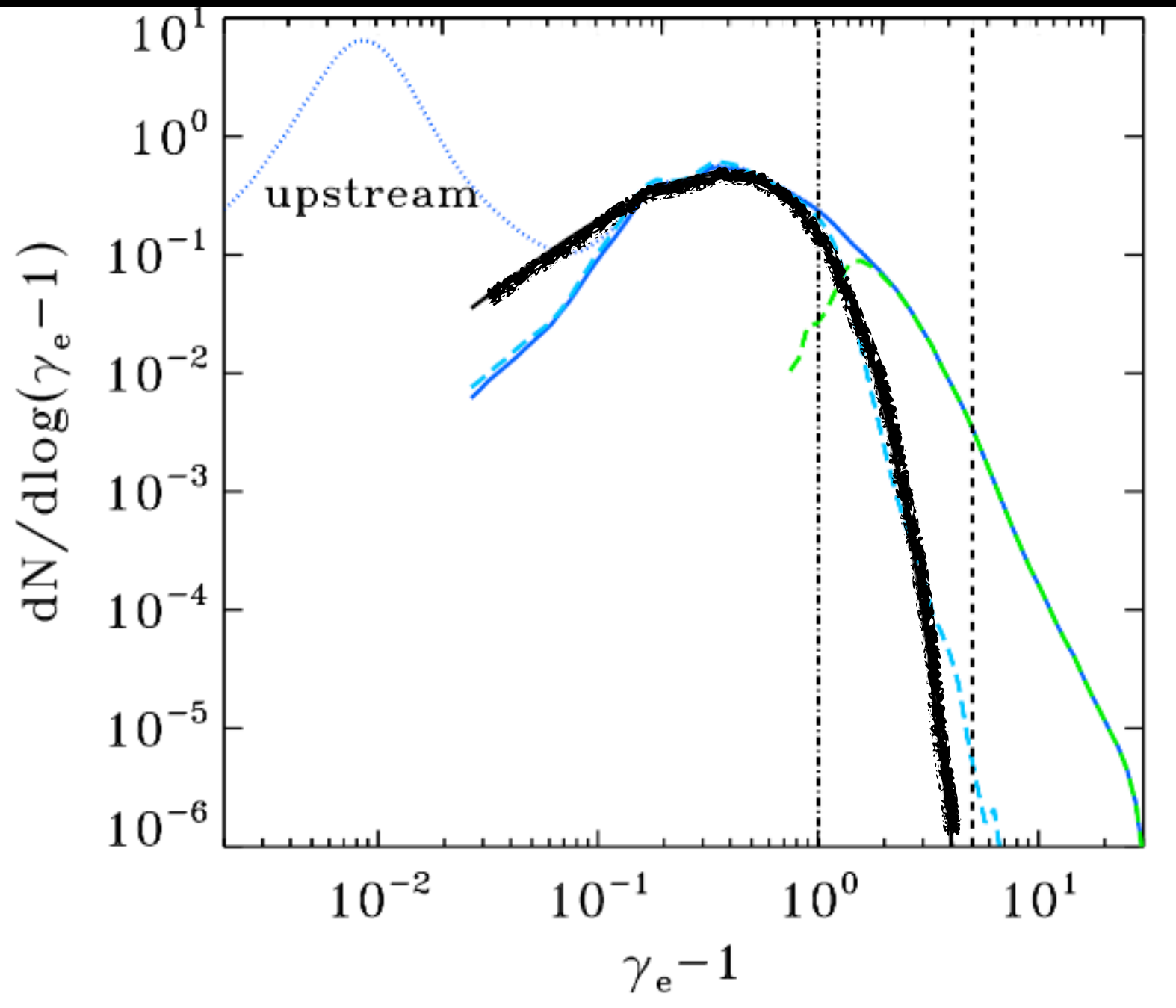
$ct/L=0.1$



The total IC power is dominated by the IC power resulting from trans-rel bulk motions.

# Particle energy spectrum

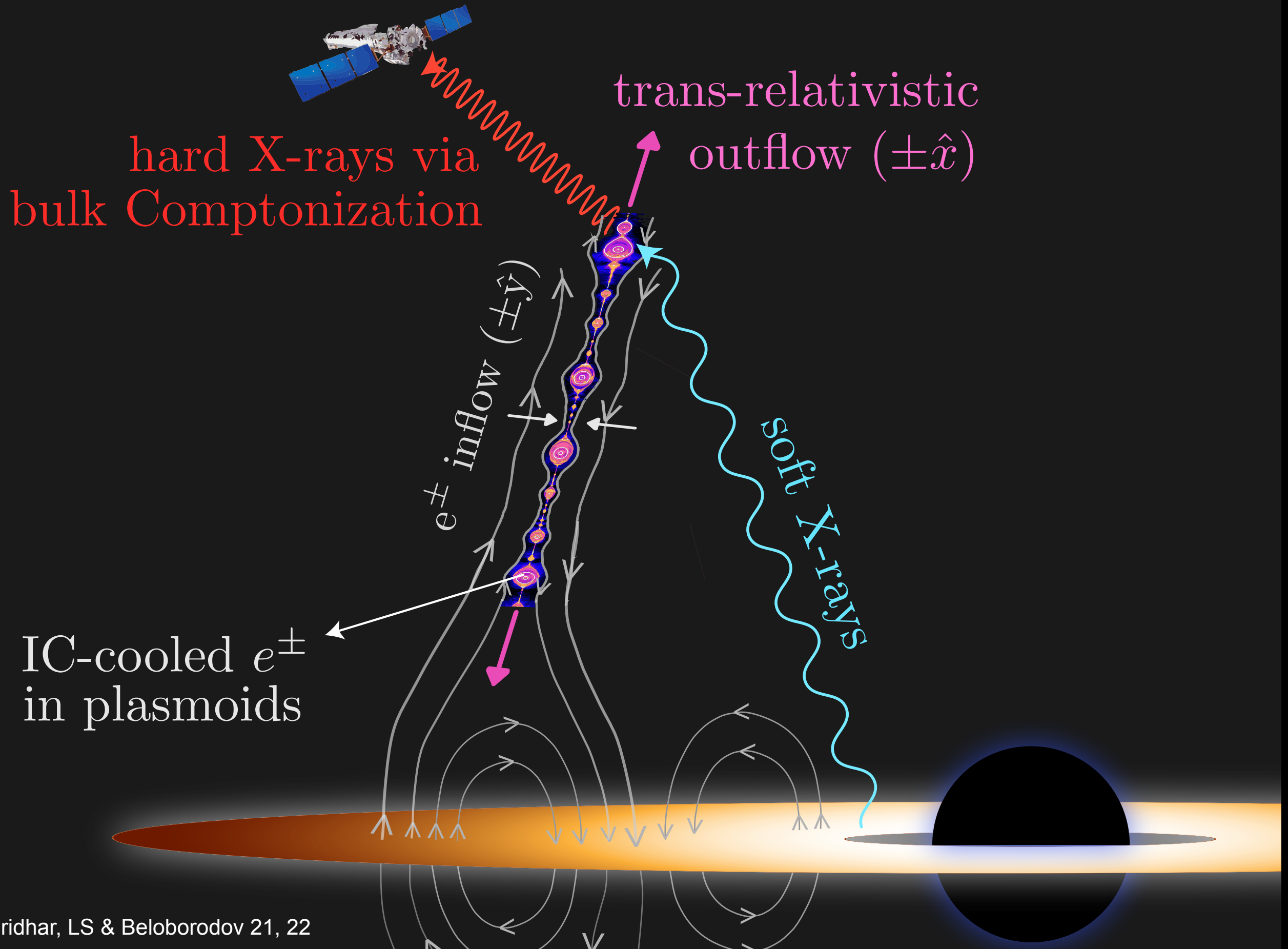
$\gamma_{\text{cr}}=16$



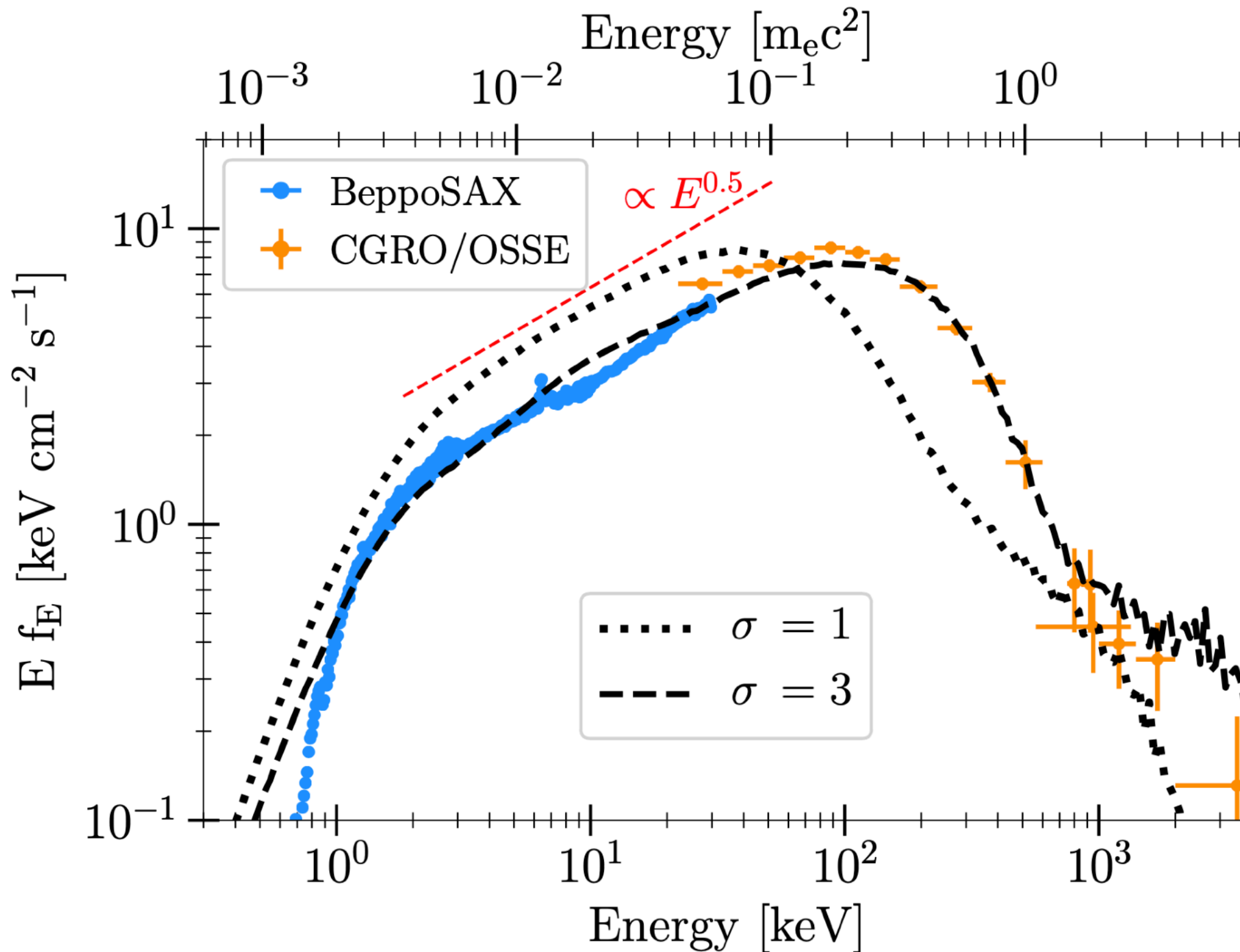
(LS & Beloborodov 20;  
Sridhar, LS & Beloborodov  
21, 22)

- The bulk energy spectrum resembles a Maxwellian with  $T \sim 100$  keV
- Bulk Comptonization in the plasmoid chain mimics thermal Comptonization

# A reconnection model for hard X-rays



# X-ray photon spectrum



# Overarching summary

## Relativistic reconnection can:

- efficiently dissipate magnetic energy (at rate  $\sim 0.1 c$ ).
- produce non-thermal particles with hard power-law slopes.
- serve as injection process for subsequent (non-reconnection) acceleration:  
e.g., Fermi acceleration at shocks, stochastic acceleration in turbulence,  
shear acceleration at jet boundaries.
- imprint strong pitch-angle anisotropy.
- produce trans-relativistic bulk motions.

# <https://thea.astro.columbia.edu/>

 **COLUMBIA** | Theoretical High Energy Astrophysics Group

[Home](#) [Research](#) [People](#) [Opportunities](#) [Seminars](#) [Contact](#) [Gallery](#)



## Welcome to THEA!

We are the Theoretical High Energy Astrophysics (THEA) group at Columbia University. We are located in the Columbia Departments of Physics and Astronomy in Pupin Hall on the Columbia Morningside campus. Our interests are broad, covering many topics in contemporary theoretical astrophysics (compact objects, gravitational wave sources, and other high-energy phenomena) and which call upon a wide range of physics topics (general relativity, radiation hydrodynamics, collision-less plasmas / stellar dynamics, and nuclear astrophysics). Click on the links below to learn about us and our research work.